

Danmarks Geologiske Undersøgelse  
*Geological Survey of Denmark . Yearbook 1982*

---

# Årbog 1982



---

I kommission hos C. A. Reitzels Forlag  
København 1983



Danmarks Geologiske Undersøgelse  
*Geological Survey of Denmark. Yearbook 1982*

---

# Årbog 1982

---

I kommission hos C. A. Reitzels Forlag  
København 1983



D.G.U. Årbog 1982  
er sat med fotosats Times  
og trykt i offset i 1000 eksemplarer  
hos AiO as, Odense.  
Bogen er trykt på Thai-cote 115 g  
fra a/s De forenede Papirfabrikker.  
ISBN 87-421-0735-0  
ISSN 0105-063X

*Redaktion:* Bent Aaby

Date of publication: 1983-11-30



# Contents

## Indhold

Niels Balslev Jørgensen: Foreløbige sedimentologiske undersøgelser i fluviale sedimenter i egnen omkring V. Nebel, Østjylland . . . . .	5
Arne Villumsen, Ole Stig Jacobsen, and Carsten Sønderkov: Mapping the vulnerability of ground water reservoirs with regard to surface pollution . . . . .	17
Lise Holm: Subsidence history of the Jurassic sequence in the Danish Central Graben . . . . .	39
Tove Birkelund, Claus Koch Clausen, Henrik Nøhr Hansen, and Lise Holm: The <i>Hectoroceras kochi</i> Zone (Ryazanian) in the North Sea Central Graben and remarks on the Late Cimmerian Unconformity . . . . .	53
Søren Priisholm: Geothermal reservoir rocks in Denmark . . . . .	73
Peter Klint Jensen: Principles of temperature mapping . . . . .	87
Peter Klint Jensen: Formation temperatures in the Danish Central Graben . . . . .	91
Erik Nygaard: <i>Bathichnus</i> and its significance in the trace fossil association of Upper Cretaceous chalk, Mors, Denmark . . . . .	107
Publications issued 1982 . . . . .	138



# Foreløbige sedimentologiske undersøgelser i fluviale sedimenter i egnen omkring V. Nebel, Østjylland

Niels Balslev Jørgensen

Jørgensen, N. B.: Foreløbige sedimentologiske undersøgelser i fluviale sedimenter i egnen omkring V. Nebel, Østjylland. *Dann. geol. Unders. Årbog 1982*: 5–16, skitse 1–3. København 1983.

Observations in the continuous excavations for the natural gas pipeline in Jylland, revealed several pointbar sequences, giving evidence of a former meandering stream, and further revealed the hummocky areas around the Nørresø – Søndersø valley, consists of deposits from a braided river system.

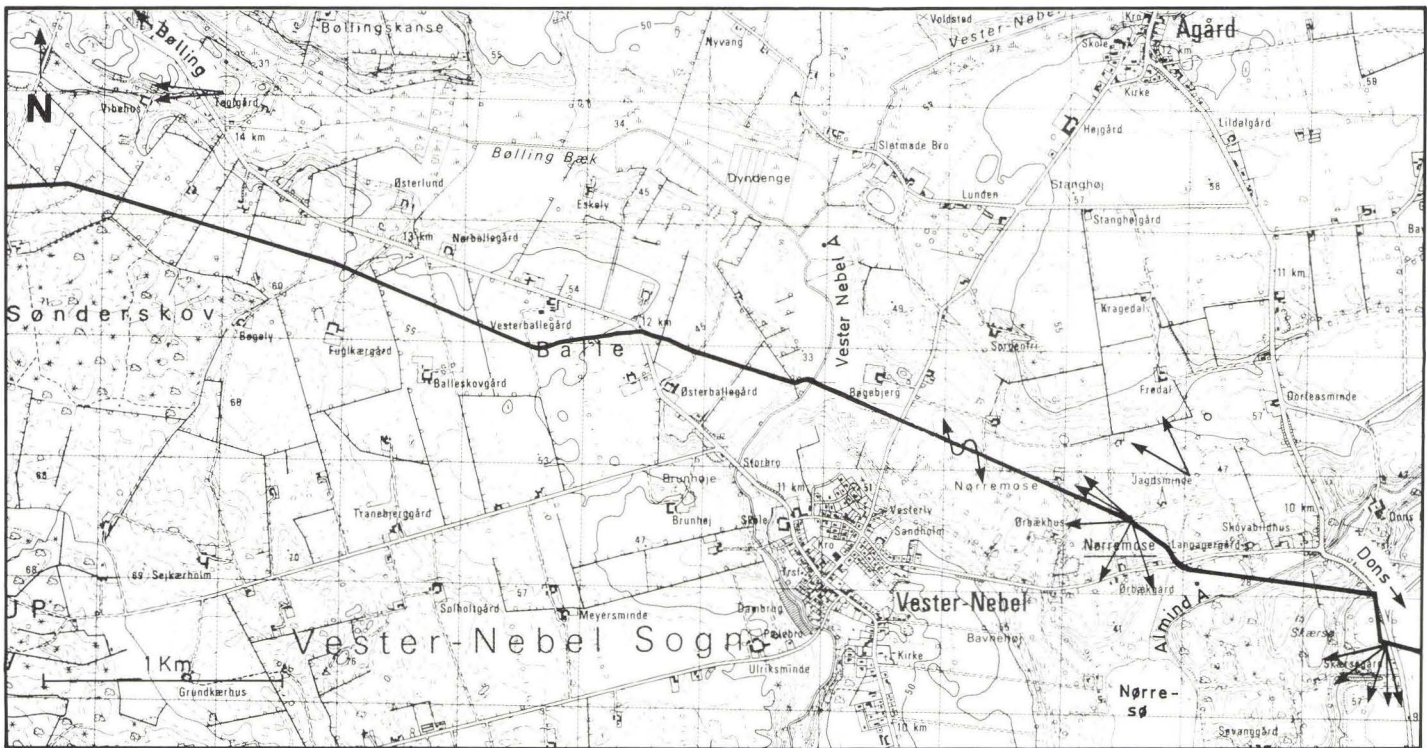
Direction of meltwater flow was bi-modal, showing northwesterly and southwesterly directions. The Almind Å-valley and the V. Nebel Å-valley presumably acted as feeder channels for the braided environment. It is suggested that the meltwater flowed towards the area around Vamdrup and Skodborg.

*Jørgensen, N. B., Geological Survey of Denmark, Thoravej 31, DK-2400 Copenhagen NV, Denmark.*

I forbindelse med nedgravningen af naturgasledningen, leder råstofgeologisk afdeling ved Danmarks Geologiske Undersøgelse et projekt, hvor der foretages systematiske undersøgelser langs udgravningerne. De i denne artikel behandlede data er indsamlet i perioden 30/6–7/7–82 på strækningen V. Nebel-Dons, eller nærmere betegnet fra 10790 m til 13963 m (se fig. 1).

Området er karakteriseret ved nogle markante dalsystemer, hvoraf den største er den op til to kilometer brede nord-syd gående Nørresø-Søndersø dal. Den nordlige forlængelse af denne dal deler sig i tre mindre dale: Almind Å-dal, V. Nebel Å-dal og dalen med Bølling bæk (fig. 1). Denne dalforgrening er af Milthers (1948) og Nordmann (1958) omtalt i forsigtige vendinger: “En anden dal strækker sig fra Egtved mod sydøst forbi Bølling omtrent til V. Nebel. Den er ret smal men har typisk præg af at være opstået ved erosion under isen. I tilslutning til denne dal er det muligvis, at den sørække er opstået, som strækker sig 6–7 kilometer nordpå fra Harte, vest for Kolding. De tre dalretninger afspejler da muligvis, at der en tid i egnen mellem Vejle og Kolding dalene har været israndstillinger liggende i buet form med selve Kolding omtrent i centrum” (Milthers 1948, side 134); Nordmann (1958 side 75) skriver “Denne tanke skal ikke diskuteres nærmere her; måske støttes







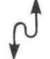
-  Gasledning
-  Strømretning
-  Kanalretning

Fig. 1. Oversigtskort. Kortgrundlag 1213 III NØ JORDRUP. Gengivet med tilladelse A 881/76 af G.I.

den af en forestilling hos ham (Milthers) om, at smeltevandsfloden, som har udformet Elbodalen, skulle have haft strømretning fra SV til NØ. Dette er der dog kun liden grund til at antage; når de andre store tunneldale har haft deres afløb mod SV eller V til trods for, at deres glaciale bund højner sig i denne retning, er der al grund til at tro, at Elbodalen også har haft det”.

Tidligere i sin afhandling skrev Nordmann: “Den mulighed er dog næppe udelukket, at søerne (navnlig Stallerup sø) er af tektonisk oprindelse. Hvis de skulde være “langsøer” i en tunneldal, må denne have en ganske anden retning end de øvrige tunneldale på kortbladet, hvilket ikke er meget sandsynligt” (side 16).

Af kortudsnittet (fig. 1) fremgår det at ledningen føres gennem de lavt liggende områder NØ for V. Nebel, og passerer på vejen det lidt højereliggende område, hvorover vejen mellem V. Nebel og Ågård er ført. Ved den østlige Nørremose bliver landskabet stadig mere kuperet med en uregelmæssig topografi. Efter at have passeret Almind Å-dal føres ledningen igen gennem småkuperet landskab, omkring Skærso, for at ende på plateauet ved Dons. Området er således beliggende mellem det af Milthers (1948) beskrevne bueformede israndsstrøg og et mere lineært nord-syd gående strøg, beliggende lidt vestligere.

## De opmålte profiler

Den kontinuerte opmåling foregår fortrinsvis ved opmåling af sedimentologiske log. Derudover er der også foretaget opmåling af længdeprofiler. En kombination af disse profiltyper for udvalgte strækninger danner basis for denne artikel.

### *Profil ved 11410 m – 11455 m og 12012 m – 12028 m*

Profil 11410 m – 11455 m ligger på østsiden af V. Nebel Å, mens profil 12012 m – 12028 m ligger ca. 200 m øst for vejen til Ågård (fig. 1). Generelt er begge profilerne domineret af ret finkornede sandede og siltede aflejringer med underordnede lerede lag. På skitse 1 og skitse 3 (vedlagt bag i bog) ses udsnit af de opmålte længdeprofiler, der er domineret af en storskala, rytmisk opbygget, sigmoidal skrålejring der dykker omkring 26°–32°, dels i nordvestlig, dels i østlig retning. Skrålejringen er opbygget af mindre enheder, bundter, af forsæt med varierende tykkelse og varierende hældning/strygning. I de enkelte forsæt ses storskala trug- og planar skrålejring, mens strukturløse forsæt dominerer (fig. 2). I ganske få forsæt er observeret småskala planar skrålejring.





Fig. 2. Udsnit af pointbar sekvens fra profilet 12012–12028 m. Bemærk den rytmiske opbygning af skrålejringen (Epsilon-skrålejringen). Profilet ca. 1,80 m højt.

Sekvensen 11410 m – 11455 m overlejres af strukturløst sand, stedvis igen overlejret af tørv (skitse 3). Der ses enkelte normalforkastninger, hvoraf nogle er synsedimentære, med forkastningsplanet hældende mod Ø.

På grund af den relativ fine kornstørrelse og den karakteristiske opbygning af forsættene med interne primære sedimentære strukturer opfattes disse strækninger som profiler i pointbar sekvenser opbygget af typisk Epsilon (longitudinal) – skrålejring. Den dominerende strømretning har været mere eller mindre vinkleret på profilvæggen, men der har også været strømkomponenter op ad forsættene i form af småskala ribber, repræsenteret i profilet ved småskala skrålejring. Dette fortolkes som et resultat af det undertiden spiralformede strømningsmønster i en meanderbue (Puidefabragas, 1973). Der er foretaget målinger af hældningen af forsættene, hvilket, har givet et indtryk af orienteringen af kanalerne i forhold til gasledningen. På figur 3 er angivet en mulig fortolkning af måleresultaterne. Det ses at profilet kan tænkes at repræsentere dels “neck cut-off” hvor en kanal bryder igennem på det smalleste sted i en meanderbue, dels “Chute cut-off” hvor gennembrudet sker konformt med pointbar opbygningen (se Reineck & Singh, 1975). Der er dog ikke i profilet observeret større ændringer i kornstørrelse, hvor speciel “neck cut-off” viser sig ved ret finkornede aflejringer.



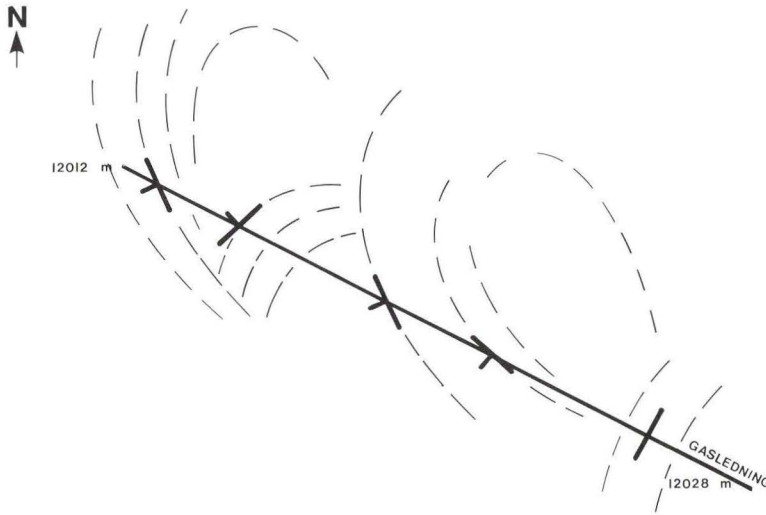


Fig. 3. Forslag til rekonstruktion af kanalforløbet ud fra de indsamlede data i profilet 12012–12028 m. Der kan tilsyneladende udskilles to meanderbuer der hver især er afskåret, den ene (til venstre) ved “chute-cut-off” den anden ved “neck-cut-off”.

#### *Profilet ved 11790 m – 11870 m*

Dette profil er opmålt i det højereliggende område ved vejen mellem V. Nebel og Ågård. I den nordvestlige del af profilet ses horisontal til subhorisontal lamination i godt sorteret fin- til mellemsand, overlejret af et linseformet legeme af siltet finsand med småskala skrålejring (fig. 4, skitse 1). Internt ses lerede lag, der draperer skrålejringen. Over det linseformede legeme ses stedvis et leret 5–15 centimeter tykt lag, med enkelte gruspartikler.

Toppen af profilet udgøres af næsten strukturløst stenet sand. Der ses dog enkelte skrålejrede sæt. Dette øvre lag har tilsyneladende en ret stor lateral udbredelse i nordvestlig retning, hvor der i den underlejrede sekvens ses storskala planar- og trug-skrålejring mellemlagt af finkornede bænke. Der er målt strømretninger mod NV og SV (se skitse 1, vedlagt).

Profilet ændrer gradvis karakter mod sydøst, idet et gråbrunt, leret, gytjeholdigt lag kiler sig ind ved omkring 11830 m (skitse 1). Længere mod sydøst udgør dette lag, her opspaltet i to horisonter med organisk indhold adskilt af et sandet lag, undergrænsen for en enhed med rytmisk lagdeling. Sandede strukturløse lag på omkring 5–10 centimeters tykkelse skifter med mere siltede-lerede lag på omkring 2–5 centimeters tykkelse. De ofte normalgraderede, sandede lag dominerer sekvensen.

En pollenanalyse af det øvre organiske lag, udført af Else Kolstrup, gav

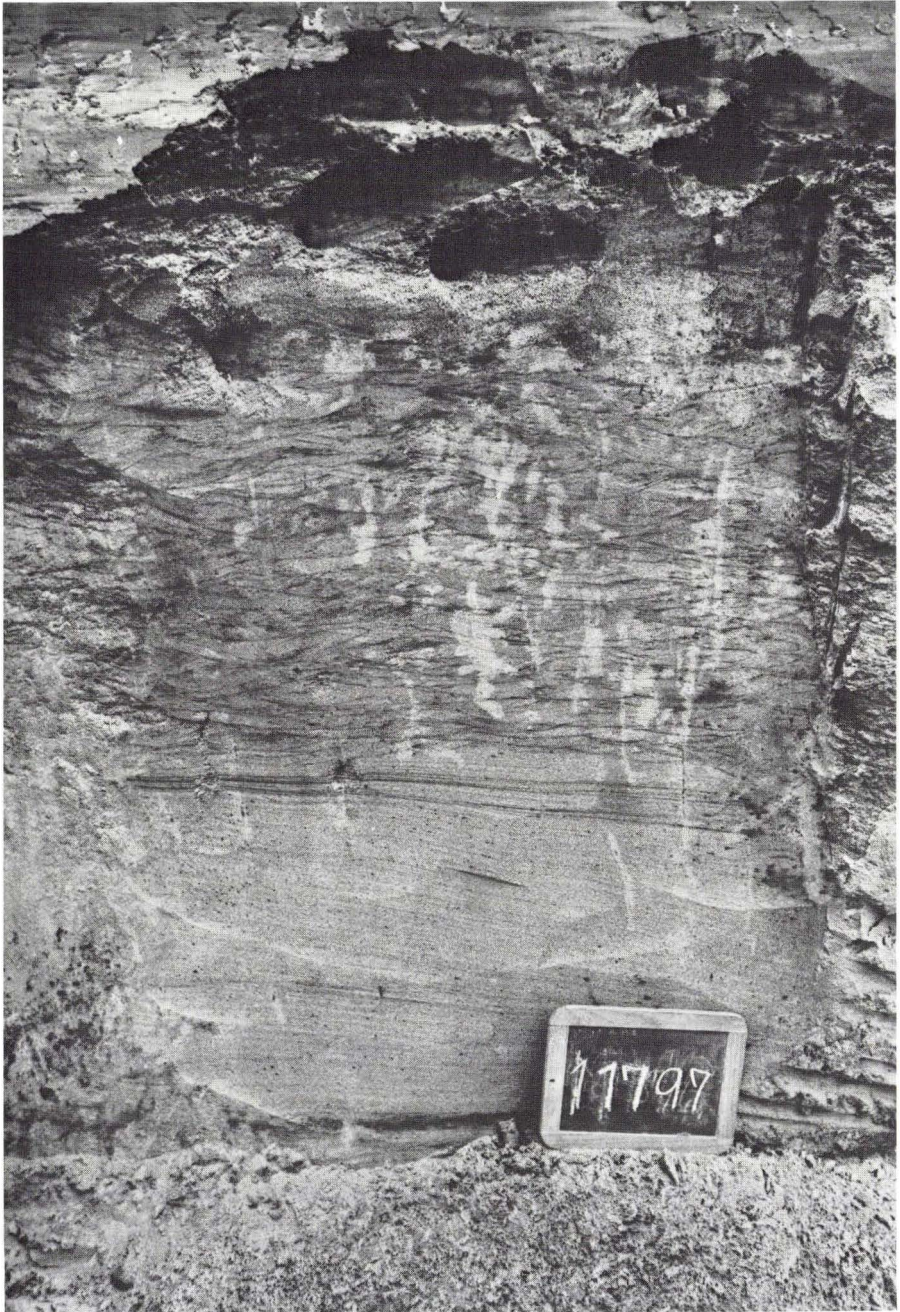


Fig. 4. Profilet ved 11797 m. To facies er repræsenteret, nederst horisontal til subhorisontal lamination, øverst småskala skrånlejrning. Se også skitse 1.



høje procenter af græsser og halvgræsser og lave procenter af fyr, birk og pil.

Den nordlige del af dette profil antages at repræsentere en pointbar sekvens, i dette tilfælde opbygget ved lateral tilvækst, hvor sedimenterne hovedsagelig aflejres ved aftagende vandføring (se fx. Reineck & Singh, 1975: Allen, 1964, fig. 10). Profilet ses således at være et "finning-up" profil, hvor toppen udgøres af det lerede lag, der kan opfattes som en leve- eller "swale" dannelse (Allen, 1964). Ifølge Reineck & Singh (1975) er en pointbar sekvens generelt opbygget af linseformede legemer, der internt viser følgende opbygning: (fra bunden) storskala trug-skrålejring – horisontal lamination – småskala skrålejring – og i toppen lerede aflejringer. "Finning-up" tendensen i det her omtalte profil understreges således dels texturelt og strukturelt, men også et set i relation til flow-regime. Den horisontale lamination i bunden er antagelig aflejret under øvre flow-regime betingelser i de dybere dele af kanalen, mens småskala skrålejringen er aflejret under nedre flow-regime betingelser i roligere vand længere oppe ad den hældende aflejringsflade (se Southard, 1975).

De synsedimentære forkastninger tyder på at sedimenterne har været understøttet på aflejringsstidspunktet.

Den rytmiske lagdeling med fine kornstørrelser, i den østlige del af profilet, peger på et roligt lav-energi aflejringsmiljø (submiljø). Sedimenterne er antagelig aflejret fra pulserende sedimentmættede smeltevandsstrømme.

Da profilet ikke viser tegn på isoverskridelse, antages det at denne sekvens hører hjemme i sen Mellem Weichsel eller Sen Weichsel.

#### *Profilet ved 12461 m – 12655 m*

Omkring 1 kilometer øst for vejen mellem V. Nebel og Ågård bliver terrænet kuperet og når op i 47–49 m.o.h. Her skifter profilet karakter til relativ grove sandede, grusede sedimenter med storskala primære sedimentære strukturer. I tilknytning til opmåling langs udgravningen er der foretaget observationer i en grusgrav ved Jagdsminde (skitse 2). Endvidere er der foretaget opmåling i udgravningen ved 13969 m, umiddelbart øst for Skærso. (Der var på dette tidspunkt ikke foretaget udgravning på tværs af Almind Å).

I profilet er registreret fire dominerende sedimentære facies. 1) Storskala trug-skrålejring, bestående af overvejende stenet, ofte dårligt sorteret, fint til groft sand, med stor lateral udbredelse (fig. 5, 6). Lerklater i forsættene ses hyppigt. Strukturerne antages at hidrøre fra migration af linguoide mega-ribber, migrerende ved nedre flow-regime betingelser (se Southard, 1975). Migrationen er antagelig foregået i større kanaler der efterhånden er blevet udfyldt (Cant & Walker, 1978). Et eksempel på en sådan udfyldning ses ved 12503 m, skitse 2. I andre tilfælde er der påbegyndt en ny større kanal



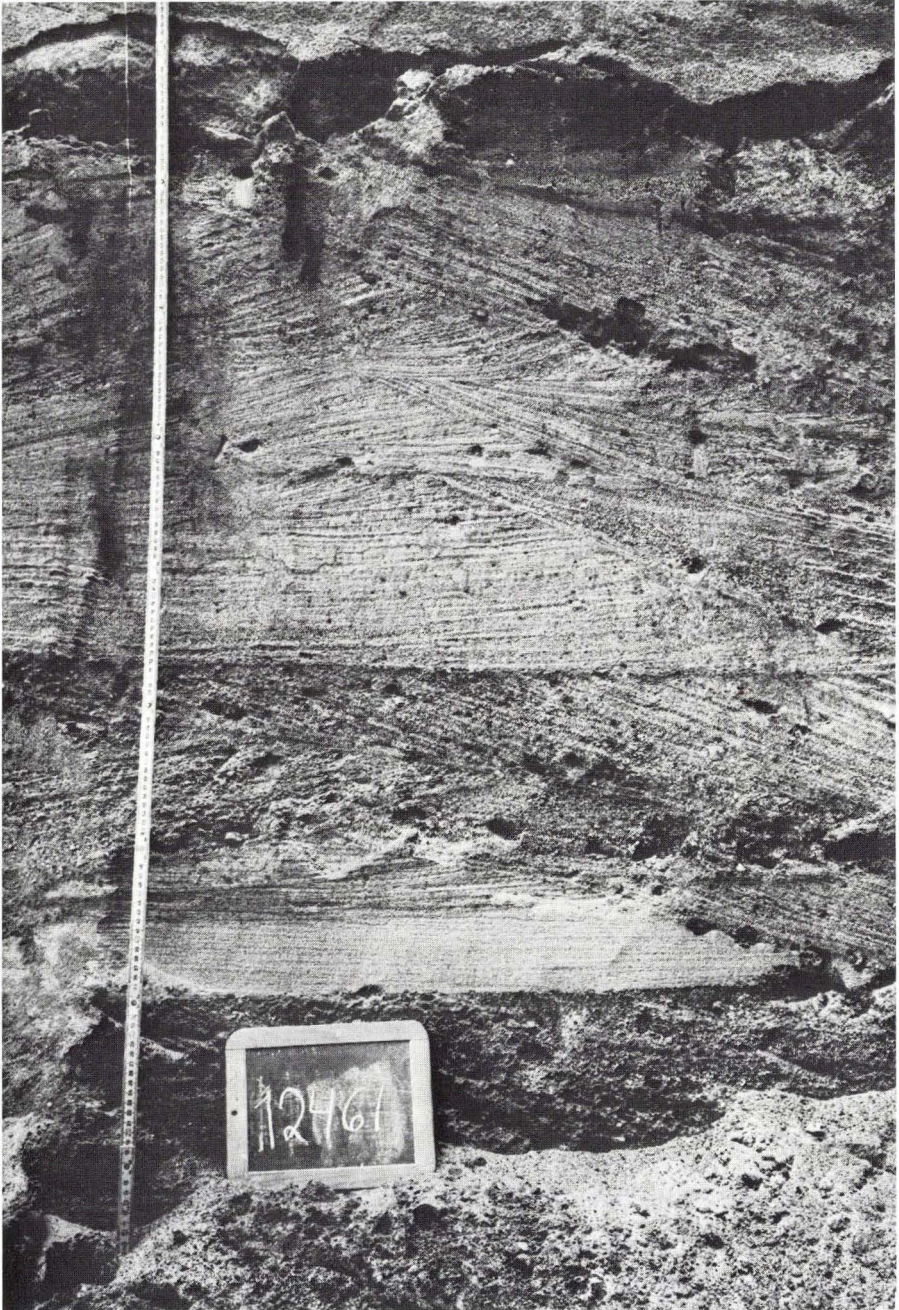


Fig. 5. Profilet ved 12461 m. Storskala trugskrålejringer dominerer, med underordnede lag med horisontal lamination. Se også skitse 2.





Fig. 6. Profilet ved 12563 m. Storskala trug skrålejring. Den øverste del af billedet viser meget stor skala trugskrålejring med interne underordnede skrålejringer (lige over midten).

umiddelbart over den netop udfyldte (se 12461 m, 12563 m, 12655 m, skitse 2 samt fig. 5,6). 2) Scour udfyldninger eller kanaludfyldninger. Disse forekommer enkeltvis i mellem- til grovkornet sand, ofte med en gruset, stenet, undergrænse. En sådan kanal eller scour forekommer ved 12638 m, skitse 2. 3) Horisontal til subhorisontal lamination i fin- til grovkornet sand med enkelte klaster. Denne facies har stor lateral udbredelse (skitse 2) og antages at være dannet ved øvre flow-regime betingelser dels i kanaler, dels ved vertikal tilvækst af "sand flats" (Cant & Walker, 1978). Den nedre del af profilerne ved 12461 m og 12655 m fortolkes således som "sand flat" sekvenser, der senere er blevet gennembrudt af nye kanaler. 4) Småskala skråløjring i leret, siltet, finsand; forekommer i tynde linseformede lag, men er sjældne. Strømdata for storskala strukturer er angivet på fig. 1. I skrænter er der ofte observeret små normalforkastninger.

Den relativ grove kornstørrelse, den ret dårlige sortering, kombinationen af facies med dominans af stor skala trug skråløjring, og deres indbyrdes forhold, med hyppige erosive grænser, synes at pege på et braideret flodsystem som det overordnede aflejringsmiljø (se fx. Miall, 1977). Ifølge Miall's lithofacies typer for braidrede strømme svarer de her beskrevne profiler til "Donjek-typen". Længere opstrøms, mod øst i Almind Å-dalen, findes grusgrave, der indeholder meget grovere sedimentter og viser profiler der nærmest svarer til "Scott typen" i Miall's klassifikation. De her opmålte profiler må således antages at svare til de centrale dele af et større hedeslettekompleks. Strømretningsdata opmålt i en grusgrav nær Bølling (fig. 1), tyder også på en sammenhæng mellem sedimentterne omkring V. Nebel-Dons og de sandede, grusede strøg op gennem dalen til Bølling (se Milthers, 1948).

## Model for området

På grundlag af de indsamlede data, og landskabets udformning, foreslås en tentativ model for området (fig. 7):

1) Området omkring V. Nebel mod slutningen af istiden, med fordeling af gletcheris og fluvioglaciale sedimentter. Udbredelsen af sedimentterne er taget fra Nordmann (1958). Det antages, ud fra de målte strømretninger og kornstørrelse data, at sedimentterne for en stor del er tilført gennem det der i dag fremstår som Almind Å-dal. Herefter deler strømmen sig i en nordvestlig strøm der antagelig fortsætter til Bølling, og en sydvestlig strøm der formodes at fortsætte til egnen omkring Vamdrup og Skodborg, sydvest for Kolding.

Sedimentterne er antagelig strømmet ud over et dødisområde, hvor fordybninger i isen er blevet udfyldt, på samme måde som Milthers (1925) foreslog



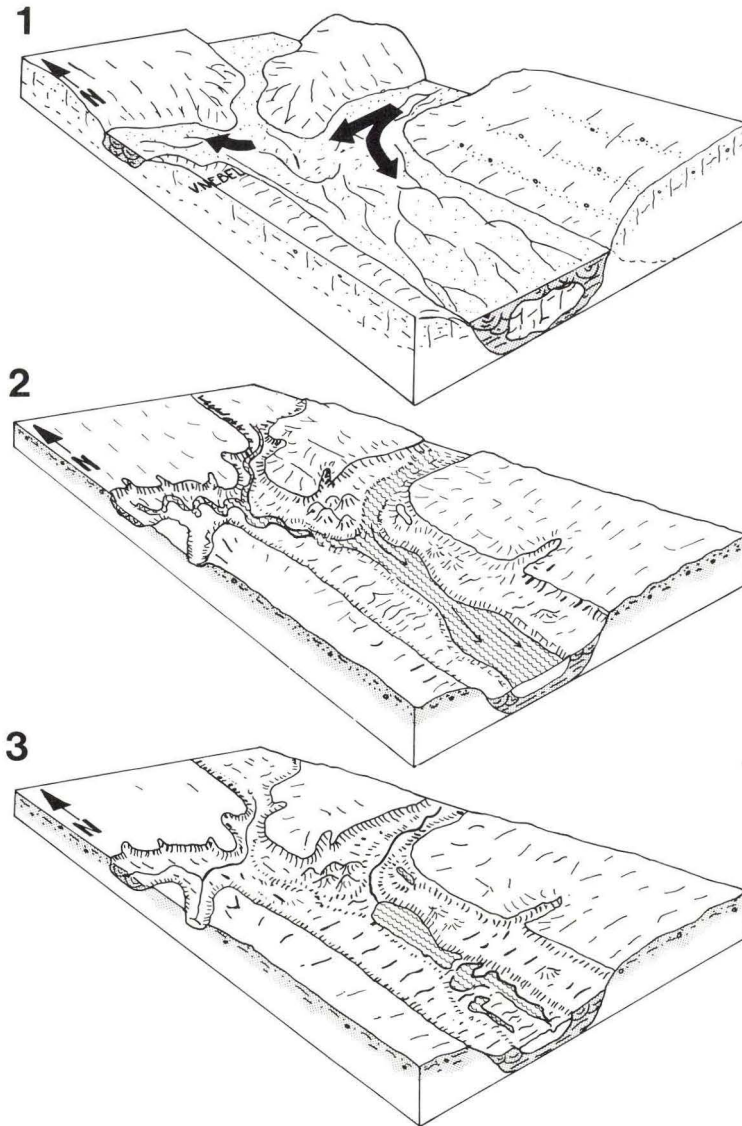


Fig. 7. Model for områdets opbygning fra sidste istid. Se teksten.

det for området vest herfor, nærmere betegnet Knudsbøl Plantage. Det kan ikke udelukkes at gletcheris er stagneret netop her på grund af en markant fordybning i prækvartæret (se også Nordmann, 1958).

2) Isen er smeltet bort. Fra Almind Å-dal og sydover strækker sig et bredt

flodløb, hvis eksistens godtgøres af de skrænter der endnu står tilbage (fig. 1). Nord for V. Nebel snor sig en meanderende strøm, der er repræsenteret i profilerne ved pointbar sekvenser.

Området nord for Nørresø ses at være småbakket på grund af at sedimenterne oprindeligt blev aflejret udover, og i, hulninger i isen.

3) Nutiden. Det brede flodløb er blevet til Nørresø (og Søndersø) som et resultat af indsynkning på grund af smeltning af begravet is. V. Nebel Å løber vest om V. Nebel, og i lave områder er der opstået moser.

Det skal bemærkes, at modellen er hypotetisk. Således er det reelt kun de øverste jordlag i området der er kendt (bortset fra profilerne) idet området er ret tyndt besat med dybere borer.

*Tak.* Denne artikel er udarbejdet ud fra en lille del af det store datamateriale der i disse år bliver indsamlet langs naturgasledningen. Der rettes derfor en tak til D.O.N.G. A/S for muligheden for at foretage disse opmålinger.

Bent K. Hansen takkes for godt samarbejde i felten, og Peter B. Konradi og Ib Marcussen takkes for diskussioner omkring landskabets dannelse og kritisk gennemlæsning af manuskriptet. Else Kolstrup takkes for at udføre pollenanalyse, og gennemlæsning af manuskriptet.

Tegnarbejdet er for en stor del udført af elev Jannie Knudsen og tegner Danuta Kestenbaum, som takkes herfor. Sidst, men ikke mindst, takkes Irma og Carlos Torres for at udføre fotografisk arbejde, og Karen Jensen og Lone Andreasen for renskrift af manuskriptet.

## Litteratur

- Allen, J. R. L., 1964: Studies in fluvial sedimentation: Six cyclothems from the lower Old Red Sandstone, Anglo-Welsh Basin. *Sedimentology*, 3: 163–198.
- Cant, D. J. & Walker, R. G., 1978: Fluvial processes and facies sequences in the sandy braided South Saskatchewan River, Canada. *Sedimentology*, 5: 625–648.
- Miall, A. D., 1977: A review of the braided-river depositional environment. *Earth sci.rev.*, 13: 1–62.
- Milthers, V., 1925: Kortbladet Bække. Résumé en français. *Danm. Geol. Unders. I rk.*, 15: 1–175.
- Milthers, V., 1948: Det danske Istidslandskabs terrænformer og deres opståen. *Danm. Geol. Unders. III rk.*, 28: 1–233.
- Nordmann, V., 1958: Kortbladet Fredericia. *Danm. Geol. Unders. I Rk.*, 22-A: 1–125.
- Puigdefabregas, C., 1973: Miocene point-bar deposits in the Ebro Basin, northern Spain. *Sedimentology*, vol. 20: 133–144.
- Reineck, H. E. & Singh, I. B., 1975: Depositional sedimentary environments, with reference to terrigenous clastics. Springer Verlag, Berlin, Heidelberg, New York 1975: 1–439.
- Southard, J. B., 1975: Bed configuration, I “Depositional environments as interpreted from primary sedimentary structures and stratification sequences”. S.E.P.M. short course no. 2. Dallas 1975.

# Mapping the vulnerability of ground water reservoirs with regard to surface pollution

Arne Villumsen, Ole Stig Jacobsen, and Carsten Sønderskov

Villumsen, A., Jacobsen, O. S., and Sønderskov, C.: Mapping the Vulnerability of Ground Water Reservoirs with regard to Surface Pollution. *Danm. Geol. Unders., Årbog 1982*: 17–38, 2 pls., København, 1983.

Data for geology, hydrogeology, and ground water chemistry have been used to evolve a preliminary ground water vulnerability map. By this type of map the possibility of ground water pollution can be predicted. The map may be of use in the land use planning and water planning.

As a test area in the ground water vulnerability project the 1120 km<sup>2</sup> large peninsula Djursland, in Jutland, Denmark, has been selected because of its geological, hydrogeological and chemical conditions which are representative for large areas in Denmark as well as in other countries.

By use of the geological basic data maps of Djursland a determination of the aquifer distribution, the piezometric head of each aquifer, and the inter-aquifer-flow relationships has been made.

EDP has been used to calculate and present the basic parameters necessary for the estimate of the vulnerability. The basic parameters include the following:

- total thickness of the geological deposits above the aquifers
- permeability of the deposits above the aquifers
- piezometric head
- hydraulic percolation time through the geological deposits above the aquifers
- reduction capacity and sorption capacity of layers above the aquifers.

The above-mentioned factors are combined and depicted in a ground water vulnerability map, which is preliminary verified by comparison with ground water chemistry maps, indicating the actual ground water quality.

The work has been supported financially by the EEC.

*A. Villumsen, O. S. Jacobsen, and C. Sønderskov, Geological Survey of Denmark, 31 Thoravej, DK-2400 Copenhagen NV, Denmark.*

The major part of the Danish population relies on ground water for drinking water supplies. Less than 5% of the total water consumption is supplied from surface waters.

Compared to surface water supplies, the ground water supply is naturally protected against microbiological and chemical contamination. This has long been considered a persistent phenomenon. However, during the last decades



there have been several major incidents of ground water contamination from sources such as chemical disposals, landfills, agricultural land use, and use of fertilizers.

As a result of a systematic hydrogeological mapping in accordance with the Danish Water Supply Act (1973; Amended by the Act 1978), the knowledge of the possibility of contaminating ground water has increased. At present, maps showing geology, hydrogeology, and ground water chemistry (the so-called hydrogeological map series, Miljøstyrelsen 1979) have been produced for most parts of Denmark. The maps – and the corresponding data files – are used a.o. in the water supply planning and the land use planning.

The situation at present is, that shallow aquifers, often, and deeper situated ground water, occasionally, contain nitrate, which may indicate pollution. Regional as well as local differences in e.g. geology, and pollution intensity are decisive for the particular situation.

In order to predict the possibility of ground water contamination it is necessary to use the basic information of the geological and hydrogeological conditions in different areas.

The objective of the research is to develop a method (tool) by which it is possible to predict the risk of ground water pollution caused by substances induced to the surface.

## The ground water vulnerability concept

The ground water vulnerability is defined as the risk of chemical substances – used or disposed on or near the ground surface – to influence ground water quality.

Ground water vulnerability depends on a series of parameters, dynamic as well as static.

Some of the important parameters are:

- the thickness, the lithology, the permeability, and the water content of geological deposits above the aquifer
- the type of polluting compounds
- the ability of the deposits above the aquifer to neutralize, retain, or delay the actual polluting compounds
- the hydraulic conditions
- the pollution intensity in the aquifer
- the exploitation of the aquifers

The present project concerns only the *static* parameters disregarding the *dynamic* and historical events in the studied area. The static parameters include informations about geology, hydrogeology, and hydrochemistry.

The chemical composition of the ground water may be used as an indicator of the vulnerability, which can be estimated based on geological and hydrogeological data.

Chemical elements and compounds which may indicate a hydraulic contact with the surface are a.o.: nitrate ( $\text{NO}_3$ ), sulphate ( $\text{SO}_4$ ), and in many cases excessive carbon dioxide. Besides, water-rock interactions in the unsaturated zone and in the aquifers can be judged by the hydrochemical data.

In the vulnerability project the hydrogeological map series and the corresponding data files are used as much as possible to secure that the vulnerability maps at a later stage can be produced with a minimum of resources.

In the research programme preliminary vulnerability maps have been produced. In addition, the work has given valuable information of the basic lack of knowledge in the understanding of the transport and conversion of contaminants from the introduction at the ground surface to the appearance in the aquifer. This evaluation of the state of art in ground water protection is of great importance for reinforced research in this particular interdisciplinary science.

## Previous investigations

Two main types of ground water vulnerability concepts have earlier been treated in the literature. The first type of concept bases the vulnerability statements on geological (lithological) information only, while the second type of concept bases the vulnerability statements on a combination of geological, hydrogeological and hydrochemical information. Examples of geological vulnerability are expressed in the maps produced by BRGM (e.g. BRGM, 1975) and maps described by Becker-Platen et al. (1979). LeGrand (1964) described the different factors influencing the vulnerability and called attention to the importance of geology, hydrogeology, and hydrochemistry in the estimate of vulnerability. LeGrand's approach is close to the proposal in the present project concerning vulnerability mapping. However, LeGrand did not use his idea for map preparation.

## Test area

The peninsula, Djursland, fig. 1, has been selected as test area for the inves-



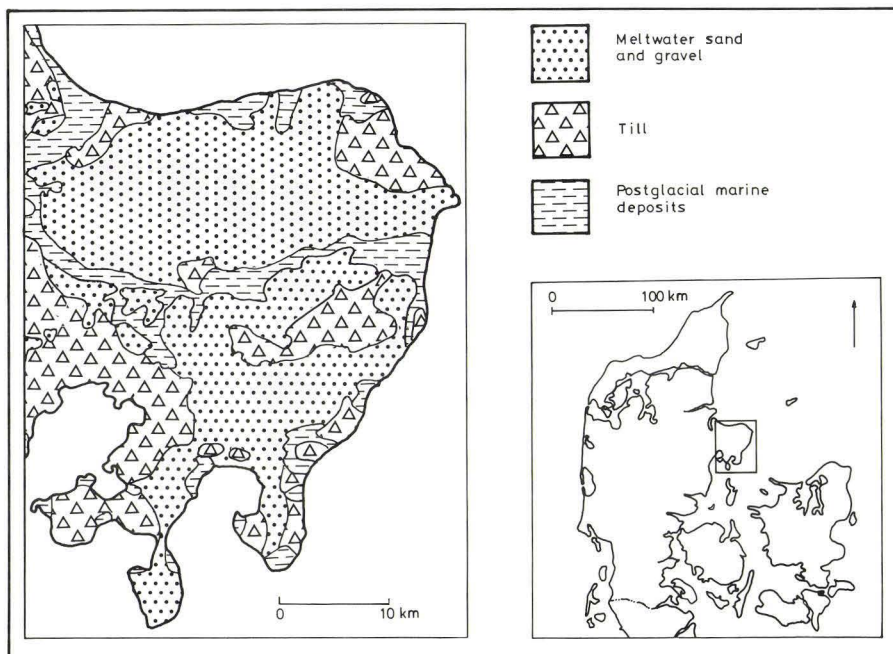


Fig. 1. Location and Quaternary geology of the test area, Djursland (simplified after Bornebusch and Milthers (1935) and Milthers (1948)).

tigations, partly due to the significant variety in the geological conditions and the related hydrogeological properties in the area, partly because indications of nitrate pollution in the area have been demonstrated through a recent ground water quality mapping (Villumsen and Kristiansen, 1979).

Finally it should be mentioned that Århus amtskommune has expressed an interest in getting an estimate of the vulnerability of the aquifers in areas, for which waste water infiltration is under consideration.

### Geology of the test area

The geological conditions in the test area have been described by a.o.: Harder (1908), Grönwall and Harder (1907), Jessen (1920), Milthers (1919) and (1932), Ødum (1926), Gry (1935) and Rasmussen (1977).

The *pre-Quaternary* rocks in Djursland consist in the northern part of the area of Danian limestone. In the southern part of Djursland the Danian limestone is overlaid by Paleocene and Eocene clay and marl deposits.

*Quaternary* deposits are present almost everywhere in the test area, (Fig. 1). These deposits are mostly till, meltwater sand and gravel. Pre-Quaternary

deposits are, moreover, present as floes in the till, especially in the southern part of Djursland. The thickness of the Quaternary deposits exceeds 100 m in several areas. In the north-eastern part of the test area the Quaternary deposits are very thin and in places only consisting of a thin layer of soil.

Postglacial marine deposits are present in a central narrow zone stretching from east to west, and in several but often small areas near to the coast. Fresh water deposits (peat and gyttja) are scattered all over Djursland.

In Djursland four categories of aquifers are identified. The main aquifer is the Danian limestone. Additionally a lower glacial and an upper glacial (Quaternary) aquifer consisting of sandy meltwater deposits are present. Of minor importance is the Postglacial sand aquifer of marine origin, Fig. 1 and 2.

### Data available from the area

The basic data for this research consists mainly of ground water well records, which contain information of the lithology and the technical installation of the wells. Besides, chemical analyses of ground water in the area have been used.

The data was available in computer files at the Survey and at Århus amtskommune. Århus amtskommune has kindly placed its geological database (Thomsen, 1980) to the disposal of the Survey for the vulnerability project.

The test area contained a total of 1360 well records, at the start of the project. After an inspection in order to confirm data reliability and after an updating this number was reduced to about 1000. These well records were filed in two versions, one in an IBM 3033 at the NEUCC-center and another in an UNIVAC 1100/82 at the RECKU-center.

The files stored in the UNIVAC-version have been used for the production of the geological basic data maps (cyclogram-well-record-map, as described by Andersen (1973)).

These maps contain information of the interpretation of the geological profiles, represented by different colours, well dimensions, position of water level, position of screened intervals, specific yield etc.

### Method of vulnerability mapping

During the research a number of thematic maps have been produced in order to visualize the different steps of the production process of the vulnerability maps. The thematic maps are described in the following chapters.

According to themes as



- aquifer distribution
- piezometric head
- inter-aquifer flow

the interpretation from point information to a 3-D geometric model has been carried out *manually*. Border lines for the aquifer distribution, iso-lines for piezometric head and limitation of the inter-aquifer flow areas have been drawn manually on pre-drawn computer maps. All other thematic maps have been calculated on a *computer*, using the same basic matrix programme and the same graphics (Appendix 1).

The following parameters were mapped by the computer:

- piezometric head
  - layer-thickness of sediments above the aquifers (isopach maps)
  - permeability index
  - interflow index
  - hydraulic percolation time
  - reduction capacity
  - sorption capacity
  - vulnerability index
- } chemical reaction index

### Information density

Only 528 well records from the test area contained information usable for the computer calculations of the thematic maps. These well records were extracted for information of aquifer category (categories), vertical aquifer limitations, piezometric head, and of any vertical continuities between different aquifers.

The interpreted material was filed in a special software at the NEUCC computer center and combined with files of topography, lithology, geographical location, and different auxiliary table functions.

Table 1 shows the information density of the four aquifer categories in the area.

One of the main thresholds, which would prevent a total use of computer manipulation of geological informations is the interpretation of one-dimensional information to three-dimensional models. The general problem is that the density of the geological information often is very low compared to the presumed discontinuities in the lithological elements, vertical as well as horizontal. This was the situation in the test area.

However, in order to evolve the computer drawn maps it was necessary to assume continuity between neighbouring data points. The lack of data may result in a diminished disintegration due to the density of information, which

Aquifer category	Number of wells	Total size of aquifers km <sup>2</sup>	Number of separate aquifers	Wells pr. km <sup>2</sup>
Postglacial	40	90	4	0.44
Upper glacial	314	680	3	0.46
Lower glacial	90	390	5	0.23
Danian	249	890	1	0.28
Total	528	1120	–	0.47

Table 1.

varies between 0.2 and 0.5 km<sup>-2</sup> for the four different categories of aquifers (Table 1).

### Aquifer distribution map

Using the geological basic data maps of Djursland, and a newly constructed map of the Danian surface, an aquifer distribution map, Fig. 2, was produced manually.

The map has been constructed by a geological interpretation of the presence and spatial extension of actually observed aquifers. In this way the well records have been correlated and four different aquifers in the horizontal as well as the vertical direction could be distinguished. The four different aquifers can be categorized as follows:

- a) Postglacial aquifer
- b) Upper glacial aquifer
- c) Lower glacial aquifer
- d) Danian aquifer

In some areas it has not been possible to define an aquifer. Either because of the geological conditions being too complicated, and/or the density of information being too poor.

### Piezometric head map

Because of lack of data it has not been possible to produce a map of the piezometric head for each category of aquifer (mentioned above).

However, based on information from the geological basic data maps and the aquifer distribution map, two maps showing the piezometric head have been produced (manually). One map represents the piezometric head of the



AQUIFER DISTRIBUTION

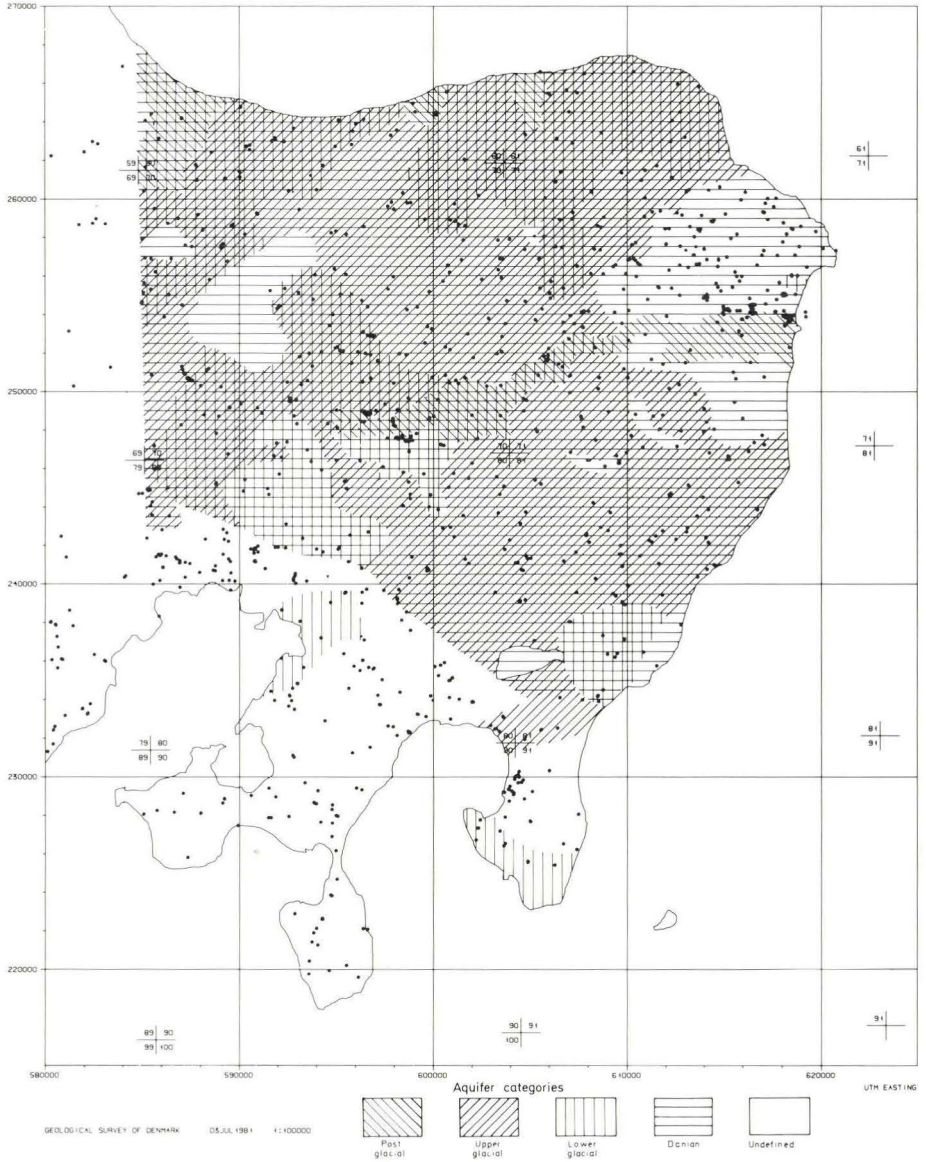


Fig. 2. Aquifer distribution showing the horizontal distribution of the different aquifer categories observed in the area. Black dots indicate location of wells.

INTER-AQUIFER FLOW MAP

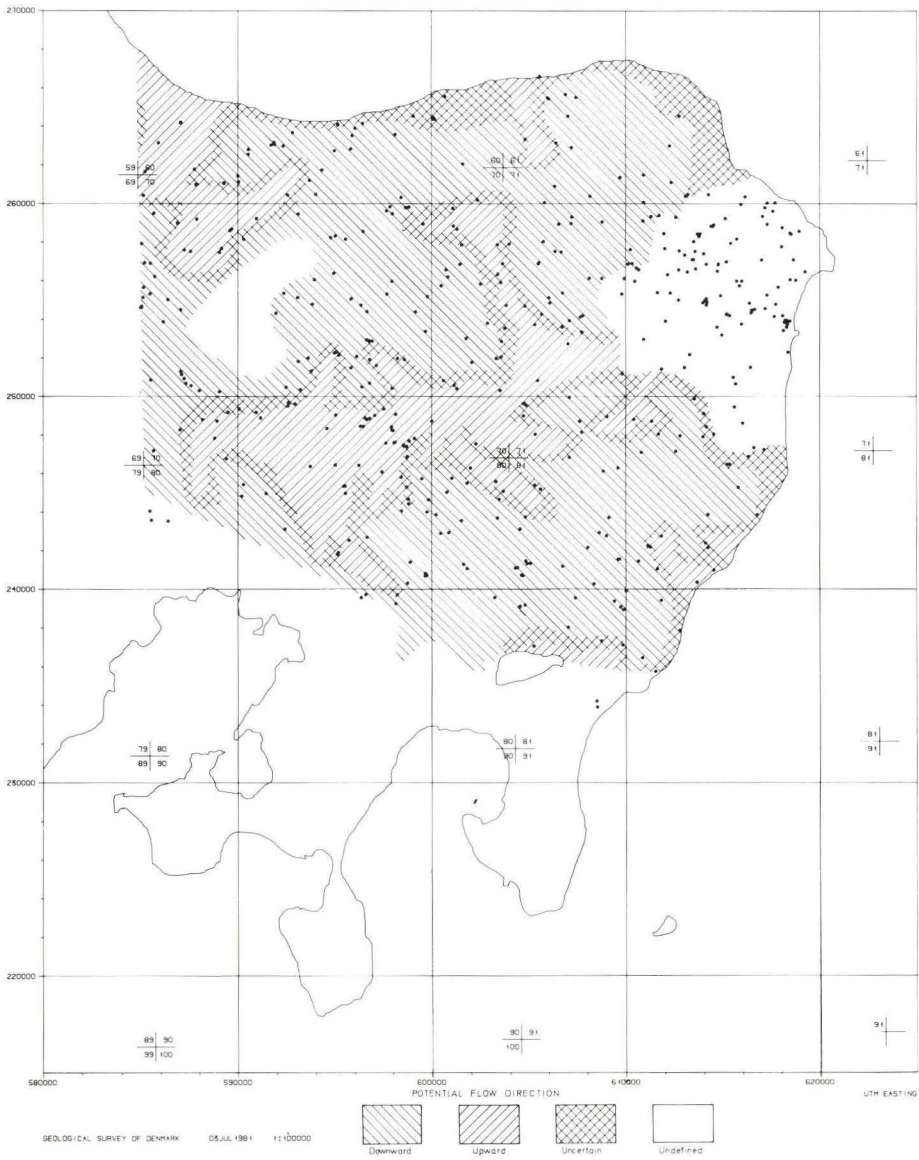


Fig. 3. Potential inter-aquifer flow direction between the glacial and the Danian aquifers according to the difference in piezometric heads. Black dots indicate location of wells.



Danian aquifer, and the other map represents the piezometric head of the main glacial (Quaternary) aquifer.

The main glacial aquifer consists predominantly of the upper glacial aquifer.

### Inter-aquifer-flow map

An inter-aquifer-flow map has been constructed for the two main aquifers in the Djursland area. The two main aquifers consist of the Danian aquifer and the main glacial aquifer (either the lower glacial aquifer or the upper glacial aquifer).

By use of the above-mentioned piezometric head maps and the geological basic data map it has been possible to construct a map which shows the potential flow direction between the two main aquifers.

The map depicts four different types of areas

- a) Areas with a potential downward flow direction
- b) Areas with a potential upward flow direction
- c) Areas with an uncertain flow direction
- d) Areas with an undefined flow direction

The information of this map is valuable as a supplement to the vulnerability map because it may be possible by means of this to predict whether a contaminant in one aquifer may be transferred to another aquifer, Fig. 3.

### Estimating subsurface water transfer ability (ART)

Infiltration to the uppermost aquifer depends on the hydraulic condition in the unsaturated zone and the piezometric head of the aquifer. Infiltration to an aquifer, which is not the uppermost, depends on the piezometric head difference between which the water transfer takes place.

In case of potential negative difference no transfer of water will take place. If the gradient is positive e.g. higher piezometric head in the upper aquifer than in the lower, a transfer is possible.

As mentioned above information on the different aquifers may not be suitable in any case to calculate the transfer possibility. Consequently an approximate calculation has been made in order to estimate the possibility of entrance in an aquifer as the difference (ART) between aquifer top and piezometric level.

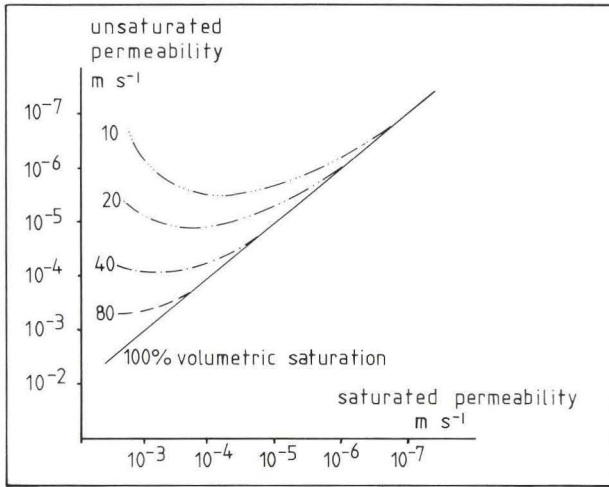


Fig. 4. The relationship between saturated and unsaturated permeability in homogeneous sediments.

### Isopach maps

The total thickness of geological deposits above the aquifer is of great importance to the prevention of contamination of the aquifer.

Consequently, maps showing the total thickness of the covering layers above the aquifers have been constructed. As this thickness may vary in accordance with the surface contours a correction according to this has been calculated, by use of the surface contour matrix, see Appendix 1.

### Permeability index maps

In order to evaluate the overall resistance against recharge of the different aquifers, calculations of a permeability index have been carried out.

Each lithological type, e.g. meltwater sand, till, limestone, etc. has been given a specific permeability ( $k_p$ ). Approximate average of measured values given in the literature, e.g. Todd (1959) is used. As reliable values of unsaturated permeability coefficients are not available a consequent use of saturated values has been decided although this may induce a general higher level of permeability coefficients, Fig. 4. The permeability index is a relative value indicating the total hydraulic resistance from soil surface to the aquifers given by

$$P_i = \sum_{j=1}^n Z_j / k p_j,$$

where  $n$  is the number of layers between aquifer and soil surface,  $Z_j$  is the thickness in metres of layer  $j$ , and  $k p_j$  is the permeability coefficient (m/sec.) of layer  $j$ .

### Interflow index map

As an estimate of the possibility of a non-vertical water movement during infiltration an interflow index has been calculated. The assumption is that the ability of horizontal water movement in the layers above the aquifer depends on changes in permeability. Water flow through a porous medium with high permeability reaching a medium with low permeability tends to change flow velocity and direction.

On the other hand, the opposite situation may not induce a radical change in flow direction, assuming that the layers have field capacity of water saturation.

This implies that a decrease (negative change) in permeability will increase the possibility of interflow and discharge. Therefore an interflow index has been calculated for each well and aquifer given by

$$I = \sum_{j=1}^n | \log_{10} k p_j - \log_{10} k p_{j+1} |, \text{ if } k p_j \geq k p_{j+1},$$

where  $k p_j$  is the permeability coefficient of layer No.  $j$ .

### Hydraulic percolation-time map

In order to estimate the travel time of water recharging an aquifer from the ground surface, a hydraulic percolation-time map has been constructed, plate 1.

The calculations are carried out assuming that the flow occurs under unsaturated conditions, no interflow is present, and that the recharge is  $0.2 \text{ m y}^{-1}$ . The flow is thus assumed to be a piston flow. Consequently, the calculated travel time will be estimated as the lowest obtainable one. Each lithological element has been given a specific retention capacity (SRC) % as the difference between the porosity and the specific yields, Fig. 5. Hence, the hydraulic retention time (RT), which is shown on plate 1, is then calculated by integration over the layers above the aquifers, writing

$$RT = \sum_{j=1}^n \int_0^{z_j} (SRC_j / 0.2) dz,$$



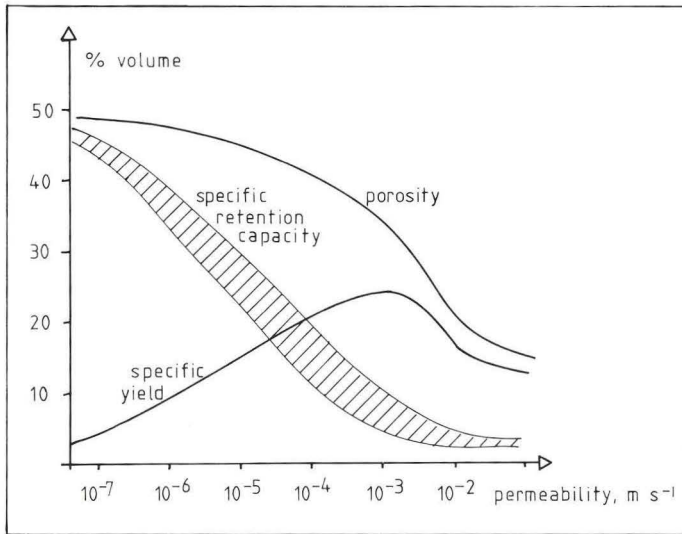


Fig. 5. Approximate volumetric porosity, specific retention and specific yield at 1 bar as a function of permeability in homogeneous sediments. (After Todd, 1959).

where  $z_j$  is the thickness of layer  $j$  (m) and  $n$  is the number of layers.

The dimension is thus years, and the hydraulic percolation-time map illustrates how fast a conservative contaminant will reach the aquifer after introduction at the ground surface.

### Chemical reaction map

The ability of the layers above an aquifer to retain reactive chemical contaminants may in many cases be one of the most dominating mechanisms to avoid pollution of the aquifer. In accordance with this two types of chemical reaction maps have been developed, showing the chemical and hydraulic resistance against percolating solutions.

As the number of chemical reactions which can take place in the subsoils is so large, some main processes must be chosen to give a rough estimate of the chemical resistance. In the present study only two main processes have been taken into consideration, namely processes depending on the reduction capacity and processes depending on the sorption capacity.

Each lithological element has been given relative values of reduction capacity and sorption capacity. It is assumed that the ability of reactions is proportional to the hydraulic retention time in each lithological element. The chemical reaction index is then given by

$$SA = \sum_{j=1}^n RT_j * CEC_j$$

and

$$RA = \sum_{j=1}^n RT_j * ROX_j,$$

where SA is the relative sorption ability,  
RA is the relative reduction ability  
RT<sub>j</sub> is the hydraulic retention time in layer j,  
CEC<sub>j</sub> is the relative sorption capacity in layer j, and  
ROX<sub>j</sub> is the relative reduction capacity in layer j.

## Vulnerability maps

The possibility of contaminating an aquifer with chemical compounds used or deposited on the ground surface depends on several physico-chemical conditions of the layers above the aquifers.

In addition to these more static properties, many more dynamic factors have to be taken into account in the prediction of the risk of contamination.

During the calculation several static parameters have been included:

- the thickness of layers above the aquifers
- permeability and specific retention capacity
- reduction capacity
- sorption capacity
- infiltration flow velocity
- aquifer category and piezometric head
- interflow

Although many parameters have been combined during calculation of the thematic maps, only four themes were used for calculation of the vulnerability index, namely

- 1) the water transfer ability, ART.
- 2) the interflow index, I.
- 3) the reduction ability, RA.
- 4) the sorption ability, SA.

The interflow index, the sorption ability, and the reduction ability are converted to values from 0 to 4 by proportional reduction.

The piezometric head parameter (ART) has been converted as follows:

0–5 metres difference corresponds to  $ART' = 3.5$

5–15 metres difference corresponds to  $ART' = 2.5$

15–30 metres difference corresponds to  $ART' = 1.5$

>30 metres difference corresponds to  $ART' = 0.5$

Values of the four thematic parameters were equally weighted according to their significance to the vulnerability.

The vulnerability index is then calculated as a mean value of the four parameters,

$$VUL = MEAN (ART', SA', RA', I').$$

where the apostrophe denotes the converted parameters.

The vulnerability index has subsequently been corrected to surface contours, and the three vulnerability maps have been produced by use of an element size of the matrix of  $(0.5 \times 0.5)$  km<sup>2</sup>, plate 2. A vulnerability map of the Postglacial aquifer has not been calculated as the data of thematic parameters were too scattered.

Appendix 2 contains an example of the calculation of the vulnerability for a ground water well in the test area.

## Verification of the vulnerability maps

Chemical analyses of the ground water can be used for a preliminary verification of the vulnerability estimate (page 19). In the hydrochemical basic data map, which is included in the hydrogeological map series (Miljøstyrelsen, 1979), the water analyses are not related to the different aquifers found in the mapped area. Therefore these maps are not directly suitable for the verification as the vulnerability estimate is aquifer-related.

## Aquifer-related hydrochemical basis-data maps

A total of 250 chemical analyses of ground water were available from the four aquifers in the Djursland area. New aquifer-relevant hydrochemical basic-data maps were drawn on these analyses and compared with the vul-



nerability maps. Due to inadequate data only about 1/3 of the total analyses could be used for this preliminary verification.

### Comparison of the predicted vulnerability and the ground water chemistry

As already pointed out, the occurrence of some chemical components in the ground water may be an indication of a geologically vulnerable area. Thus, by using single chemical parameters as indicators attention has been drawn to more time-depending and dynamic factors, as for example groundwater movement, point sources and historical contaminant load.

As a preliminary test (verification) of the predicted vulnerability a comparison between the vulnerability maps and the ground water chemistry maps depicting the nitrate content has been performed. The test showed for each of the aquifers that high nitrate concentrations were only present close to predicted vulnerable areas.

On the contrary, in some areas of high vulnerability only low concentrations of nitrate were present. However, as the historical element has not been considered, this may imply that the vulnerability cannot be detected by the water quality itself.

Accordingly, a more comprehensive verification of the vulnerability maps is necessary and a detailed plan for this has been composed.

### Use of the vulnerability maps

The purpose of the present research project was to develop a method of producing ground water vulnerability maps, based on existing records and general principles.

During this research a number of different problems occurred because of the lack of knowledge of many physico-chemical and hydraulic processes which made it necessary to include several assumptions. Subsequently, some of these processes had to be estimated by relative values. Other processes were known under saturated, but not under unsaturated conditions, and hence the estimate of the processes has been given, assuming saturated conditions, and this may lead to an overestimate of the final vulnerability prediction.

As a consequence of these assumptions it is evident that the vulnerability map will depict only the general tendency of the possibility of contamination in the aquifers.

As already mentioned the information density is lower than  $0.5 \text{ km}^{-2}$ ,

implying that only diffuse permanent pollution sources can be related to the vulnerability prediction of the maps. Therefore it is recommended that these maps are used for regional planning only and with a supplement of some other information about the historical development in the contamination of the areas, information about point sources, and about the horizontal groundwater movement.

The preliminary vulnerability maps produced by the method described above may be a new and promising tool for future groundwater protection management.

The degree of details in the maps is attuned to the density of the available background information; and it serves as a general limitation that specific, detailed questions of groundwater protection cannot be solved by means of the vulnerability maps alone. The maps, however, may be a valuable tool for planning by means of which a.o. the need for further investigations in site-specific cases can be estimated.

## Further investigations

With the termination of this stage of the vulnerability project an important result has been achieved. The planning of the ground water protection is one of the main questions in Denmark at the moment. Therefore, the results of the vulnerability project have to be evaluated, critically, and the basis of the vulnerability maps has to be improved.

In phase 2 of the vulnerability project, which is financially supported by a.o. the EEC, the Survey has planned investigations for this purpose. The main elements in this study are *a verification* of the preliminary vulnerability maps and detailed hydraulic and chemical investigations of *the unsaturated zone*, i.e. the zone between the terrain and the ground water aquifer. Finally *microbiological vulnerability* studies are included together with *geological mapping*.

The verification phase is necessary to evaluate the applicability of the maps, which are produced entirely on existing data.

One of the most uncertain factors in the estimate of the vulnerability is attached to the unsaturated zone. In order to increase the reliability of the preliminary vulnerability maps it is necessary to gain access to data for bulk process kinetics and for the quantitative nitrate and sulphate reduction in the unsaturated zone in various geological deposits.

The above mentioned investigations were started in the autumn of 1982 as a co-work with the following participants:

The Geological Survey of Denmark, State Laboratory for Soil and Crop

Research, Århus amtskommune, and Institute of Hygiene, University of Århus.

## Concluding remarks

The risk of polluting compounds, used or disposed on or near the ground surface, to influence ground water quality is in the present study illustrated in preliminary ground water vulnerability maps, which have been produced for the test area, Djursland, Denmark.

By the estimate of the ground water vulnerability geological, hydrogeological, and chemical conditions have been taken into account. Verification of the vulnerability maps has been performed by use of data for the chemical compositions of ground water.

The preliminary vulnerability maps, now available, have been produced under assumptions not totally valid for water movement and chemical reactions in the unsaturated zone. This has been necessary, however, as the exact values for factors influencing the ground water vulnerability, especially in this zone, are not known at present. It should be stated, that despite this weakness, the vulnerability maps in the present version may be used for practical purposes e.g. the planning of ground water protection. Research work on a.o. chemical reactions in the unsaturated zone has recently been started at the Survey as a second phase of the ground water vulnerability project. It is expected that this work will contribute to an improvement of the basis on which the future vulnerability maps can be produced.

*Acknowledgements.* Århus amtskommune is thanked for placing its geological database to the disposal of the Survey. Per Jacobi, Lyngby, has evolved the software and performed the technical preparation of the thematic maps, produced by computer. For the permission to publish the technical description (Annex 1) and for valuable discussions we express our gratitude to Per Jacobi. The study has been supported by grants from the EEC.

## Dansk sammendrag

DGU har i efteråret 1981 afsluttet første etape af det såkaldte sårbarhedsprojekt, hvor der for et forsøgsområde (Djursland) er fremstillet sårbarhedskort, der viser risikoen for at forurenende stoffer fra jordoverfladen kan påvirke grundvandets kvalitet.

Grundvandets sårbarhed afhænger af en række faktorer, geologiske, hydrogeologiske, fysiske og kemiske – alle egenskaber ved de lagserier, der ligger over grundvandsreservoirerne.

I princippet udarbejdes der ét sårbarhedskort for hver reservoirtype. På Djursland, hvor der



findes 3 reservoirtyper, der har praktisk betydning (Danienkalk og to glaciale smeltevands-sandreservoirer) bliver der således tale om 3 sårbarhedskort.

De faktorer, der er medtaget i den nu afsluttede fase af sårbarhedsprojektet er følgende:

- den umættede zone/dæklagets tykkelse, permeabilitet og specifikke vandindhold
- bjergarternes reduktionskapacitet
- bjergarternes adsorptionskapacitet
- infiltrationshastigheden
- reservoirets type og trykforhold
- lagfølgenes permeabilitetsændring
- geografisk placering og topografi.

Disse faktorer danner grundlag for en beregning af et sårbarhedsindex, der ved hjælp af EDB udtegnes som et skraveret kort, hvor de mørkeste skraveringer viser de mest sårbare områder (plate 2). Datagrundlaget tillader ikke en detaljeret sårbarhedsvurdering inden for mindre områder. Kortene vil derfor i første omgang være et redskab i den regionale planlægning, ligesom det ved hjælp af sårbarhedskortene kan afgøres, hvor behovet er størst for supplerende undersøgelser forud for etablering af lossepladser m.v., som kunne tænkes at true grundvandet.

Ved hjælp af foreliggende kemiske analyser af grundvandet er der foretaget en foreløbig verifikation af sårbarhedskortene.

Amtskommunerne foretager i overensstemmelse med vandforsyningsloven (1978) en hydrogeologisk kortlægning af geologiske, hydrogeologiske og grundvandskemiske forhold.

Det har vist sig at være hensigtsmæssigt at udnytte disse kort og de tilhørende databaser ved udarbejdelse af sårbarhedskort. Sårbarhedskort kan derfor opfattes som en naturlig overbygning på den hydrogeologiske kortserie.

I den næste fase af sårbarhedsprojektet, der ligesom fase 1 støttes økonomisk af EF, er det planlagt at forbedre videngrundlaget for sårbarhedskortene, specielt hvad angår vandbevægelse og kemiske omsætninger i den umættede zone. Herudover indgår i fase 2 en mere omfattende verifikation af sårbarhedskortene, opbygning af en geologisk model over Djursland for at få et bedre grundlag for beregning af lagmægtigheder og permeabilitetsforhold samt undersøgelser af mikrobiologiske forhold i relation til grundvandsbeskyttelse. I disse undersøgelser deltager DGU sammen med Statens Planteavlslaboratorium under landbrugsministeriet, Århus amtskommune og Hygiejnisk Institut ved Århus Universitet.

## References

- Andersen, L. J., 1973: Cyclogram technique for geological mapping of borehole data. Danm. Geol. Unders., III rk., 41: 1–25.
- Becker-Platen, J. D., Luettig, G., and Meine, K. H., 1979: Geoscientific maps for planning. Nat. res. Forum, 3: 167–177.
- Bornebusch, C. H. and Milthers, K., 1935: Soil Map of Denmark 1:500000. Danm. Geol. Unders. III rk., 24: 1–68.
- BRGM, 1975: Carte de Vulnérabilité des Eaux Souterraines a la Pollution. BRGM.
- Gry, H., 1935: Petrology of the Paleocene Sedimentary Rocks of Denmark. Danm. Geol. Unders. II rk., 61: 1–172.

- Grönwall, K. A. and Harder, P., 1907: Paleocæn ved Rugaard i Jylland og dets Fauna. (Résumé en Français) *Danm. Geol. Unders., II rk.*, 18: 1–102.
- Harder, P., 1908: En østjydsk Israndlinje og dens Indflydelse paa Vandløbene. *Danm. Geol. Unders., II rk.*, 19: 1–262.
- Jessen, A., 1920: Stenalderhavets Udbredelse i det nordlige Jylland. (English summary) *Danm. Geol. Unders., II rk.* 35: 1–112.
- LeGrand, H. E., 1964: Systems for evaluation of contamination potential of some waste disposal sites. *JAWWA*, 56: 959–974.
- Lov om vandforsyning m.v., Lov nr. 299 af 8. juni 1978. (Danish Water Supply Act of 1978). Miljøstyrelsen, 1979: Vandforsyningsplanlægning 1. del. Planlægning af grundvandsindvinding. Miljøstyrelsen, vejledning nr. 1, 1979. København.
- Milthers, V., 1919: Mergelen i Djursland. *Danm. Geol. Unders. III rk.*, 18: 1–41.
- Milthers, V., 1932: Israndens Tilbagerykning fra Østjylland til Sjælland-Fyn, belyst ved Ledeblokke. *Danm. Geol. Unders., IV rk.*, 2(9): 1–70.
- Milthers, V., 1948: The morphology and genesis of the glacial landscape in Denmark. *Danm. Geol. Unders. III rk.*, 28: 234 p.
- Rasmussen, H. W., 1977: Geologi på Mols. *Danm. Geol. Unders. Ser. A*, nr. 4, 1–22.
- Thomsen, R., 1980: Aarhus amtskommunes anvendelse af EDB-teknik ved behandling af geologiske data og ved vandforsyningsplanlægning. *Vannet i Norden*, nr. 2: 3–31.
- Todd, D. K., 1959: *Ground water Hydrology*. London: Wiley, 336 p.
- Villumsen, A. og Kristiansen, H., 1979: *Grundvandskemien i Århus amtskommune*. Århus Amtskommune.
- Ødum, H., 1926: Studier over Daniet i Jylland og på Fyn. (English summary). *Danm. Geol. Unders., II rk.*, 45: 1–306.

## Appendix 1

### Description of lay-out and technical preparation of maps

#### Surface contour map

In order to make most of the thematic maps by computer it was necessary to produce a simplified surface contour map.

From a geodetic map (1:50.000) about 2000 points were digitized by use of the UTM-net coordinates. The points were chosen by a subjective evaluation of the general morphological trends of the surface, i.e. points were mainly placed where marked changes in slopes were present, whereas only few points were placed in plain areas.

In addition, the values of altitude and UTM coordinates of all wells were used giving a total number of morphometric points of more than 3000.

The surface morphometric matrix was then calculated by 3-D lineary interpolation and consists of  $150 \times 204$  elements covering an area of approx. 1910 km<sup>2</sup> including coastal areas.

## Thematic Maps based on Well-data

The basic assumption during the calculation procedure was that information deriving from a specific point are representative to the area between the neighbouring points.

This implies, that the information depicted on the maps cannot be disintegrated more than the basic information density.

The present procedure for map construction uses a matrix system with an element size of  $(0.25 \times 0.25)$  km<sup>2</sup>, which corresponds to the order of magnitude of the basic information density. In the final calculation of the vulnerability index an element size of  $(0.5 \times 0.5)$  km<sup>2</sup> has been used as a consequence of a lower accuracy of this parameter.

The production of the different thematic maps is based on the following principles:

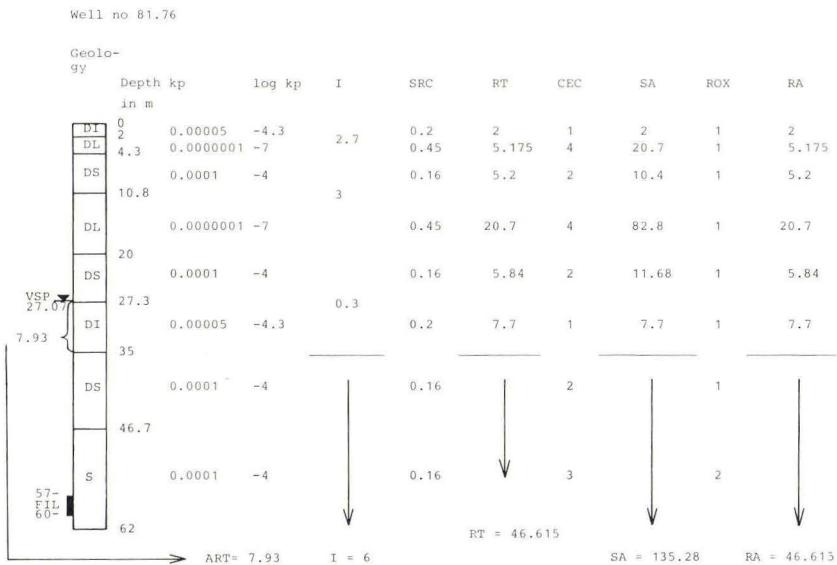
- a) Each theme is depicted on a separate map for each aquifer category.
- b) Only well records containing information of a particular aquifer are used for calculations of that aquifer.
- c) Each element in the map matrix has been calculated by lineary 3-D interpolation of the five nearest parameter values weighted by the 2. power of the distance to the element.
- d) The protomatrix for Djursland consisting of  $150 \times 204$  ( 30.600) elements has been divided into four submatrices in accordance with the distribution of the four different aquifer categories.
- e) The themes which directly depend on the surface contours have been corrected with respect to the surface contours.
- f) Many of the thematic parameters have been calculated using relative values of physico-chemical properties. As exact information is still undiscovered, the corresponding thematic parameters are given as relative index.



## Appendix 2

### Calculation of the vulnerability

Well DGU file No. 81.76 used as an example of the calculation-procedure for vulnerability of the sandlayer (DS + S) 35 m below ground surface. The single steps in the procedure as well as some of the pre-defined values of kp, SRC, CEC and ROX for the given geological layers are illustrated:



$\overline{ART}' :$	$\overline{I}' :$	$\overline{SA}' :$	$\overline{RA}' :$
ART = 0-5 m $\overline{ART}' = 3.5$	$\overline{I}' = 4 - (I/4.3)$	$\overline{SA}' = 4 - (SA/300)$	$\overline{RA}' = 4 - (RA/250)$
ART = 5-15 m $\overline{ART}' = 2.5$			
ART = 15-30 m $\overline{ART}' = 1.5$			
ART = > 30 m $\overline{ART}' = 0.5$			
ART = 7.93 m $\overline{ART}' = 2.5$	$I = 6$ $\overline{I}' = 2.60$	$SA = 135.28$ $\overline{SA}' = 3.55$	$RA = 46.615$ $\overline{RA}' = 3.81$

$$VULNERABILITY = \frac{(\overline{ART}' + \overline{I}' + \overline{SA}' + \overline{RA}')}{4} = 3.12$$

Symbols :

DS	Meltwater sand	I	Interflow index
DI	Meltwater silt	SRC	Specific retention
DL	Meltwater clay	RT	Hydraulic retention time
S	Sand	CEC	Relative sorption capacity
FIL	Filter	SA	Relative sorption ability
VSP	Piezometric surface	ROX	Relative reduction capacity
kp	Permeability coefficient	RA	Relative reduction ability

# Subsidence history of the Jurassic sequence in the Danish Central Graben

Lise Holm

Holm, L.: Subsidence history of the Jurassic sequence in the Danish Central Graben. *Danm. geol. Unders., Årbog 1982*,: 39–51, København, 1983.

Subsidence diagrams for three of the structural units in the Danish Central Graben, the Southern Salt-dome Province, the Tail End Graben and the area east of the Dogger High show that the main subsidence took place in the Late Jurassic and in the Neogene/Quaternary with maximum subsidence rates of 160 m per M.y. and 125 m per M.y., respectively. The influence of compaction is considered to be of minor importance while a correction for uplift and erosion is necessary for the understanding of the dynamic history of the area.

*Lise Holm, Geological Survey of Denmark, Thoravej 31, DK-2400 Copenhagen NV.*

During recent years a detailed knowledge of subsidence history has become of increasing importance for areas with a hydrocarbon potential. The combination of burial depth and time for a given formation must be known in studies of source rock maturation, reservoir properties and timing for hydrocarbon maturation and accumulation, (cf. Waples 1980). Subsidence diagrams can also be used as a basis for the construction of temperature curves (see Jensen 1983). Further, the diagrams illustrate in a convenient way the dynamic history of an area.

The present study is a continuation of the work on the geology of the Danish Central Graben, published in Michelsen (1982). Focus has been put on the Jurassic sequence for two main reasons. First, the main source rock formation in the Danish Central Graben, informally named the J-4 unit, is Jurassic in age, and also other Jurassic formations are believed to have a source rock potential (Lindgreen et al. 1982). Second, the Jurassic sequence contains potential reservoir formations of importance as targets for the hydrocarbon exploration.

## Framework

The Danish Central Graben has been subdivided into eight structural units (Andersen et al. 1982, Michelsen & Andersen 1983) (fig. 1). Subsidence

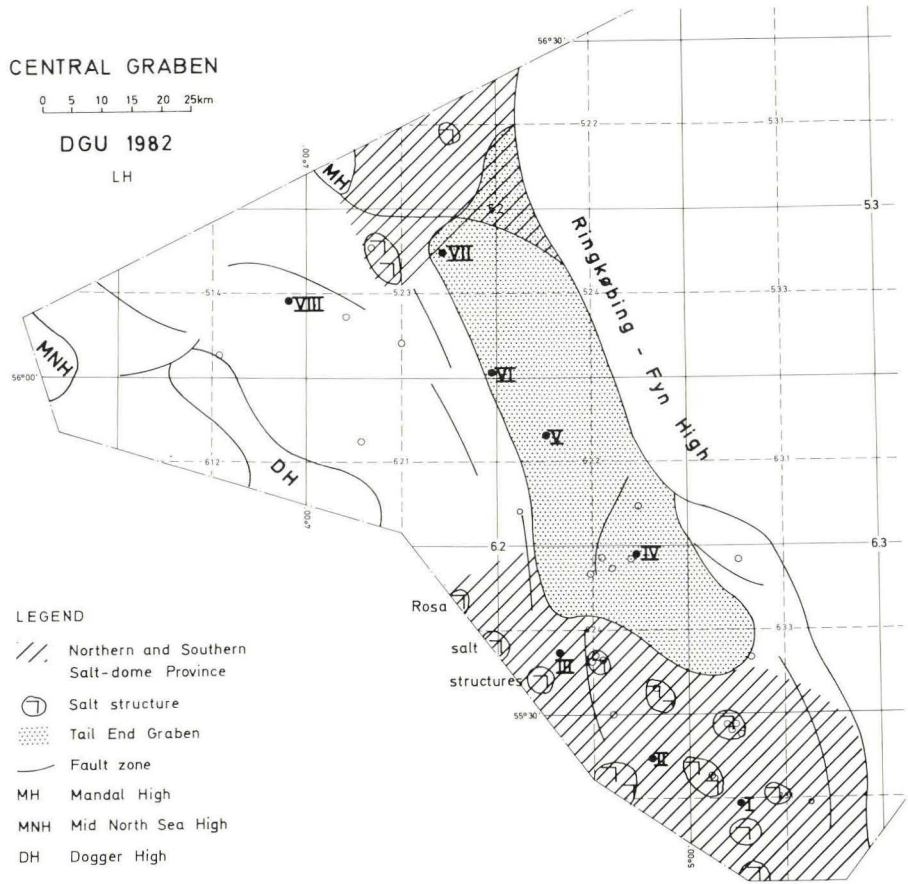


Fig. 1. Location map. Structural units of the Central Graben are indicated. After Michelsen & Andersen (1983).

diagrams have been constructed for three of these units, the Southern Salt-dome Province, represented by 3 subsidence diagrams, the Tail End Graben with 4 diagrams, and one diagram from the area east of the Dogger High.

In the Southern Salt-dome Province, the depth to the top Palaeozoic is approximately 6 km. In the Tail End Graben, the depth to the top Palaeozoic is in the region of 10–11 km, in contrast to a depth of about 3 km on the adjacent parts of the Ringkøbing-Fyn High. In the area east of the Dogger High, the depth to the top Palaeozoic is approximately 5 km. This area is the least known of the structural units dealt with in this paper.



## Method

The subsidence diagrams (figs. 2 and 3) have been constructed with the use of seismic sections, seismic maps and well data. Interval velocities used for depth conversion (table 1) have been chosen after general velocity-depth relationships for the three areas (J. C. Olsen pers. comm. 1981). The following seismic reflectors have been used:

top mid Miocene,  
top Chalk Group,  
base Chalk Group,  
top Jurassic,  
internal Jurassic reflector,  
and base Jurassic.

The internal Jurassic reflector is considered to be close to the base of the J-4 unit. In areas where this reflector has not been identified, the thickness of the J-4 unit has been estimated for adjacent wells and from the regional setting. To simplify the diagrams, the age of this horizon has been defined as the beginning of the Kimmeridgian (150 M.y. ago), on all curves. In the Cenozoic, an extra horizon on the curves has been added, which gives the Quaternary a thickness of 500 m for all three provinces.

No corrections have been made for compaction, isostatic uplift, and erosion. The implications of this approach will be discussed later.

The error of the depths given here is mainly dependent on the error of the interval velocities and is probably within  $\pm 10\%$ . The velocities are generally chosen conservatively and thus the depths and thicknesses tend to be minimum rather than maximum values. In table 1, the two-way travel times, the interval velocities and the calculated depths are presented.

Each of the diagrams has been constructed to show the subsidence history for a small local area, but the diagrams are considered to represent the general Jurassic development of the structural unit in question at the same time.

## Results

The general pattern of all the diagrams shows two main episodes of increased subsidence for the three areas, one in the Late Jurassic and the other in the Neogene/Quaternary. The latter is the period with the most widespread and rapid subsidence, with rates of 110–125 m per M.y. The subsidence rate

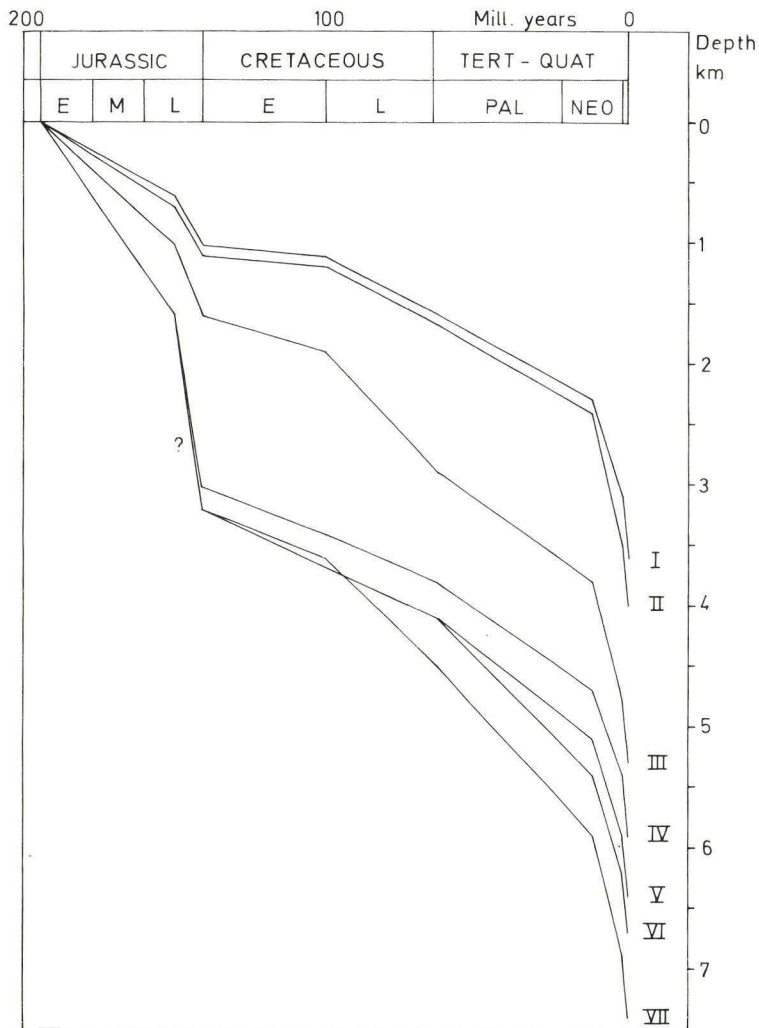


Fig. 2. Subsidence diagrams for the Southern Salt-dome Province and the Tail End Graben.

- I Southern Salt-dome Province. "Mean depth" for the Jurassic sequence.
- II Southern Salt-dome Province. Deep-seated Jurassic sequence.
- III Southern Salt-dome Province. Deep-seated Jurassic sequence east of the Rosa structures.
- IV Tail End Graben. Southern part, near the well E-1.
- V Tail End Graben. Middle, southern part.
- VI Tail End Graben. Middle, northern part.
- VII Tail End Graben. Northern part.

increases with time during the Neogene as seen from the difference in subsidence rates between the Middle and Late Miocene and the Pliocene on one hand and the Quaternary on the other hand. These are 80 m, respectively 250 m per M.y.

The rate of subsidence during deposition of the J-4 unit is, within the Central Graben, varying from 40 m to 160 m per M.y. (fig. 2). The maximum figure is uncertain, however, since it is based on seismic data only. All the figures can only be regarded as minimum values for the rate of subsidence as no correction for compaction has been made.

It should be noted that the thickness of the Lower Cretaceous sequence locally is very varying (Andersen et al. 1982, fig. 15) so a generalized picture of the Early Cretaceous subsidence is of limited value.

By comparison of the individual structural units, the following picture arises.

Since the end of the Early Cretaceous, the area east of the Dogger High has undergone the strongest subsidence of all the provinces dealt with. The top of the Jurassic sequence is here situated at a depth of 4.5 km. The Jurassic sequence is relatively thin in this area, being generally less than 1 km.

This is in strong contrast to the Tail End Graben which came into existence in Jurassic time. More than 3 km, locally 4 km of Jurassic sediments were deposited in the central part of this half-graben. The depth to the top of the Jurassic is here 3–4 km. This is due to a relatively strong Palaeogene subsidence. Besides, the Early Cretaceous sequence is relatively thick in the Graben.

Among the structural units discussed here, the Southern Salt-dome Province has suffered the most moderate subsidence since the beginning of the Jurassic.

A comparison of diagrams from a single structural unit, reveals a more detailed picture than given above. The position of the three curves for the southern Salt-dome Province (fig. 2) has been chosen to represent the Jurassic sequence at different depths and with different thicknesses: One covers the area with a mean depth (~2.5 km) to the top Jurassic reflector and a mean thickness (~1000 m) of the Jurassic sequence. The second represents areas with a deeper seated (~2.8 km) and thicker (~1200 m) Jurassic sequence, and the third curve shows the area with greatest depth (3.5–4 km) and thickest sequence (~1600 m). This last mentioned area is relatively small. The areas with the most shallow Jurassic sequence in the Southern Salt-dome Province have not been treated here.

The difference in depth between the two first areas in the Southern Salt-dome Province is due to increased subsidence of the second area since the Late Miocene. The variation in the Jurassic thickness is dependent on the



position in relation to the salt structures, as the thicker sequences are found between the structures. The relatively thick and deep-seated Jurassic sequence (fig. 2, curve no. III) is related to a major synsedimentary *en echelon* fault system (compare Michelsen 1982, fig. 13), and to the development of a rimsyncline around the Rosa salt structures, situated to the west.

Four curves have been constructed for the Tail End Graben, one in the very southern part and three along a northwestward trending line through the graben (fig. 2). The thickness of the Jurassic sequence here is 3000–4000 m with maximum thicknesses in the eastern and northern part of the graben. The depth to the top Jurassic increases from south to north, from 3 km to more than 4 km. This is a result of increasing subsidence which has happened in the Cenozoic, especially during the Palaeogene. The northernmost location, represented by curve no. VII (fig. 2), shows that the relatively thin Lower Cretaceous sequence here is overlain by a thick Chalk Group (compare profile 4 in Michelsen & Andersen 1983). This is due to inversion tectonics during the Sub-Hercynian or possibly the Laramide tectonic event (Andersen et al. 1982).

The area east of the Dogger High is only represented by one diagram (fig. 3) due to the limited knowledge of the area. The curve is considered to show a mean depth of the Jurassic sequence in that area. Only the J-4 unit is included in the diagram, with an assumed thickness of 800 m.

## Discussion

As mentioned earlier, no correction has been made for compaction, isostatic uplift or erosion. Some comments will be given here on the influence on the subsidence diagrams by using this approach.

*Compaction:* Sediments normally become compacted with increasing depth. Thus the rate of subsidence, as calculated from the present thickness becomes increasingly different (i.e. smaller than) from the “true” subsidence rate with depth. This difference is to some extent compensated by overpressuring, which tends to keep a relatively high porosity in the sediments (Magara 1978).

In the Danish Central Graben, Upper Jurassic and Lower Cretaceous shales, the Chalk Group and the Tertiary claystones below the top of the mid Miocene horizon are normally overpressured (cf. Lieberkind 1978, fig. 5). This implies that most of the sequence dealt with here in general is overpressured and thus has not suffered strong compaction.

Preliminary calculations on the compaction effect on the normally pres-

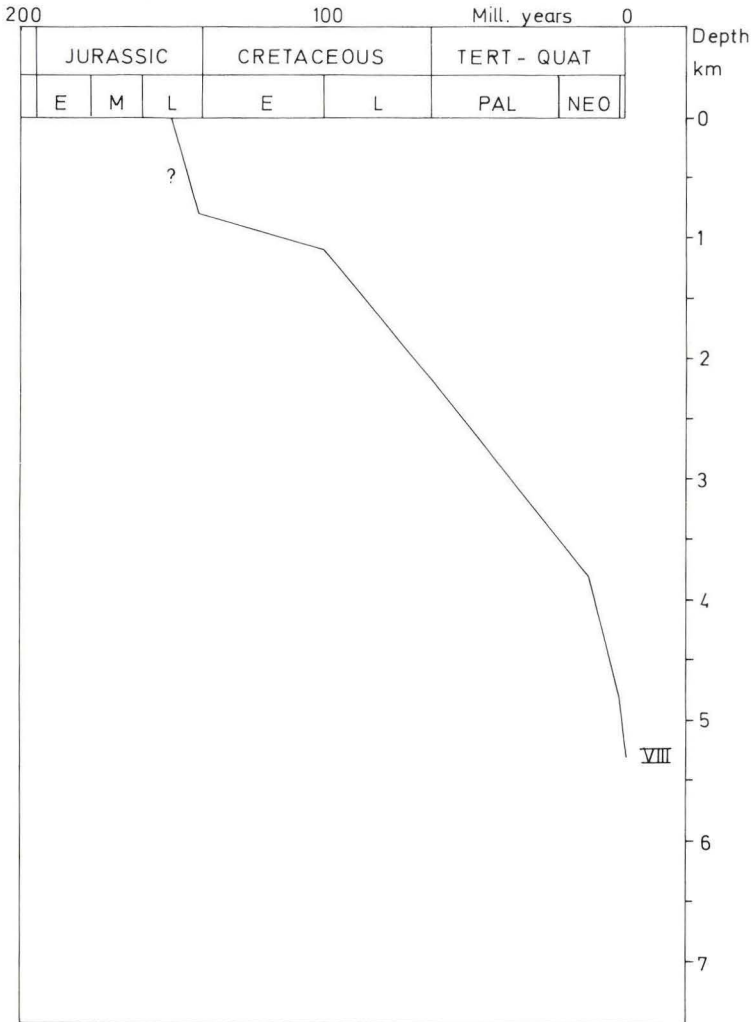


Fig. 3. Subsidence diagram from the area east of the Dogger High. Please note that the diagram starts at the base of the Kimmerigian.

sured CEN-5 and CEN-6 units, of Neogene and Quaternary age (Kristoffersen & Bang 1982) have been carried out by P. Klint Jensen (pers. comm. 1982). These calculations show that the increase in subsidence rate, from the Neogene to the Quaternary, is smaller than indicated on the diagrams, whereas the increase itself is a reality.

In summary, the lack of correction for compaction for this area is considered to be of only minor importance.

*Isostatic uplift and erosion:* Isostatic uplift can in some cases be recorded as changes in depositional environment, for instance from deep to shallow water environment, and/or as erosion of the sediments. These features can however, also be caused by eustatic fall of the sea level.

In the sequence dealt with in this paper, the greatest difference in depth of sedimentation is between the Lower Jurassic and the Middle Jurassic formations. During the deposition of these formations, the sedimentary environment in the Central Graben changed from marine shelf to terrestrial.

This difference in the depths of sedimentation is probably in the region of a few hundred metres. The magnitude of the erosion caused by the mid-Cimmerian event can be estimated by regarding the present distribution of the Lower Jurassic Fjerritslev Formation. In the wells drilled till now, only the lowest part of the Formation (member F-I) is thought to be present. The thicknesses of the two sub-members Ia and Ib of the F-I member are the same as in the Danish Subbasin, and the palaeogeographic pattern suggests similar sedimentation in the two areas in the Early Jurassic. Therefore it is assumed that the Fjerritslev Formation in the Central Graben originally had a similar thickness as in the Danish Subbasin. This implies that more than 500 m of the Formation has been removed by erosion.

Thus, the relatively uplift is in the region of 600–800 m. It is due to a combined effect of isostasy and eustasy. The isostatic movement may be related to a regional crustal arching in the North Sea area occurring at end-Toarcian (Eynon 1981). He suggests a rising mantle plume centred in the Outer Moray Firth area as the probable causal phenomenon. The eustatic changes include a regional regression at the end of the Toarcian, and a regional transgression, beginning in the Callovian and continuing into the Late Jurassic (Vail & Todd 1981). In Vail et al. 1977, fig. 2, the range of eustatic sea level changes from the Lower to the Middle Jurassic is estimated to be in the region of 100 m. This implies that isostatic uplift is the major factor in the development of the mid-Cimmerian unconformity in the Danish Central Graben.

The tectonic events in the Late Jurassic-Early Cretaceous caused erosion and/or non-deposition in the area around and on the Dogger High, and in the Northern Salt-dome Province. In the area east of the Dogger High, marked unconformities are present at this level but the magnitude of the erosion is not known. In the Tail End Graben and the Southern Salt-dome Province, no major hiatus from this period is known (compare Birkelund et al. 1983), but the very top of the Upper Jurassic J-4 unit is absent in many wells, indicating minor erosion. According to Rawson & Riley (1982), the unconformities in the latest Jurassic-Early Cretaceous in the North Sea Basin are of eustatic



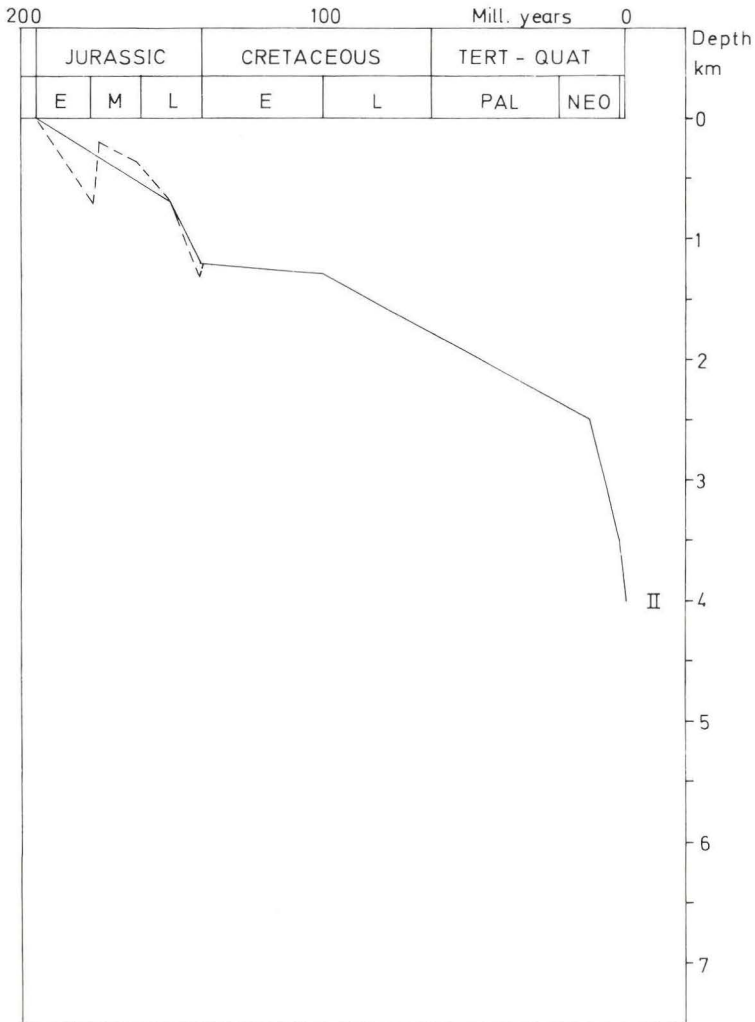


Fig. 4. Subsidence diagram from the Southern Salt-dome Province. The stippled curve is corrected for uplift and erosion.

origin. The associated isostatic uplifts have probably been limited in magnitude.

In relation to the Sub-Hercynian and the Laramide tectonic events, non-deposition rather than extensive erosion is thought to have taken place.

In summary, incorporation of isostatic uplift and erosion in the subsidence diagrams would only have changed the diagrams significantly in relation to

the mid-Cimmerian event. In fig. 4, a diagram is shown which has been roughly corrected for uplift and erosion. The example is from the Southern Salt-dome Province which is the best known structural unit. The diagram shows that the subsidence in the Early Jurassic in this province was in the same order as in the Late Jurassic. The uplift in the Middle Jurassic was in the region of 500 m.

The subsidence diagrams show the general subsidence history of the structural units. If the diagrams are used to show the dynamic history of the area, a correction for uplift and erosion is necessary while the correction for compaction is of minor importance.

*Acknowledgements.* I want to thank my colleagues at the Geological Survey of Denmark, especially Olaf Michelsen, for fruitful discussions.

## Dansk sammendrag

Indsynkningsdiagrammer på basis af seismiske data er konstrueret for 3 strukturelle enheder i Central Graven. Disse omfatter Den sydlige saltstruktur Provins, Tail End Graven og området øst for Dogger Højdestruktur.

Diagrammerne viser, at hovedindsynkningen fandt sted i sen Jura og i Neogen/Kvartærtiden med maksimumshastigheder på henholdsvis 160 m og 125 m per million år. I Jura fandt den største indsynkning sted i Tail End Graven, mens den største indsynkning i sen Kridt, Tertiær og Kvartærtiden foregik i området øst for Dogger Højdestrukturen.

Betydningen af at korrigere diagrammerne for isostatisk hævnning og erosion diskuteres. I forbindelse med den midt Cimmeriske tektoniske fase er der sket en hævnning og erosion af Fjerritslev Formationen i størrelsesordenen 500 m. Erosion i forbindelse med de sen Cimmeriske og Laramiske faser skønnes at være lille i Den sydlige saltstruktur Provins og i Tail End Graven. I området øst for Dogger Højdestruktur kendes omfanget af erosionen ikke.

Betydningen af at korrigere for kompaktion i diagrammerne diskuteres og vurderes til at være af underordnet betydning for forståelse af den dynamiske udvikling af området.

## References

- Andersen, C., Olsen, J. C., Michelsen, O. and Nygaard, E. 1982: Structural outline and development. *In:* Michelsen, O. (ed.) 1982: 9–25.
- Birkelund, T., Clausen, C. K., Hansen, H. N. and Holm, L. 1983: The *Hectoroceras Kochi* Zone (Ryazanian) and remarks on the Late Cimmerian Unconformity in the North Sea Central Graben. *Danm. geol. Unders., Årbog* 1982: 53–72.
- Eynon, G. 1981: Basin Development and Sedimentation in the Middle Jurassic of the Northern North Sea. *In:* Illing, L. V. & Hobson, G. D. (eds.): *Petroleum Geology of the Continental Shelf of North-West Europe*. Heyden & Son Ltd. for Inst. of Petroleum, London: 196–204.

- Jensen, P. K. 1983: Formation temperatures in the Danish Central Graben. Danm. geol. Unders., Årbog 1982: 91–106.
- Koch, J. O., Holm, L. and Michelsen, O. 1982: Jurassic. *In*: Michelsen, O. (ed.) 1982: 37–44.
- Kristoffersen, F. N. and Bang, I. 1982: Cenozoic excl. Danian limestone. *In*: Michelsen, O. (ed.) 1982: 61–70.
- Lieberkind, K. 1978: A conventional log evaluation method for detection of lithology and hydrocarbons in the Danish North Sea well M-1x. Danm. geol. Unders., Årbog 1977: 113–129.
- Lindgreen, H., Thomsen, E. and Wrang, P. 1982: Source rocks. *In*: Michelsen, O. (ed.) 1982: 73–86.
- Magara K. 1978: Compaction and fluid migration. *Developments in Petroleum Science*, 9, Elsevier Scientific Publishing Company, Amsterdam: 1–319.
- Michelsen, O. (ed.) 1982: Geology of the Danish Central Graben. Danm. geol. Unders., Ser. B, 8: 1–133.
- Michelsen, O. and Andersen, C. 1983: Mesozoic structural and sedimentary development of the Danish Central Graben. *Geol. Mijmbouw*, V. 62: 93–102.
- Rawson, P. F. and Riley, L. A. 1982: Latest Jurassic – Early Cretaceous Events and the “Late Cimmerian Unconformity” in North Sea Area. *Am. Assoc. Petrol. Geol. Bull.* V. 66: 2628–2648.
- Vail, P. R., Mitchum, R. M. and Todd, R. G. 1977: Eustatic model for the North Sea during the Mesozoic. *Mesozoic northern North Sea symposium proceedings*, Oslo, Norway. October 17–18, 1977, Norwegian Petroleum Society.
- Vail, P. R. and Todd, R. G. 1981: Northern North Sea Jurassic Unconformities, Chronostratigraphy and Sea-level Changes from Seismic Stratigraphy. *In*: Illing, L. V. & Hobson, G. D. (eds.): *Petroleum Geology of the Continental shelf of North-West Europe*. Heyden & Son Ltd. for Inst. of Petroleum, London: 216–235.
- Waples, D. W. 1980: Time and Temperature in Petroleum Formation: Application of Lopatin’s Method to Petroleum Exploration. *Am. Assoc. Petrol. Geol. Bull.* V. 64: 916–926.

*Table 1.*

*Table 1.* Two-way travel times (TWT), interval velocities ( $V_{int}$ ), and calculated thicknesses and depths for some seismic reflectors. TMM=top mid Miocene, TCh=top Chalk Group, TLCr=base Chalk Group, TJ=top Jurassic, JI=internal Jurassic reflector, TTr=base Jurassic.

	TWT sec.	TWT thickness sec.	$V_{int}$ km/sec.	Thickness km	Depth km
I Southern Salt-dome Province. “Mean-depth” for the Jurassic sequence					
TMM	1.3	1.3	2.0	1.3	1.3
TCh	2.0	0.7	2.0	0.7	2.0
TLCr	2.3	0.3	3.6	0.5	2.5
TJ	2.4	0.1	2.8	0.1	2.6
TTr	3.05	0.65	3.0	1.0	3.6
(J-4 Unit				0.4)	



	TWT sec.	TWT thickness sec.	V <sub>int</sub> km/sec.	Thickness km	Depth km
II Southern Salt-dome Province. Deep-seated Jurassic sequence					
TMM	1.5	1.5	2.0	1.5	1.5
TCh	2.2	0.7	2.0	0.7	2.2
TLCr	2.5	0.3	3.6	0.5	2.7
TJ	2.6	0.1	2.8	0.1	2.8
TTr	3.4	0.8	3.0	1.2	4.0
(J-4 Unit				0.5)	
III Southern Salt-dome Province. Deep-seated Jurassic sequence east of the Rosa structures					
TMM	1.5	1.5	2.0	1.5	1.5
TCh	2.4	0.9	2.0	0.9	2.4
TLCr	2.9	0.5	4.0	1.0	3.4
TJ	3.1	0.2	3.0	0.3	3.7
TTr	4.1	1.0	3.2	1.6	5.3
(J-4 Unit				0.6)	
IV Tail End Graben. Southern part, near the well E-1					
TMM	1.2	1.2	2.0	1.2	1.2
TCh	2.1	0.9	2.0	0.9	2.1
TLCr	2.3	0.2	3.6	0.4	2.5
TJ	2.6	0.3	2.8	0.4	2.9
JJ	3.5	0.9	3.0	1.4	4.3
TTr	4.6	1.1	3.0	1.6	5.9
V Tail End Graben. Middle, southern part					
TMM	1.3	1.3	2.0	1.3	1.3
TCh	2.3	1.0	2.0	1.0	2.3
TLCr	2.5	0.2	3.6	0.4	2.7
TJ	2.85	0.35	2.8	0.5	3.2
TTr	>4.85	>2	3.2	>3.2	>6.4
(J-4 Unit				1.6)	

	TWT sec.	TWT thickness sec.	$V_{int}$ km/sec.	Thickness km	Depth km
VI Tail End Graben. Middle, northern part					
		1.3	2.0	1.3	
TMM	1.3	1.3	2.0	1.3	1.3
TCh	2.6	0.2	4.0	0.4	2.6
TLCr	2.8	0.35	3.0	0.5	3.0
TJ	3.15	1.0	3.2	1.6	3.5
JI	4.15	1.0	3.2	1.6	5.1
?TTr	5.15				26.7
VII Tail End Graben. Northern part					
		1.5	2.0	1.5	
TMM	1.5	1.4	2.0	1.4	1.5
TCh	2.9	0.4	4.4	0.9	2.9
TLCr	3.3	0.27	3.0	0.4	3.8
TJ	3.57	1.0	3.2	1.6	4.2
?JI	4.57	1.0	3.2	1.6	25.8
?TTr	5.57				27.4
VIII Area east of Dogger High					
		1.5	2.0	1.5	
TMM	1.5	1.6	2.0	1.6	1.5
TCh	3.1	0.45	4.8	1.1	3.1
TLCr	3.55	0.2	3.4	0.3	4.2
TJ	3.75				4.5
(J-4 Unit				0.8)	





# The *Hectoroceras kochi* Zone (Ryazanian) in the North Sea Central Graben and remarks on the Late Cimmerian Unconformity

Tove Birkelund, Claus Koch Clausen, Henrik Nøhr Hansen and Lise Holm

Birkelund, T., Clausen, C. K., Hansen, H. N., and Holm, L.: The *Hectoroceras kochi* Zone (Ryazanian) in the North Sea Central Graben and remarks on the Late Cimmerian Unconformity. *Danm. geol. Unders., Årbog 1982*: 53–72, København 1983.

Ammonites, inoceramids and dinoflagellate cysts found in core material from the E-1 well in the Tail End Graben of the Danish part of the Central Graben are described. The core belongs to the upper, highly radioactive part of the Kimmeridge Clay Formation (unit J-4) and includes the ammonite *Hectoroceras kochi* indicating the basal Cretaceous, Lower Ryazanian *H. kochi* Zone. Dinoflagellates indicate the *Cannosphaeropsis thula* Subzone. Dinoflagellates from cuttings immediately below and above the boundary between the Kimmeridge Clay Formation and the overlying Valhall Formation indicate a Valanginian age for the boundary (*Spiniferites ramosus* Zone). No hiatus between the two formations is discernible in the dinoflagellates. The “Late Cimmerian unconformity” is discussed in the light of the new stratigraphic data from the well.

*Tove Birkelund, Claus Koch Clausen, and Henrik Nøhr Hansen, Institute of Historical Geology and Palaeontology, Øster Voldgade 10, DK-1350 Copenhagen K., Lise Holm, Geological Survey of Denmark, Thoravej 31, DK-2400 Copenhagen NV.*

One of the early wells in the southern part of the Danish North Sea, E-1, drilled in 1965 in the Central Graben (Fig. 1), yielded a fossiliferous core of laminated, organic-rich shale from the upper part of the Kimmeridge Clay Formation (core 8, 9783' – 9792'). The core was summarily described by Rasmussen (1978) in a review of eight North Sea wells in the Danish sector. In that work the age of the core was suggested as being Late Jurassic on the basis of poorly preserved miospore and microplankton assemblages, from preliminary determinations by F. Bertelsen. However, in a figured well log (Fig. 12) in the same work it was referred to the lowermost part of the Cretaceous.

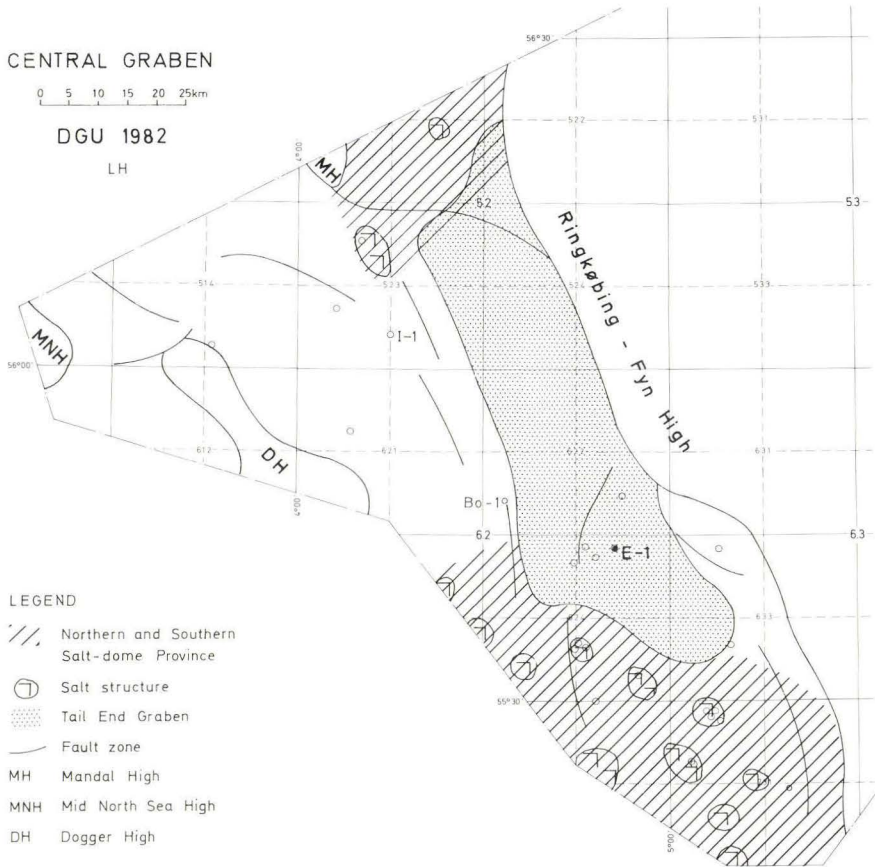


Fig. 1. Map showing structural units of the Danish part of the Central Graben (after Michelsen & Andersen 1983). Location of the E-1, Bo-1 and I-1 wells indicated.

In a recent survey of the geology of the Danish Central Graben (Michelsen 1982), Koch et al. referred the core to an informal J-4 unit, equivalent to the Kimmeridge Clay Formation described by Deegan & Scull (1977). The boundary with the overlying Valhall Formation (see Deegan & Scull 1977) was placed at 9727', 56' above the top of the core, and the entire J-4 unit was referred to the Kimmeridgian-Portlandian.

The discovery of ammonites in the core now makes it possible to determine the age precisely as the *Hectoroceras kochi* Zone of the Lower Ryazanian and this, in turn, provides a fine age calibration for the dinoflagellate assemblage of the core.

Dinoflagellate dating of cuttings from the uppermost part of the Kimmeridge Clay Formation above the core, and from the lowermost part of the

overlying Valhall Formation indicate close to continuous sedimentation in this part of the Central Graben. The boundary between the Kimmeridge Clay Formation and Valhall Formation is discussed further below in relation to the "Late Cimmerian Unconformity".

## Geological setting and lithology of the core

The E-1 well is situated in the southernmost part of the Tail End Graben (Andersen et al. 1982, Michelsen & Andersen 1983) (Fig. 1). The well was drilled on a structural closure at the level of the "Top Chalk Group" (the Tyra Field). The structure is an antiformal flexure caused by Late Cretaceous – Early Tertiary inversion tectonics.

The Tail End Graben is the area showing the greatest subsidence during the Jurassic in the Danish part of the Central Graben (Holm 1983), especially during the Late Jurassic. The total Jurassic sequence is 3000 m thick in the southern part, and the maximum thickness is more than 4000 m further northwards. The thickness of the J-4 unit is estimated to be at least 1600 m in the area around the E-1 well. After deposition of the J-4 unit, a period of relatively slow subsidence followed during which the Valhall Formation was deposited.

The J-4 unit is characterized by high gamma ray activity and a low sonic velocity, interspersed with many high velocity peaks representing dolomite stringers (Koch et al. 1982) (Fig. 2). The E-1 well penetrated one of the most complete developments of the upper part of the J-4 unit in the Danish part of the Central Graben. In the uppermost part, an interval of 25 m with very high radioactivity is found, corresponding to the Mandal Formation in the northern part of the Central Graben (Hamar et al. 1983). In the Danish part of the Central Graben this highly radioactive interval is known from only two other wells, Bo-1 and I-1 (Fig. 1). In the well Bo-1 this interval is 30 m thick and displays the highest gamma ray readings. In the I-1 well the highly radioactive interval attains the greatest thickness, more than 100 m, but this may be due to structural complexity.

The core described here belongs to this highly radioactive interval. It consists of a dark, finely laminated, organic-rich shale deposited under euxinic conditions. An x-radiograph of the rock shown in Fig. 3 reveals the microlaminated character of the rock, with a fine first- and second-order cyclicity.

The organic matter of the J-4 unit in the E-1 well is dominated by liptinite, mainly alginite, associated with varying amounts of vitrinite and inertinite. A remarkable increase in liptinite, mainly alginite, characterizes the top of the unit (Lindgreen et al. 1982).



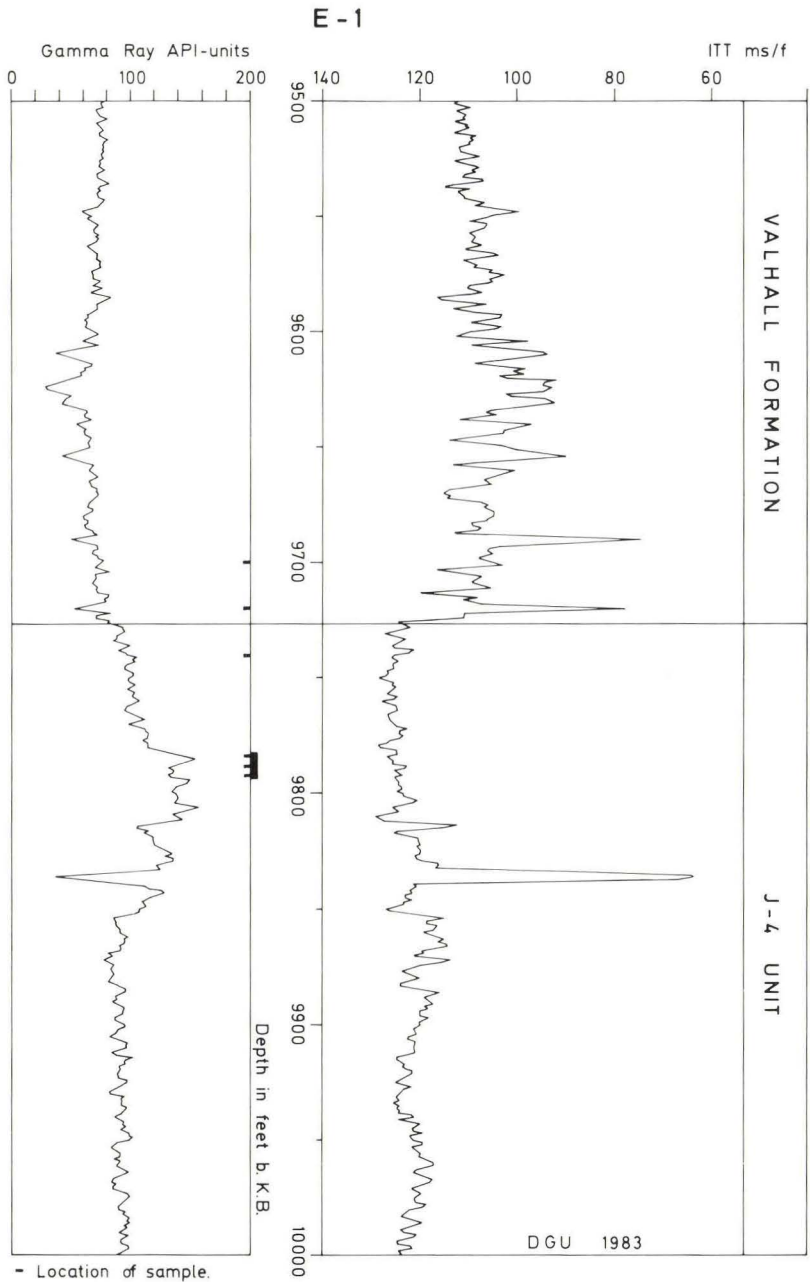


Fig. 2. Logs of the upper part of the J-4 unit and the lower part of the Valhall Formation in the E-1 well. Location of the investigated core and cutting samples indicated.

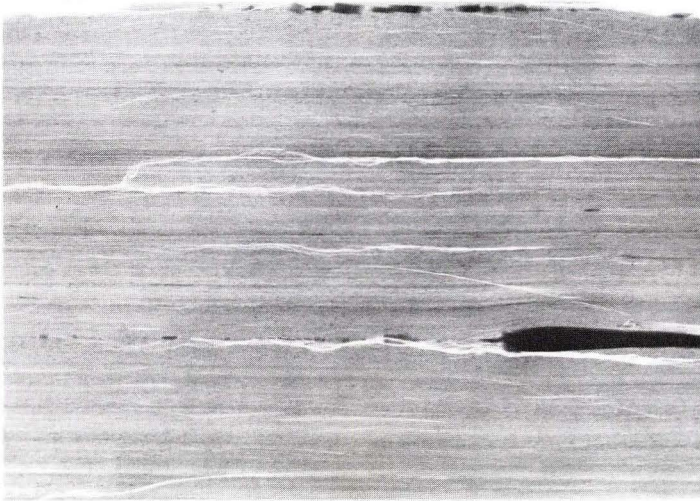


Fig. 3. X-radiograph of core 8 showing the micro-laminated character of the rock,  $\times 1$ .

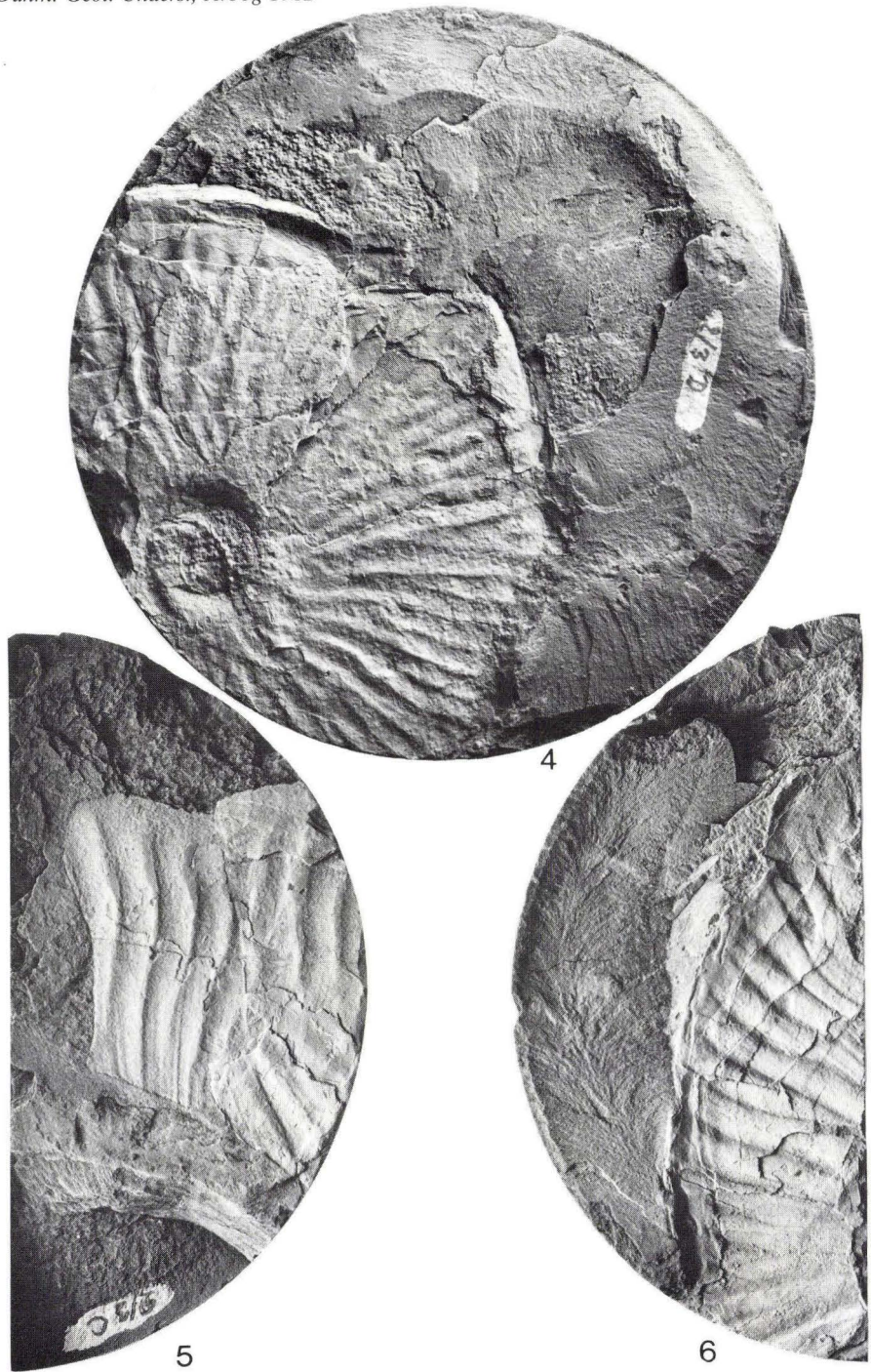
### Ammonites (T. B.)

Three fragments of ammonites have been recovered from the core, one 120–130 cm below top, one 106–108 cm below top, and one 33–43 cm below top. The first is fairly complete, while the others are fragments, probably of body chambers. All of them belong to the Boreal genus *Hectoroceras*.

This genus was established by Spath (1947) who referred it to the family Craspeditidae. It is characterized by its narrow, high-walled umbilicus and compressed oxycone coiling with flat sides and a blunt venter. The ribbing is flexuous, with long primaries which branch above the middle of the flat whorl sides. The ribs tend to terminate close to the venter, leaving the venter smooth. The suture line is very simple, but with numerous auxiliaries.

Besides the type species, *Hectoroceras kochi* Spath, 1947, which is by far the best known, only a few other species have been referred to the genus: *H. larwoodi* Casey, 1973, and *H. tolijense* (Nikitin, 1884) by Klimova (1972).

The best preserved specimen from the core (Fig. 4) seems to be rather close to the type species, *H. kochi*, which is primarily known from Spath's description of rich collections from southern Jameson Land (Spath 1947, p. 21, pl. 1, figs 1–5; pl. 2, figs 1–4 (fig. 2 holotype); pl. 3, fig. 1; text fig. 5). Topotypes have also been figured in Surlyk et al. (1973, pl. 4, figs 1–2) and occurrences further north, in Wollaston Forland, have been figured by Surlyk (1978, pl. 5, fig. 5). Occurrences in the northern USSR have been described by e.g. Shulgina (1972, p. 173, pl. 3, fig. 2) and in England by Casey (1961,



Figs 4–6. *Hectoroceras* cf. *kochi* Spath, 1947 from core 8. 4: Crushed phragmocone, 120–130 cm below top MGUH 16077; 5: Fragment of body chamber, 106–108 cm below top, MGUH 16078; 6: Fragment of body chamber, 33–43 cm below top, MGUH 16079. All  $\times 1$ .



1973, p. 244, pl. 7, figs 1–3). The specimens from these scattered localities all lie within the range of variation of the rich collections from the type area of the species in southern Jameson Land.

The most complete specimen from the core (Fig. 4) has less flexuous ribs than most figured specimens, but is in this respect very close to the holotype, which also has rather straight ribs. One of the large fragments (Fig. 6) closely matches large specimens from East Greenland, while the other fragment (Fig. 5) is less certain.



Fig. 7. Distribution of the genus *Hectoroceras* in the Lower Ryazanian. Palaeogeography mainly after Casey (1973) and Ziegler (1982). Projection after Smith & Briden (1977), slightly modified.

## Stratigraphy

The wide distribution of *Hectoroceras* (Fig. 7) during a short interval in the Ryazanian makes it an excellent stratigraphic marker (Surlyk 1978; Callomon & Birkelund 1983, table 2).

It characterizes the upper part of the Lower Ryazanian, the *Hectoroceras kochi* Zone, in East Greenland, eastern England, N and NW Siberia and is also known from the Volga Basin. In East Greenland the *H. kochi* Zone is underlain by the *Praetollia maynci* Zone (Surlyk 1978), in England by the *Praetollia (Runctonia) runctoni* Zone (Casey 1973, Casey et al. 1977), and in Siberia by zones characterized by the genus *Chetaites*, in the upper part of which *P. maynci* also has been found (Shulgina 1972). The discovery of *Hectoroceras* in the Volga Basin in the lower part (but not the lowermost part) of the former *Riasanites riasanensis* Zone ties the stratigraphy of Siberia and the Russian Platform nicely together (see Casey et al. 1977, Mesezhnikov et al. 1979).

## Inoceramid bivalves (C.K.C.)

Recrystallized bivalves occur scattered throughout the core, but only specimens from the upper part are suitable for closer description.

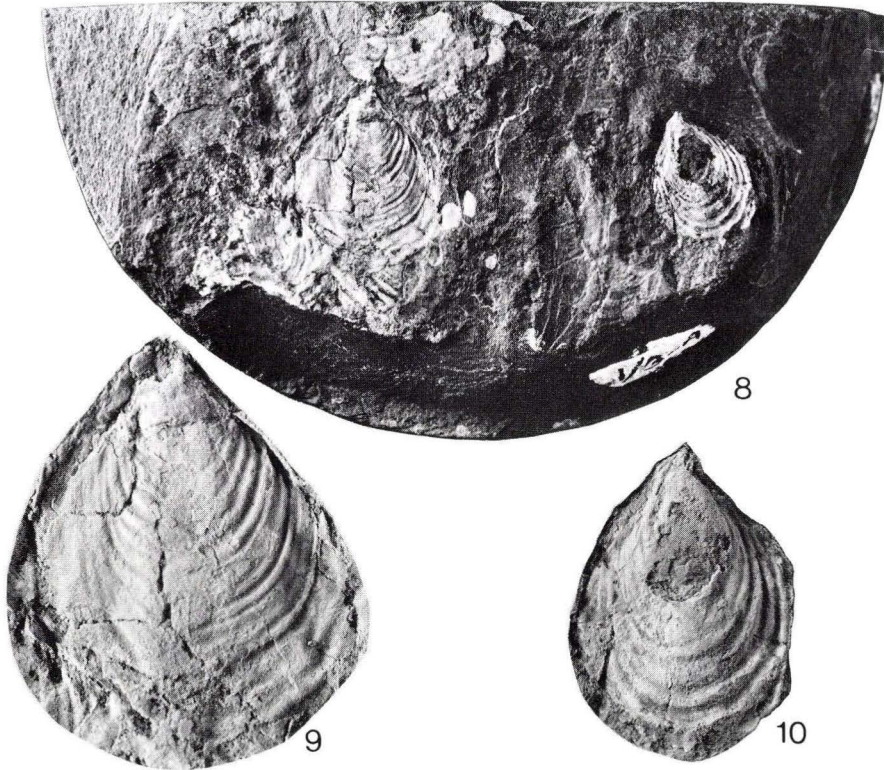
Two bivalved specimens and one fragment from a level 25–28 cm below the top of the core are tentatively referred to *Inoceramus vereshagini* Pochialaynen, 1969 (Figs. 8–10).

The specimens are equivalved or slightly inequivalved and have a prominent commarginal ribbing of well-defined ribs. The outline is ovate and the ratio between height and width 1.2. A small wing is developed. The beaks are subterminal with an angle of 70–80°. The umbones are gently prosogyrate, projecting only weakly above the hinge-line. The hinge-line is rather long and straight, with a uniform series of narrow ligament-pits (only six pits visible). The pits are separated by thin, raised interspaces. Muscle scars are not visible.

The specimens seem to be close to *I. vereshagini*. According to Zakharov & Turbina (1979) this species is highly variable in sculpture, changing with growth, as are the outline of the test and the value of the anterioligamental angle (50–70°).

## Stratigraphy

*I. vereshagini* has been recorded by Zakharov & Turbina (1979) as ranging



Figs 8–10. *Inoceramus* aff. *vereshagini* Pochialaynen, 1969. 8: Bedding plane with the two bivalved specimens and one fragment,  $\times 1$ . 9: Largest specimen, bivalved, showing right valve, MGUH 16080, c.  $\times 3$ . 10: Small bivalved specimen showing right valve, MGUH 16081, c.  $\times 3$ .

from the *Craspedites taimyrensis* Zone (Upper Volgian) to the *Chetaites sibiricus* Zone (lowermost Ryazanian) in the northern part of central Siberia (the Katanga depression), and from the Valanginian in the north-east and far east (the northern Sikhote-Alin) of USSR.

### Palaeoecology

In a discussion of some Late Jurassic inoceramid bivalves Crame (1982) suggested that the replacement of the genus *Retroceramus* by the genus *Inoceramus* in the Early Cretaceous reflected the adoption of an epibyssate mode of life.

The occurrence of *Inoceramus* in non-bioturbated, laminated rock would suggest, according to Kauffman's (1975) interpretation of the benthonic life



habit of the bivalve, a small content of free oxygen in the bottom waters. Such oxic environment may have been of temporary duration in an otherwise generally anoxic sea floor, since there is no other evidence apart from *Inoceramus* of active benthos.

### Dinoflagellate cysts (H. N. H.)

Three samples from the core were used in the palynological analysis: Sample 1 from core interval 9783'–9785', 40–45 cm below the top of the core; sample 2 from core interval 9785'–9788', 99–101 cm below the top of the core, and sample 3 from core interval 9788'–9792', 165–175 cm below the top of the core.

Preparation of the samples: After a standard palynological preparation with HCl and HF it was barely possible to identify any palynomorphs. The dominating organic matter is amorphous, probably of marine algal origin as it exhibited UV induced fluorescence. Strong oxidation with HNO<sub>3</sub> for 17 minutes and 30 minutes treatment in an ultrasonic bath (80 000 HZ) were necessary to clean the palynomorphs from some of the amorphous organic matter.

### Discussion of the dinocyst distribution and the age of the core

The dinocyst species identified in the three samples are listed in Fig. 11. As may be seen, the three samples contain almost the same species, dating the interval 9783'–9792' as in the *Cannosphaeropsis thula* Subzone (Davey 1982) of the Lower Ryazanian (see Fig. 12). The stratigraphically most diagnostic species are:

*Batioladinium radiculatum* Davey 1982, *B. ponum* Davey 1982 (Fig. 22) and *Gonuaulacysta* sp. A Davey 1979 all appear at the base of the subzone.

*Cannosphaeropsis thula* Davey 1982 (Fig. 21) defines the top of the subzone by its last occurrence.

Further, the presence of *Gochteodinia villosa* (Vozzhennikova 1979) Norris 1975 indicates a Late Volgian – Late Ryazanian age.

It is also worth mentioning that the species *Stiphrosphaeridium dictyophorum* (Cookson & Eisenack 1958) Davey 1982 (Figs 13–14) occurs commonly in all three samples. According to Davey (1982) it is similarly common in the two ammonite zones of the Lower Ryazanian in eastern England: The *Praetollia runctoni* and *Hectoroceras kochi* Zones.

The age determination is further supported by the absence of the genus *Muderongia* Cookson & Eisenack 1958, which is only missing in the *Canno-*

Core	Cuttings	
9783'-85'	9700'	
9785'-88'	9720'	
9788'-92'	9740'	
Selected dinoflagellate cysts		
x x x		<i>Batioladinium pomum</i> Davey, 1982
x x x		<i>Batioladinium radiculatum</i> Davey, 1982
x x x		<i>Canningia compta</i> Davey, 1982
x x x		<i>Cannosphaeropsis thula</i> Davey, 1982
x x x		<i>Chlamydothorea membranoidea</i> Vozzhennikova, 1967
	x x	<i>Cleistosphaeridium tribuliferum</i> (Sarjeant, 1966) Davey et al., 1969
x x x		<i>Dingodinium spinosum</i> (Duxbury, 1977) Davey, 1979
x	x	<i>Gochteodinia villosa</i> (Vozzhennikova, 1976) Norris, 1978
x x x		<i>Gonyaulacysta</i> sp. A Davey, 1979
x x x		<i>Pareodinia</i> spp.
x x x		<i>Stiphrosphaeridium dictyophorum</i> (Cookson & Eisenack, 1958) Davey, 1982
x x x	x x x	<i>Gonyaulacysta</i> spp.
x x x	x x x	<i>Hystrichodinium voigtii</i> (Alberti, 1961) Davey, 1974
x	x	<i>Isthmocystis distincta</i> Duxbury, 1979
x x x	x x x	<i>Scriniodinium pharo</i> (Duxbury, 1977) Davey, 1982
	x x	<i>Sirmiodinium grossii</i> Alberti, 1961
	x x	<i>Tanyosphaeridium</i> spp.
x	x	<i>Tubotuberella apatela</i> (Cookson & Eisenack, 1960) Ioannides et al., 1977
	x	<i>Canningia</i> aff. <i>compta</i> Davey, 1982
	x x x	<i>Dingodinium albertii</i> Sarjeant, 1966
	x x x	<i>Gochteodinia villosa multifurcata</i> Davey, 1982
	x x x	<i>Heslertonia heslertonensis</i> (Neale & Sarjeant, 1962) Sarjeant, 1966
	x x	<i>Hystrichosphaeridium</i> cf. <i>recurvatum</i> (White, 1842) Davey & Williams, 1966
	x x x	<i>Kleithriasphaeridium</i> spp.
	x x	<i>Lagenorhysis delicatula</i> (Duxbury, 1977) Duxbury, 1979
	x x x	<i>Muderongia simplex</i> Alberti, 1961
	x x x	<i>Phoberocysta neocomica</i> (Gocht, 1957) Millioud, 1969
	x x x	<i>Pseudoceratium pelliiferum</i> Gocht, 1957
	x x x	<i>Scriniodinium campanulum</i> Gocht, 1959
	x x x	<i>Surculosphaeridium</i> sp. III Davey, 1982
	x x x	<i>Trichodinium ciliatum</i> (Gocht, 1959) Eisenack, 1964
	x	<i>Concavissimisporites verrucosus</i> (Delcourt & Sprumont, 1955) Dörhöfer & Norris, 1977

Fig. 11. List of selected dinoflagellate cysts from the investigated core and cuttings.

AGE		BOREAL AMMONITE ZONES	DINOCYST ZONATION (after Davey 1979)		
			SUBZONES	ZONES	
Valanginian	late	"Astieria" fauna		<i>Spiniferites ramosus</i>	
		<i>tuberculata</i> *			
		<i>bidichotomoides</i> *			
		<i>triptychoides</i> *			
		<i>pitrei</i>			
	<i>Dichotomites</i> spp.				
early	<i>Polyptychites</i>				
	<i>Paratollia</i>				
Ryazanian	late	<i>albidum</i>	<i>Scriniodinium pharo</i>	<i>Pseudoceratium pelliferum</i>	
		<i>stenomphalus</i>			
		<i>icenii</i>			
	early	<i>kochi</i>			<i>Cannosphaeropsis thula</i>
		<i>runctoni</i>			
Portlandian	late	<i>lamplughi</i>	<i>Egmontodinium expiratum</i>	<i>Gochteodinia villosa</i>	
		<i>preplicomphalus</i>			
		<i>primitivus</i>			
		<i>oppressus</i>			
		<i>anguiformis</i>			
	early	<i>kerberus</i>		<i>Dingodinium spinosum</i>	
		<i>okusensis</i>			
		<i>glaucolithus</i>			
		<i>albani</i>			
					<i>Avellodinium culmulum</i>

\* German Boreal Zones

Fig. 12. Correlation of the dinocyst zonation to the Boreal ammonite zonation for the Portlandian to Valanginian (after Davey 1982).

*sphaeropsis thula* Subzone, the *C. thula/Egmontodinium expiratum* Subzone and the *Dingodinium spinosum* Zone in the late Jurassic – early Cretaceous dinocyst sequence of the North Sea area (see Davey 1982, Fig. 3).

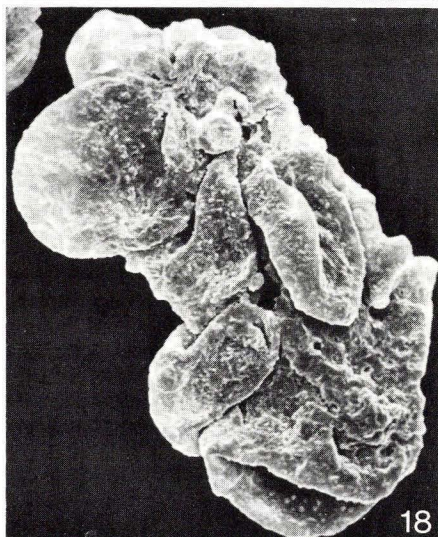
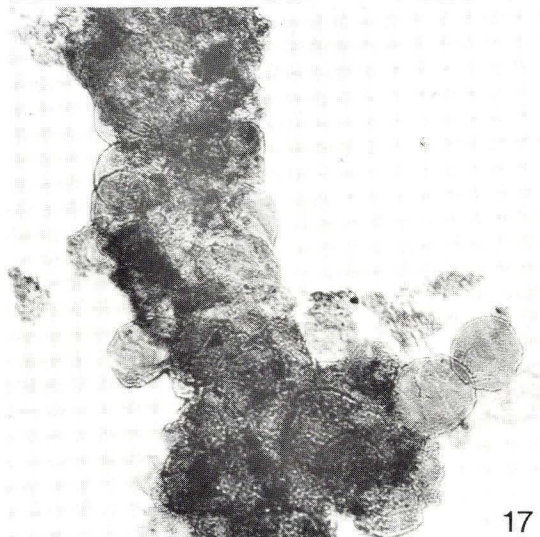
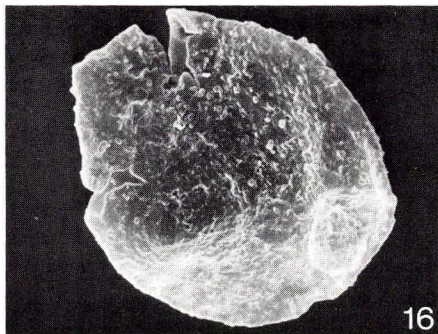
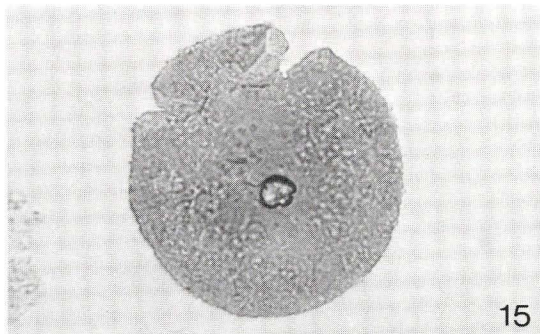
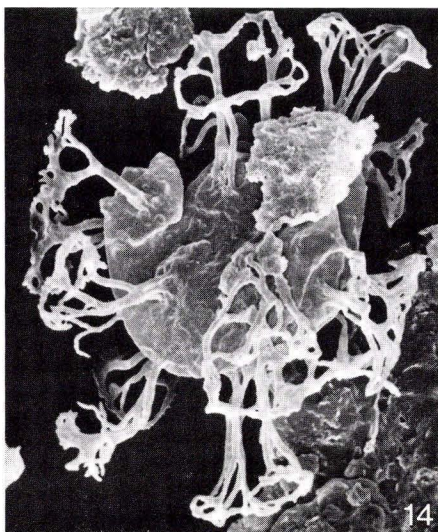
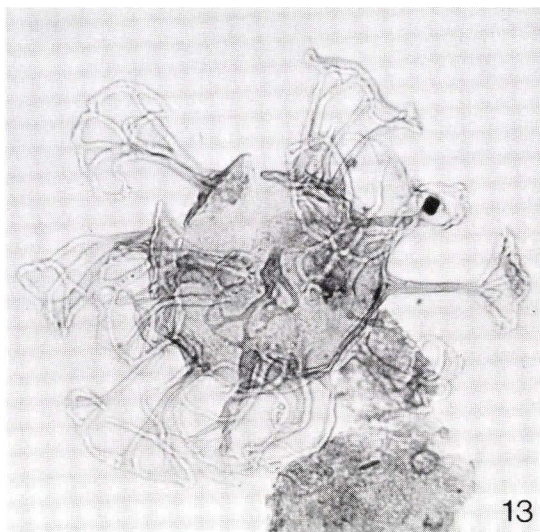
*Egmontodinium expiratum* Davey 1982, characterizing the lowermost part of the *Gochteodinia villosa* Zone, has not been found in any of the three samples. In England it has been reported from the *Praetollia runctoni* Zone but not from the *Hectoroceras kochi* Zone. This supports correlation of the core interval 9783'–9792' with the top of the *C. thula* Subzone, in good agreement with the occurrence of *Hectoroceras kochi*.

*Canningia compta* Davey 1982 constitutes up to 60% of the dinocyst assemblages in sample 9788'–9792'. Some occur as single specimens (Figs

---

Figs 13–18. 13: *Stiphrosphaeridium dictyophorum*, sample 9788'–9792', MGUH 16082, c. × 550. 14: *S. dictyophorum*, sample 9788'–9792', MGUH 16083, c. × 550. 15: *Canningia compta*, sample 9788'–9792', MGUH 16084, c. × 550. 16: *C. compta*, sample 9788'–9792', MGUH 16085, c. × 550. 17: Coprolitic lump of *C. compta*, sample 9788'–9792', MGUH 16086, c. × 150. 18: Coprolitic lump of *C. compta*, sample 9788'–9792', MGUH 16087, c. × 300. Authors of these taxa are given in fig. 11.







15–16), but the most common occurrence of the species is in strings or lumps (Figs 17–18), the specimens being cemented together with amorphous organic matter. These lumps are not destroyed even after treatment with nitric acid and ultrasonics. On the basis of shape and coherence, these lumps are interpreted as coprolites, probably of pelagic organisms if the anoxic bottom conditions did not allow much benthonic life. The abundant occurrence in the core of this species is remarkable, as it is stressed by Davey (1982) that the species flourished in the relatively shallow shelf seas of eastern England during the Volgian and the Ryazanian, but not in the same abundance over most of the North Sea Basin.

F. Bertelsen (1968) reported *Cleistosphaeridium tribuliferum* (Sarjeant, 1966) Davey et al. 1969 from core 8 and on that basis dated the core interval to an Oxfordian age. According to Davey (1982) *C. tribuliferum* continues into the *C. thula*/*E. expiratum* Subzone, but the present investigation extends its known occurrence to the *C. thula* Subzone.

#### Dinocysts from cuttings around the J-4 unit/Valhall Formation boundary

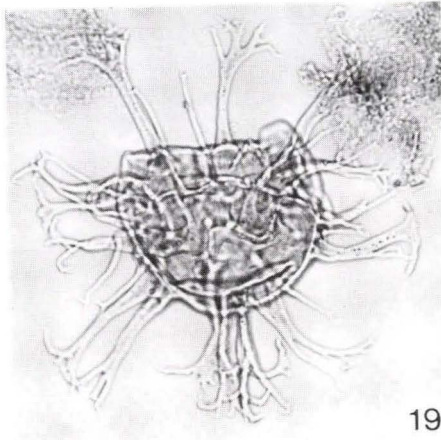
According to Michelsen (1982) the boundary between the J-4 unit and the Valhall Formation in the E-1 well lies at 9727', 56' above the dated core. To get an idea of the age of that boundary cuttings from the levels 9740', 9720' and 9700' were investigated.

The organic content of the samples reflects the character of the two formations. Thus, the sample from 9740' contains a good deal of unstructured organic matter, while the samples from level 9700' and 9720' contain mainly structured organic matter, following the change from anoxic to oxic bottom conditions at the boundary between the formations. Nevertheless, some mixing of the material must be expected.

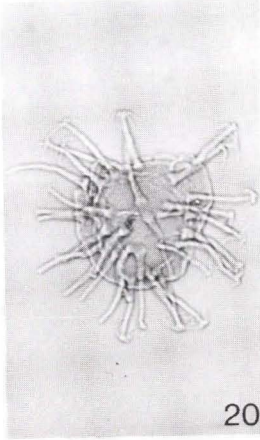
The identified species from the three samples are listed in Fig. 11. They contain the same assemblage of species, dating the interval 9700'–9740' to the Valanginian *Spiniferites ramosus* Zone (Davey 1979) (see Fig. 12). The exact age within the Valanginian, however, is uncertain.

---

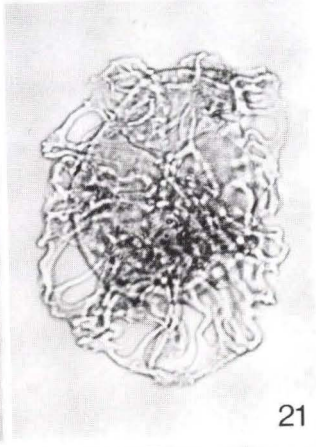
Figs 19–27. 19: *Surculosphaeridium* sp. III, sample 9720', MGUH 16088. 20: *Hystrichosphaeridium* cf. *recurvatum*, sample 9740', MGUH 16089. 21: *Cannosphaeropsis thula*, sample 9788'–9792', MGUH 16090. 22: *Battioladinium pomum*, sample 9788'–9792', MGUH 16091. 23: *Pseudoceratium pelliferum*, sample 9700'. MGUH 16092. 24: *Phoberocysta neocomica*, sample 9700', MGUH 16093. 25: *Gochteodinia villosa multifurcata*, sample 9720', MGUH 16094. 26: *Lagenorhytis delicatula*, sample 9700', MGUH 16095. 27: *Concavissimisorites verrucosus*, sample 9720', MGUH 16096. All c. × 550. Authors of these taxa are given in fig. 11.



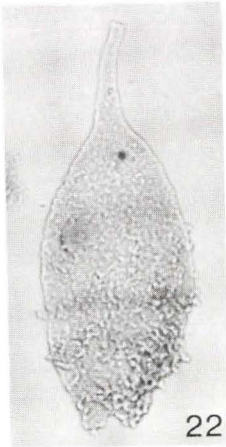
19



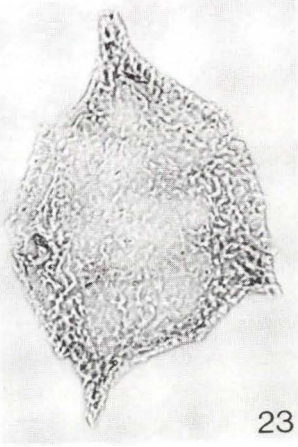
20



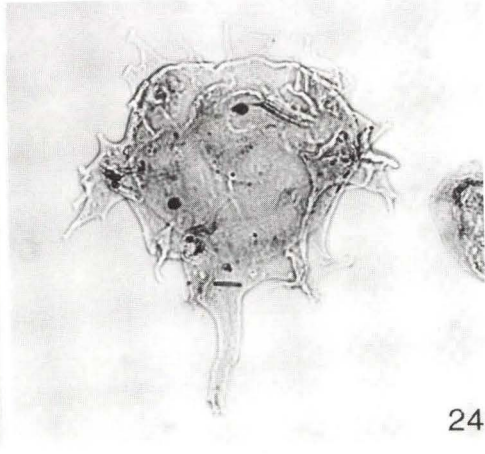
21



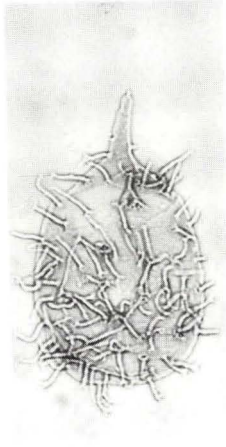
22



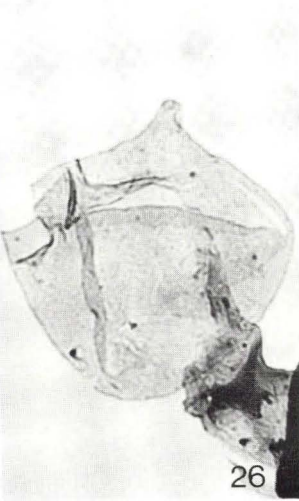
23



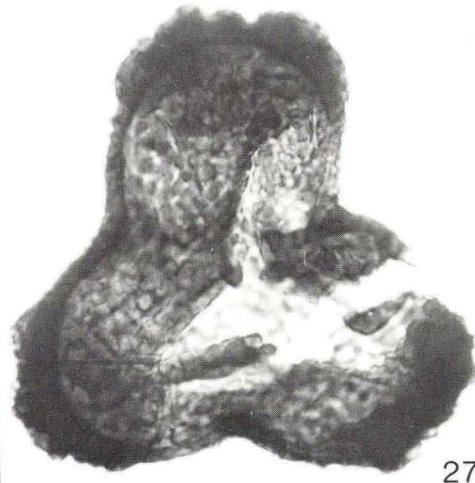
24



25



26



27



*Gochteodinia villosa multifurcata* Davey 1982 (Fig. 25) appears near the Ryazanian-Valanginian boundary and extends throughout the Valanginian into the early Hauterivian (Davey 1982).

*Phoberocysta neocomica* (Gocht 1957) Millioud 1969 (Fig. 23) appears a little later in the Valanginian, at the base of the *S. ramosus* Zone s.str. in the Haldager 1 borehole (see Davey 1982, Fig. 3), and should thus exclude the lowermost Valanginian. On the other hand, the persistent occurrence of *Scrinidinium pharo* (Duxbury 1977) Davey 1982 in all three samples points to a very early Valanginian age. In addition, the occurrence of *Surculosphaeridium* sp. III Davey 1982 (Fig. 19), up to now found only in beds D3 and D4 of the Lower Valanginian at Speeton, may indicate an early Valanginian age. Well preserved specimens of that species have been found in the samples, confirming the description given by Davey (1982) on the basis of fragmented material.

Pollen and spores have not been examined in any detail, but the spore *Concavissimisporites verrucosus* (Delcourt & Sprumont 1955) Dörhöfer & Norris 1977 (Fig. 27) occurs in the cuttings from 9720'. It is reported from Hills 4 palynozone (Dörhöfer & Norris 1977) covering the Upper Ryazanian, Lower Valanginian and the lower part of Upper Valanginian in south England and north Germany. Generally, species characterizing the Hauterivian *Discorsia nanna* Zone (Davey 1979) are not present. Only *Hystrichosphaeridium* cf. *recurvatum* (White 1842) Davey & Williams 1966 (Fig. 20), described from the *D. nanna* Zone in the Haldager 1 bore-hole by Davey (1982), has been found in the cuttings from 9700' and 9720'.

In conclusions, no hiatus is apparent in the J-4 unit – Valhall Formation boundary interval on the basis of the cuttings described here. The boundary between the formations lies in the Valanginian, probably in the early part.

## Biostratigraphical conclusions

Ammonites and dinoflagellates date the core interval 9783'–9792' to the Lower Ryazanian *Hectoroceras kochi* Zone and the *Cannosphaeropsis thula* dinocyst Subzone, while dinoflagellates from cuttings from the top of the J-4 unit and the base of the Valhall Formation (9700'–9740') indicate a Valanginian age for that interval (*Spiniferites ramosus* Zone).

The early Cretaceous age of the highly radioactive upper part of the Kimmeridge Clay Formation (J-4 unit) of the Central Graben of the Danish sector is in good agreement with other parts of the Central- and Viking Grabens. Thus, Fyfe et al. (1980), Costa (1981), Rawson & Riley (1982), and Hamar et al. (1983) all agree that the organic mudstone facies of the

Upper Jurassic persists into the Ryazanian, and Hamar et al. (1983) has now established a separate formation for the hot shales of Ryazanian age from the northern part of the Central Graben: the Mandal Formation.

The age of the boundary between the Kimmeridge Clay Formation (Mandal Formation) and the Valhall Formation (viz. the change from anoxic to oxic conditions) was claimed to be Late Ryazanian by e.g. Fyfe et al. (1980), Riley & Tyson (in Fyfe et al. 1980), Rawson & Riley (1982), and Hesjedal & Hamar (1983). The present work seems to show that the boundary is early Valanginian in the E-1 well described here.

## The Late Cimmerian Unconformity

Many authors have applied the term "Late Cimmerian" in a general sense to tectonism in the late Jurassic and early Cretaceous.

Ziegler (1978, 1982) used the term "the Late Cimmerian phase" in a restricted sense for a major rifting pulse which, according to him, affected the entire Arctic – North Atlantic rift system in Early Cretaceous time, and is believed to have coincided with a sharp eustatic drop in sea-level (Vail et al. 1977). The term has been applied in the North Sea especially to the so-called "Late Cimmerian regional unconformity" between the Kimmeridge Clay Formation (J-4 unit) and the Valhall Formation. In a number of papers in Michelsen (1982) this unconformity was considered to be characterized by a major hiatus in the Danish part of the Central Graben and to be of Late Jurassic age at least partly. The present work shows that the hiatus has been overestimated in at least some parts of the Central Graben and that the age of the unconformity (defined by the base of the Valhall Formation) is in fact Early Cretaceous and thus belongs to the Late Cimmerian phase in the strict sense of Ziegler.

Some authors have recently questioned whether there is a regional unconformity at the top of the Kimmeridge Clay formation at all (Riley & Tyson in Fyfe et al. 1980). Rawson & Riley (1982) claimed that although a major hiatus (or a condensed sequence) may occur at basin margins or above structural highs over most of the North Sea, the base of the Valhall Formation is conformable with underlying sediments, and Hesjedal & Hamar (1983) stress that no angular unconformity can be traced in the central part of the Graben north of the Danish sector. Likewise, in the E-1 well described here, no unconformity could be seen, but in the area around the E-1 well, a weak seismic angular unconformity seems to mark the base of the Valhall Formation (K. Damtoft Poulsen, pers. comm. 1983).

In addition, both the Jurassic-Cretaceous boundary and the top of the

Lower Ryazanian (*Hectoroceras kochi* Zone) are characterized by erosional unconformities in eastern England, which may reflect slightly earlier local movements (Casey 1973, Rawson & Riley 1982).

The distinct seismic reflector at the base of the Valhall Formation represents a lithological boundary, which is considered isochronous by some authors (Riley & Tyson in Fyfe et al. 1980, Rawson & Riley 1982, Hesjedal & Hamar 1983), as it marks a change from mainly anoxic conditions (deposition under a stratified water column) to well oxygenated bottom conditions. However, the boundary is not necessarily strictly isochronous. The Valanginian (and not Ryazanian) age of the boundary in the E-1 well may very well be explained by the persistence of anoxic conditions in some of the deeper parts of the basin, but more exact biostratigraphic datings are needed to map the boundary in detail.

In conclusion, it seems as if the Late Cimmerian phase in the strict sense (early Early Cretaceous) was reduced to relatively minor movements in Ryazanian and ?Early Valanginian time in the North Sea basin, while oscillations in sea-level caused characteristic lithological changes around the Ryazanian – Valanginian boundary.

*Acknowledgements.* We thank O. Michelsen, E. Håkansson, R. G. Bromley and J. H. Callomon for helpful discussion of the manuscript. We are in particular indebted to S. Piasecki for advice on the dinoflagellate cysts, and to V. A. Zakharov for advice on the bivalves.

## Dansk sammendrag

En borekerne fra E-1 boringen i Tail End Graben indeholder ammoniter, inoceramer og dinoflagellatcyster, der daterer kernen til Nedre Ryazanien. Kernen tilhører den særlig radioaktive øvre del af den såkaldte J-4 unit (svarende til Deegan & Scull's Kimmeridge Clay Formation) og er beliggende ca. 50' under grænsen mellem J-4 enheden og Valhall Formationen. Grænsen mellem de to enheder kan på grundlag af dimoflagellatcyster fra cuttings dateres til Nedre Valanginien og der kan ikke påvises nogen lakune mellem de to formationer på grundlag af disse. Den såkaldte "Late Cimmerian Unconformity" diskuteres i lyset af denne boring, og det konkluderes, at Nordsøen kun var svagt påvirket af tektonisk uro i tidlig tidlig kridt.

## References

- Andersen, C., Olsen, J. C., Michelsen, O. & Nygaard, E. 1982: Structural outline and development. *In*: Michelsen, O. (ed.): Geology of the Danish Central Graben. Geol. Surv. Denmark, Ser. B, No. 8: 9–26.
- Bertelsen, F. 1968: Dansk Nordsø E-1, rapport nr. 2. Mikroplanktonindholdet i kærne 8, 9783'–9792' og tillæg til rapport nr. 2. Geol. Surv. Denmark, internal report.



- Callomon, J. H. & Birkelund, T. 1983: The ammonite zones of the Boreal Volgian (Upper Jurassic) in East Greenland. *Can. Soc. Petrol. Geol. Mem.* 8: 349–369.
- Casey, R. 1961: Geological age of the Sandringham Sands. *Nature* 190: 1100.
- Casey, R. 1973: The ammonite succession at the Jurassic-Cretaceous boundary in eastern England. *Geol. Jour. Spec. Iss. No. 5*: 193–266. Seel House Press, Liverpool.
- Casey, R., Mesezhnikov, M. S. & Shulgina, N. I. 1977: Correlation of the boundary deposits of the Jurassic and Cretaceous of England, Russian Platform, the Sub-Polar Urals and Siberia. *Akademia Nauk SSSR, Ser. Geol.* 1977, 7: 14–33 (in Russian).
- Costa, L. I. 1981: Palynostratigraphy, Upper Jurassic to Lower Cretaceous in the wells 2/7–1 and 2/7–3. *In: Geology of the Eldfisk Area. Norwegian Petroleum Directorate NPD Paper No. 30*: 17–21.
- Crame, J. A. 1982: Late Jurassic inoceramid bivalves from the Antarctic Peninsula and their stratigraphic use. *Palaeontology* 25(3): 555–603.
- Davey, R. J. 1979: The stratigraphic distribution of dinocysts in the Portlandian (latest Jurassic) to Barremian (Early Cretaceous) of Northwest Europe. *AASP Contr. Ser. No. 5B*: 49–81.
- Davey, R. J. 1982: Dinocyst stratigraphy of the latest Jurassic to Early Cretaceous of the Haldager No. 1 borehole, Denmark. *Geol. Surv. Denmark, Ser. B, No. 6*: 1–56.
- Deegan, C. E. & Scull, B. J. (compilers) 1977: A proposed standard lithostratigraphic nomenclature for the Central and Northern North Sea. *Rep. Inst. Geol. Sci. No. 77/25*: 1–36.
- Dörhöfer, G. & Norris, G. 1977: Palynostratigraphische Beiträge zur Korrelierung jurassisch-kretazischer Grenzschieften in Deutschland und England. *N.Jb. Geol. Paläont. Abh.* 153(1): 50–69.
- Hamar, G. P., Fjæran, T. & Hesjedal, A. 1983: Jurassic stratigraphy and tectonics of the south-southeastern Norwegian offshore. *Geol. Mijnbouw* 62 (1): 103–114.
- Hesjedal, A. & Hamar, G. P. 1983: Lower Cretaceous stratigraphy and tectonics of the south-southeastern Norwegian offshore. *Geol. Mijnbouw* 62 (1): 135–144.
- Holm, L. 1983: Subsidence history of the Jurassic sequence in the Danish Central Graben. *Danm. geol. Unders. Årbog* 1982: 39–51.
- Kauffman, E. G. 1975: Dispersal and biostratigraphic potential of Cretaceous benthonic bivalvia in the Western Interior. *Geol. Ass. Canada Spec. Paper* 13: 163–194.
- Klimova, I. G. 1972: Berriasian marine faunas. Ammonites from West Siberia. *In: Saks, V. N. (ed.): The Jurassic-Cretaceous boundary and the Berriasian stage in the Boreal Realm. Nauka, Novosibirsk*: 194–204 (in Russian).
- Koch, J. O., Holm, L. & Michelsen, O. 1982: Jurassic. – *In: Michelsen, O. (ed.): Geology of the Danish Central Graben. Geol. Surv. Denmark Ser. B., No. 8*: 37–45.
- Lindgreen, H., Thomsen, E. & Wrang, P. 1982: Source rocks. *In: Michelsen, O. (ed.): Geology of the Danish Central Graben. Geol. Surv. Denmark, Ser. B., No. 8*: 73–107.
- Mesezhnikov, M. C., Zakharov, V. A., Shulgina, N. I. & Alekseev, S. N. 1979: The stratigraphy of the Ryazanian horizon in the region of Oká River. *In: Saks, V. N. (ed.): The Upper Jurassic and its boundary with the Cretaceous system. "NAUKA", Novosibirsk*: 71–81.
- Michelsen, O. (ed.) 1972: Geology of the Danish Central Graben. *Geol. Surv. Denmark, Ser. B, No. 8*: 1–133.
- Michelsen, O. & Andersen, C. 1983: Mesozoic structural and sedimentary development of the Danish Central Graben. *Geol. Mijnbouw* 62 (1): 93–102.
- Rasmussen, L. B. 1978: Geological aspects of the Danish North Sea sector. With a report on the well Dansk Nordsø E-1, E-2, F-1, G-1, H-1, I-1, J-1, and K-1. *Geol. Surv. Denmark, III ser., No. 44*: 1–85.

- Rawson, P. F. & Riley, L. A. 1982: Latest Jurassic – Early Cretaceous Events and the “Late Cimmerian Unconformity” in North Sea Area. *Amer. Ass. Petr. Geol. Bull.* 66(12): 2628–2648.
- Shulgina, N. I. 1972: Berriasian marine faunas. Review of ammonites in the Boreal Realm. Ammonites from the North of Middle Siberia. *In: Saks, V. A. (ed.): The Jurassic-Cretaceous boundary and the Berriasian stage in the Boreal Realm. “NAUKA” Novosibirsk: 117–175 (in Russian).*
- Smith, A. G. & Briden, J. C. 1977: Mesozoic and Cenozoic paleocontinental maps. Cambridge University Press: 63 pp.
- Spath, L. F. 1947: Additional observations on the invertebrates (chiefly ammonites) of the Jurassic and Cretaceous of East Greenland. I. The *Hectoroceras* faunas of S. W. Jameson Land. *Medd. Grønland* 132 (3): 1–69.
- Surlyk, F. 1978: Submarine fan sedimentation along fault scarps on tilted fault blocks (Jurassic-Cretaceous boundary, East Greenland). *Grønlands geol. Unders.* 128: 1–108.
- Surlyk, F., Callomon, J. H., Bromley, R. G. & Birkelund, T. 1973: Stratigraphy of the Jurassic-Lower Cretaceous sediments of Jameson Land and Scoresby Land, East Greenland. *Grønlands geol. Unders.* 105: 1–76.
- Vail, P. R., Mitchum, R. M., Todd, R. G., Widmier, J. M., Thompson, S., Sangree, J. B. Bubb, J. N. and Hatfield, W. G. 1977: Seismic stratigraphy and global changes in sea level. *In: Payton, C. E. (ed.): Seismic stratigraphy: application to hydrocarbon exploration. Amm. Ass. Petrol. Geol. Mem.* 26: 49–212.
- Zakharov, V. A. & Turbina, A. S. 1979: Early Neocomian inoceramids from Northern Siberia and their role in the bottom community. *In: Sachs, V. N. & Zakharov, V. A. (eds): The ecology of Mesozoic marine Boreal faunas. Akademia “NAUKA” SSSR, Siberian branch, Trudy Inst. Geology and Geophysics,* 411: 23–36 and 120–142.
- Ziegler, P. A. 1978: North-Western Europe: Tectonics and basin development. *In: van Loon, A. J. (ed): Key-notes of the MEGS-II-Geol. Mijnbouw,* 57: 589–626.
- Ziegler, P. A. 1982: Geological Atlas of Western and Central Europe: 1–130. Shell Internationale Petroleum Maatschappij B. V.

# Geothermal reservoir rocks in Denmark

Søren Priisholm

Priisholm, S.: Geothermal reservoir rocks in Denmark. *Danm. geol. Unders., Årbog 1982*: 73–86. København 1983.

An extended summary of a DGU/EEC research project is presented. The possibilities of low enthalpy energy sources in Denmark have been investigated. Particular emphasis has been placed on the reservoir characteristics with the intent, if possible, to produce synthetic reservoir assessments.

The investigations of the reservoirs have included the establishment of sedimentary environment, degree and type of diagenesis, temperature mapping, factors controlling formation brine salinity, the decrease of porosity with increased depth of burial, and the relationships between porosity and permeability.

Very simplified, the porosity of the reservoirs decrease from 30–40% at 500 m depth to 5–15% at about 3500 m depth. The significant decrease in permeability with increased depth is noted. Temperatures increase from about 55–75°C at 2000 m to 75–105°C at 3000 m depth. Temperatures of 100–150°C are reached in the central part of the sedimentary basins.

*Søren Priisholm, Geological Survey of Denmark, Thoravej 31, DK-2400 Copenhagen NV, Denmark.*

Geological and geophysical investigations of geothermal possibilities prior to 1981 indicated that a more thorough analysis of the Danish reservoirs was needed (Michelsen et al. 1981).

In 1981 the EEC supported a two year continuation of the geothermal investigations. The study carried out by DGU/EEC 1981–82 and reported by Priisholm et al. 1982, has placed particular emphasis on the reservoir characteristics of clastic and orthochemic rocks with the intent of producing synthetic reservoir assessments. These are needed for analysing the potential of the low enthalpy geothermal reservoirs in Denmark.

The study was only possible through a joint research carried out by scientists and technicians as well as senior students. The following presentation is based on major contributions by:

N. Balling*	Temperature distribution
S. Fine	Bunter Sandstone, Tønder, and Skagerrak Formations – sedimentology, petrography, diagenesis, and compilation



N. Frandsen	Gassum Formation, Haldager Sand and Frederikshavn Member – sedimentology and compilation
H. Friis*	Petrography and diagenesis of Gassum Formation, Haldager Sand, and Frederikshavn Member. Heavy mineral analysis
L. Holm	Structural development
J. I. Kristiansen*	Temperature distribution
T. Laier	Geochemistry of formation water
O. Michelsen	Regional setting
E. Nygaard	Zechstein Formations
S. Priisholm	Porosity, permeability and reservoir evaluation

\* Århus University

The paper will first deal with the parametres governing the performance of the reservoir rocks such as the sedimentary environment, diagenesis, temperature distribution, salinity, porosity versus depth, and porosity versus permeability.

SYSTEM	SERIES	FORMATION	MEMBER
LOWER CRETACEOUS and younger			
JURASSIC	UPPER	BRE ÅM	*FREDERIKSHAVN
			BØRGLUM
	MIDDLE	HALDAGER	*FLYVBJERG *HALDAGER SAND
	LOWER	FJERRITSLEV	
TRIASSIC	UPPER	GASSUM	*MEMBER G <sub>1</sub> - G <sub>4</sub>
		*VINDING	
	MIDDLE	ODDESUND	
		TØNDER	*
		FALSTER	
		ØRSLEV	
	LOWER	*SILAGERÅK	
		BUNTER SANDSTONE	*
	BUNTER SHALE		
ZECHSTEIN			
PERMIAN and older			

\* RESERVOIR FORMATIONS DISCUSSED

Fig. 1. Simplified stratigraphic subdivision of the Danish onshore area.

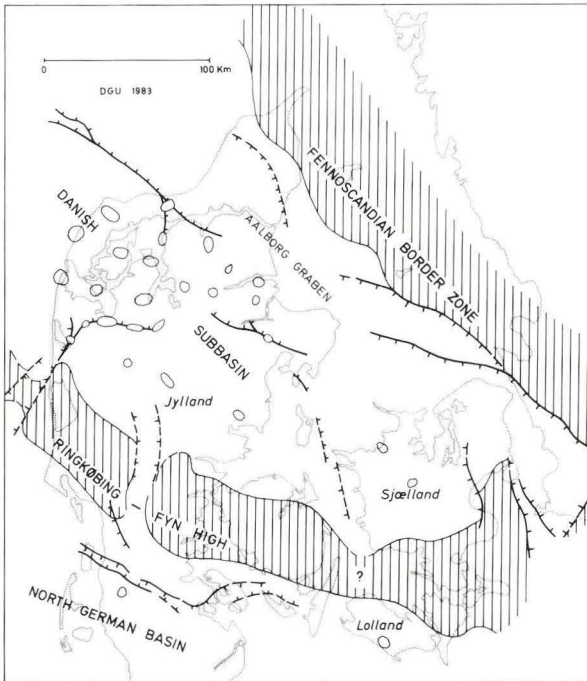



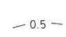


Fig. 2. Structural elements of Denmark. Pre-Upper Permian.

Legend to figures 2–8.

Abbreviation of formations:

- Bu Bunter Sandstone Formation
- Tø Tønder Formation
- Sk Skagerrak Formation
- Ga Gassum Formation
- Ha Haldager Sand
- Fr Frederikshavn Member

-  Major fault
-  Salt Structure
-  Positive area, reservoir thin or absent
-  — 0.5 — Contour. Depth or thickness in kilometres

Second, selected formations and members will be described with special reference to their geothermal reservoir possibility. Regional description of the rocks are previously published by Bertelsen (1978 and 1980), Larsen (1966), and Michelsen (1978 and 1981).

The possible reservoirs are the Zechstein carbonate deposits, the Lower Triassic Bunter Sandstone Formation, and the Middle Triassic Tønder Formation, all in the North German Basin, and the Lower to Upper Triassic

Skagerrak Formation, Upper Triassic Gassum Formation, the Middle Jurassic Haldager Sand, and the Upper Jurassic Frederikshavn Member, situated in the Danish Subbasin (fig. 1).

The structural elements of Denmark are presented in fig. 2 while the configuration of the Triassic formations is given by the general isopach map of the total Triassic (fig. 5), and the depth map to near top Triassic (fig. 6). General depth maps of the Gassum Formation, Haldager Sand, and Frederikshavn Member are presented on fig. 6–8.

## Parameters

### *Sedimentary environment*

In order to map the parameters of the sedimentary reservoir rocks, a classification into sedimentary environments has been carried out.

In general, the most high-energy environments, with the highest degree of reworking, have provided the most coarse-grained and well sorted sandstones.

The Haldager Sand and, to a lesser degree, the Skagerrak Formation, were both partly deposited in a braided river environment and are the most coarse-grained sediments of the investigated formations. This environment can provide sandstone bodies of considerable extension.

The Gassum Formation was deposited in a tidally influenced, shallow marine platform environment. The coarse-grained fraction of the Gassum Formation (fine- to medium-grained sand), is finer-grained than the above-mentioned sediments and was deposited under intermediate energy conditions.

The Frederikshavn Member was probably deposited in an near-coast intermediate-energy environment also, but no obvious relationship between energy levels and grain size can be determined.

The lowest-energy environment of the discussed formations is the sabkha regime which is exemplified by the Bunter Sandstone and Tønder Formations and provides the most fine-grained sandstones.

### *Diagenesis*

The degree of diagenesis has been evaluated with the aid of thin section, x-ray, SEM, and heavy mineral studies.

The Bunter Sandstone, Tønder and Skagerrak Formations have all suffered redbed diagenesis. The Skagerrak and Tønder Formations, when con-



taining volcanic materials, have suffered especially strong diagenetic effects which resulted in lower porosity.

The “grey formations” all have different diagenetic histories. The Gassum Formation becomes increasingly cemented with increasing temperature (depth). Dissolution of feldspars at greater depths creates secondary porosity.

The Haldager Sand has no important early cementation and thus suffers great compaction (crushing of grains) at deep levels. The Frederikshavn Member has a very early glauconitic cement which, combined with the matrix, lowers the permeability considerably.

### *Temperature*

Isotherm maps at depths of 2000 m and 3000 m and of each formation have been constructed.

Isolines generally follow the main tectonic units; the highest temperatures are predicted for the central Danish Subbasin with temperatures decreasing NE towards the Fennoscandian Border Zone and SE towards the Ringkøbing-Fyn High, above, and within which, the lowest temperatures are predicted. Temperatures range between 55°C and 75°C at 2000 m depth, and between 75°C and 105°C at 3000 m depth. In the deepest part of the Skagerrak Formation in the Danish Subbasin, temperatures may reach 100–150°C.

### *Salinity*

The formation water data have been obtained from tests and from extraction of interstitial waters in cores.

The salinity of the post-Zechstein formation waters shows an almost linear increase in salinity with depth. The major solutes are sodium-, calcium-, magnesium-, and potassium chloride. The ions found in minor concentrations are bromide, strontium, sulfate and bicarbonate.

Analyses have shown an increase in the calcium to chloride ratio with depth, and a narrow range of the bromide to chloride ratios. This indicates a common origin of the post-Zechstein formation waters.

The salinity increase is interpreted as due to filtration of the interstitial waters through semipermeable membranes which allow only H<sub>2</sub>O and some of the ions to pass through. As the compaction of the sediments proceed, the interstitial water will be progressively more concentrated.

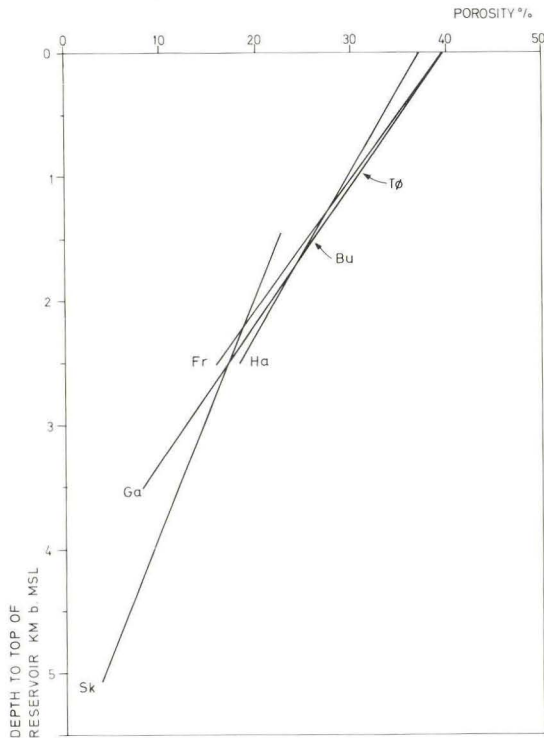


Fig. 3. Porosity gradients for geothermal reservoirs. The statistical calculated trend lines are based on log and core porosity data.

### *Depth versus porosity*

The different depth/porosity trends of the geothermal reservoirs can be illustrated by the variations in porosity gradients which are 5.3% per 1000 m for the Skagerrak Formation, 9.0% per 1000 m for the Gassum Formation, 7.8% per 1000 m for the Haldager Sand and 9.4% per 1000 m for the Frederikshavn Member. No gradients are established for the Bunter Sandstone and Tønder Formations.

A comparison between the linear regression trends of the geothermal reservoirs shows that the Frederikshavn Member, Haldager Sand, and Gassum Formations have almost the same linear decrease of porosity with depth (fig. 3), from about 35% porosity at 500 m to 20–25% at 2000 m and 10–15% at 3000 m. The data from the Tønder and Bunter Sandstone Formations have no porosity/depth trend, but the data clouds of the formations fall within the stated trend; about 30% at 1000 m and 25% at 1500 m.

The linear trend and porosity gradient of the Skagerrak Formation indicates a less drastic decrease in porosity with depth compared to the above-mentioned trend. The decrease is from about 20–25% porosity at 1500 m to 0–10% at 5000 m. Consequently, the porosity of the Skagerrak Formation is lower than for the other reservoirs at a given depth between 1500 and 2000 m, whereas the porosity of the Skagerrak Formation is higher below 2500 m. In the range 2000–2500 m, all reservoirs have porosities of 15–25%.

*Porosity versus permeability*

The porosity/air-permeability trends established for each geothermal reservoir are compared in fig. 4. They have almost the same linear trend from 40 mD permeability at 15–18% porosity down to 1 mD at 2–4% porosity. Above 40 mD at 15–18% porosity, the Skagerrak Formation and Haldager Sand have a common, “high permeability” trend with 2000 mD air-permeability.

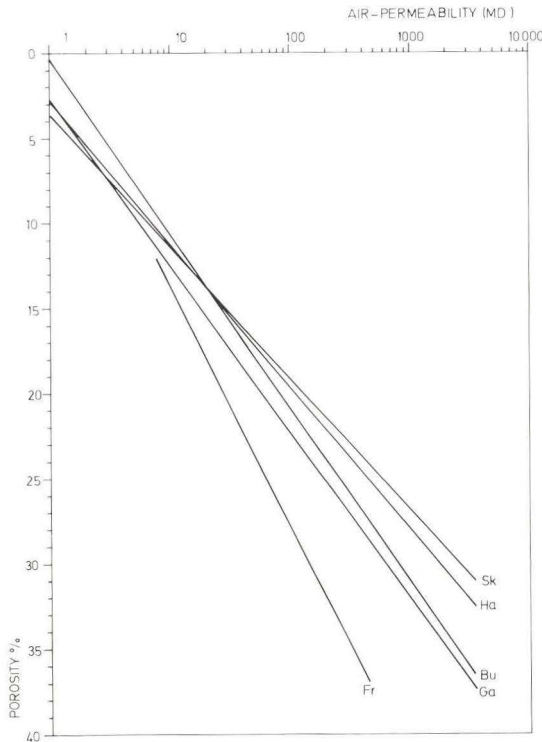


Fig. 4. Relationship between porosity and air-permeability for geothermal reservoirs. The lines of best fit are based on core data.



bility at 30% porosity, whereas the Gassum and Bunter Sandstone Formations have a trend predicting 2000 mD air-permeability at 35% porosity.

Using these trends together with the depth/porosity relations, a rough indication would be that 40 mD permeability is found at 2500 m depth and, for a given depth above 2500 m, the Haldager Sand and Skagerrak Formation will have higher air-permeability (almost a factor two higher) than will the Gassum and Bunter Sandstone Formations.

The reduction from air- to brine-permeability is found to about 50% around 100 mD air-permeability. This reduction is valid for the total permeability range of the Bunter Sandstone and Skagerrak Formations. At about 1000 mD air-permeability, the reduction is 30% for the Gassum Formation and about 25% for the Haldager Sand. Above 1000 mD, the decrease is negligible.

If the sedimentary environment, diagenesis, depth/porosity and porosity/permeability relationships are considered as a whole, it may be concluded that the relatively high-energy Haldager Sand and Skagerrak Formation, have similar porosity/high permeability trends although they differ in diagenetic history and, in certain localities, in lithology. This may cause the differences in porosity gradients where the Haldager Sand has high porosities at shallow depth of burial compared to the Skagerrak Formation. With a reduction of 25–35% from air- to brine-permeability for the Haldager Sand, compared to 50% for the Skagerrak Formation, the properties of the Haldager Sand are the most favourable of these two reservoirs. The Skagerrak Formation however, has a much greater net sand thickness but it also has a province of volcanic materials resulting in extensive diagenesis causing low reservoir quality.

Of the formations with moderate to low energy environments, a porosity gradient can only be established for the Gassum Formation. However, the data of the Bunter Sandstone and Tønder Formations appear to cluster around the same gradient. The porosity/air-permeability trends for the Gassum and Bunter Sandstone Formations are similar but a difference is noted in air- to brine-permeability reduction with better reservoir properties in the Gassum Formation.

Although the porosity gradient of the Frederikshavn Member follows the general trend as shown in fig. 3, the very early cementation with glauconite causes severe damage to the reservoir as indicated by the porosity/low permeability trend.

Despite the great differences in sedimentary environments, diagenesis, and porosity/permeability values of the reservoirs, and bearing in mind the limitation in data on which the gradients and trends are based, the geothermal

reservoirs in Denmark, as known today, have characteristics which fall within broad bands with a common decrease in porosity with depth. The porosity band is from 30–40% porosity at about 500 m depth to 5–15% at about 3500 m depth, and the brine-permeability is in the range 300–3000 mD at about 30% porosity decreasing to 10–30 mD at 15% porosity. Most likely, the reservoirs will fall, within these broad trends. The analyses presented for each reservoir indicate that the reservoir potential at depths below 2500 m is low.

## Formations

### *Zechstein Formations*

The Zechstein carbonates only have a small geothermal potential which is considered to be highest where reservoir rocks are found in combination with fracturing. This may occur along the margins of the basement blocks along the southern flank of the Ringkøbing-Fyn High. A limiting factor for the geothermal potential is the risk that poisonous hydrogen sulphide and highly corrosive, acidic pore fluids, may be present.

### *Bunter Sandstone Formation*

In the southern and southwestern part of southern Jylland, transmissivities are probably in the range of 2.5 to 25 Darcymetres. In the troughs, the formation is thicker and the transmissivity high. The reservoir bodies may be sheets. The temperatures are 50–70°C. On Lolland-Falster, the temperatures are lower (about 40°C) because of a more elevated position of the formation. The northern boundary of North German Basin, as defined by the Ringkøbing-Fyn High, may be a reservoir area because of the increasing sandy content with approach to the Skagerrak Formation further to the north. Temperatures north of the Ringkøbing-Fyn High on Sjælland are 50–70°C.

### *Tønder Formation*

In Jylland, around the Ringkøbing-Fyn High and southwards to the central part of southern Jylland, transmissivities are 5–10 Darcymetres. Temperatures are 30–50°C. The small amount of data however, makes the transmissivity estimates rather uncertain.

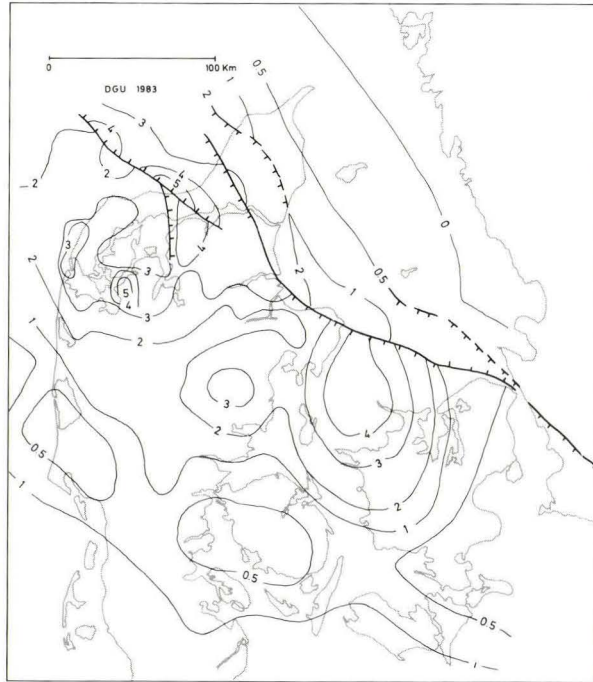


Fig. 5. Generalized isopach map of the Triassic sequence. Thickness in kilometres.

### *Skagerrak Formation*

In areas where the formation is situated above 2000–2500 m depth, and where the depositional environment is the braided river regime, transmissivities may be in the order of 20 Darcymetres.

In the central part of the Danish Subbasin, the formation is situated more deeply and thus has a lower permeability, except above salt structures where the transmissivity may be high. Further, positive temperature anomalies can be present above the salt structures. A westerly province with the volcanic materials will have reduced transmissivities.

In the Fennoscandian Border Zone, the depositional environment is dominated by poorly sorted alluvial fan deposits and thus the permeability will be lower. Sand body extension is probably relatively small.

In general, the estimates of the Skagerrak Formation are questionable because of few data.



*Gassum Formation (fig. 6)*

In areas where the formation is situated shallower than 2000 m depth, and where net sand is relatively thick, transmissivities may be greater than 5 Darcymetres. In most of the Ålborg Graben and in parts of Mid-Sjælland, these conditions should be fulfilled. The temperatures are 40–70°C here. In addition, areas above salt structures in the central part of the Danish Sub-basin may have similar, or even considerably better, reservoir properties.

In the deeper part of the Danish Subbasin, down to 3000 m, transmissivities are 0.5–5 Darcymetres and temperatures are 60–100°C. The sandy platform environment should be present in most of the above-mentioned areas and thus relatively extensive sand bodies are expected.

On Lolland-Falster, net sand thicknesses of 50–70 m are found. The depth to the formation is 500–700 m here, and the temperatures are 20–30°C. An estimate of other reservoir properties can not be given for this region at the present time.

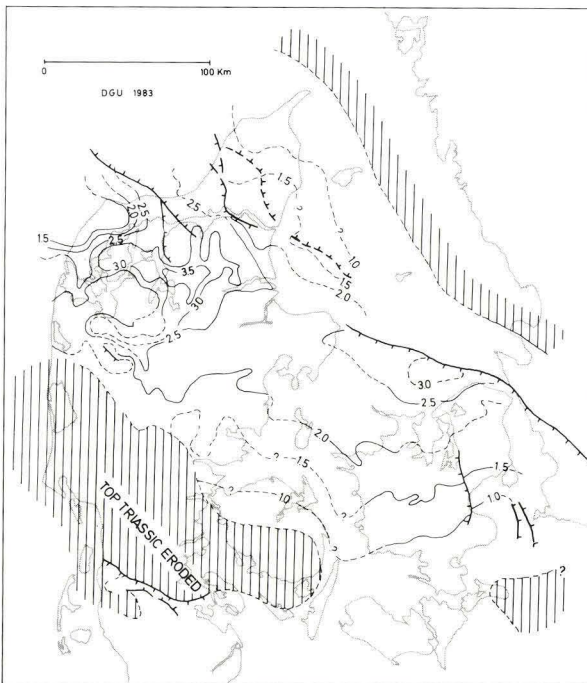


Fig. 6. Generalized depth map to top of Gassum Formation/near top Triassic. Depth in kilometres.

*Haldager Sand (fig. 7)*

In areas where the member is deposited as relatively extensive sand bodies in a braided river environment and where it is situated at depths less than 2000 m, transmissivities of 10–20 Darcymetres may be present. The net sand thickness is, however, expected to vary locally. The above-mentioned conditions are probably present in the Ålborg Graben, especially in the southern part where the braided river environment dominates. Further, in relation to salt structures in the central part of the Danish Subbasin, transmissivities may be high. The transmissivity elsewhere in the area is possibly around 1–5 Darcymetres. Temperatures in the Ålborg Graben are 40–60°C, and 60–80°C in the central part of the Danish Subbasin.

*Frederikshavn Member (fig. 8)*

In the Fennoscandian Border Zone in Jylland, in the Ålborg Graben and in the easternmost part of Jylland, transmissivities may be in the order of 10–20 Darcymetres. The lateral extension of the sand bodies may be relatively

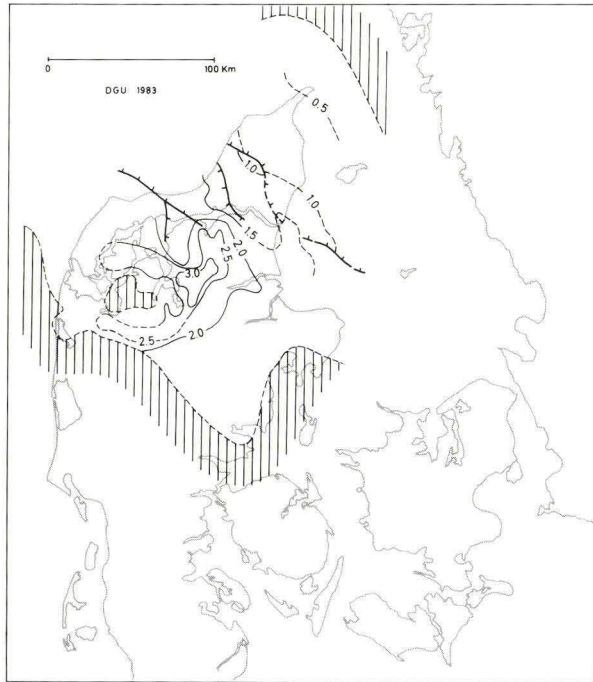


Fig. 7. Generalized depth map to top Haldager Sand. Depth in kilometres.

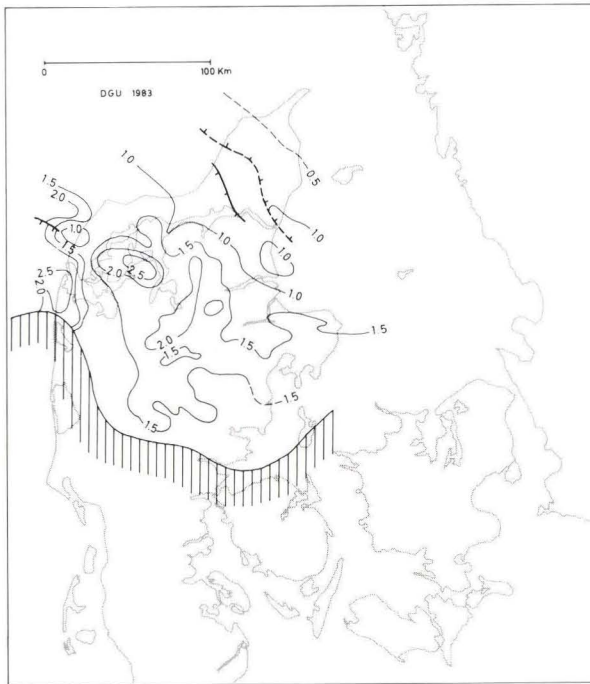


Fig. 8. Generalized depth map to top of Frederikshavn Member. Depth in kilometres.

large. Temperatures of the member are 20–40°C in northern Jylland and 50°C in the eastern part of Jylland. Due to the poor quality of the material however, the estimates of the transmissivity are uncertain and the postulated values may be too high.

*Acknowledgements.* The author is grateful to D.O.N.G, for release of confidential data.

The project summarized here was only possible by the great effort of a staff much larger than mentioned in the introduction. I would like to thank I. Abatzis, K. Andersen, G. Bertelsen, T. Bistrup, W. Brüsch, E. S. Christensen, E. Gosk, G. Grønning, O. Haslund, V. Hermansen, F. B. Hinrichsen, F. Jacobsen, P. Johannessen, U. Jørgensen, A. Kentved, J. Knudsen, J. O. Koch, F. Larsen, K. Larsen, L. A. Larsen, M. Larsen, H. Lindgreen, I. Martin-Legene, E. Melskens, A. I. Nielsen, E. Nielsen, L. H. Nielsen, T. Nielsen, B. Olfert, J. C. Olsen, G. K. Pedersen, P. A. Petersen, D. Plougmann, K. D. Poulsen, J. A. Sørensen, T. R. Sørensen, C. Torres, I. Torres, and I. Wiinberg for their participation in the project.

## References

- Bertelsen, F. 1978: The Upper Triassic-Lower Jurassic Vinding and Gassum Formations of the Norwegian-Danish Basin. – Danm. geol. Unders., Ser. B, 3: 1–26.



- Bertelsen, F. 1980: Lithostratigraphy and depositional history of the Danish Triassic, *Danm. geol. Unders., Ser. B*, 4: 1–59.
- Larsen, G. 1966: Rhaetic-Jurassic-Lower Cretaceous sediments in the Danish Embayment. – *Danm. geol. Unders., II*, 91: 1–127.
- Michelsen, O. 1978: Stratigraphy and distribution of Jurassic deposits of the Norwegian-Danish Basin. – *Danm. geol. Unders., Ser. B*, 2: 1–28.
- Michelsen, O., Saxov, S., Leth, J. A., Andersen, C., Balling, N., Breiner, N., Holm, L., Jensen, K., Kristiansen, J. I., Laier, T., Nygaard, E., Olsen, J. C., Poulsen, K. D., Priisholm, S., Raade, T. B., Sørensen, T. R. & Wurtz, J., 1981: Kortlægning af potentielle geotermiske reservoirer i Danmark, *Danm. geol. Unders., Ser. B*, 5: 1–96.
- Priisholm, S., Frandsen, N., Fine, S., Abatzis, I., Balling, N., Friis, H., Gosk, E., Holm, L., Kristiansen, J. I., Laier, T., Michelsen, O., Nielsen, A. T., Nygaard, E. 1982: Geothermal Reservoirs in Denmark. – *Danm. geol. Unders., Vol. 1–3*. Confidential Report.

# Principles of temperature mapping

Peter Klint Jensen

Jensen, P. K.: Principles of temperature mapping. *Danm. geol. Unders., Årbog 1982*: 87–90. København, 1983.

Temperature mapping can be performed by observing temperatures at different depths and by calculating mean gradients for the formations. Temperatures are calculated between wells by using surface temperature and interpolated mean gradients for each formation. Basically this principle differs from usual technique by using interpolation of mean gradients instead of interpolating mean conductivity and heat flow. In cases where interpolation of gradients are impossible due to insufficient data the gradients can be found by using the relations of the mean gradients for sedimentary sequences. Measurements of conductivity on core samples will contribute to the temperature mapping if the sampling is intensive and the porosity distribution of the formation is known, but unfortunately this is very often not the case.

Calculation of subsurface temperature is important in connection with geothermal energy exploration and the study of maturation of organic matter. This last point was the main reason why a study of subsurface temperature in the Danish Central Graben was performed (Jensen 1983).

*P. Klint Jensen, Slesvigsgade 14–311, DK-1762, Copenhagen V, Denmark.*

Temperature mapping is usually based on measured temperatures in boreholes and heat flux determinations. Heat conductivities are measured on rock samples. (See e.g. Oxburgh and Andrews & Speed 1981). But as we shall see, temperature mapping is also possible by using the observed temperatures and by assuming how mean gradients varies for the mapped area. Temperature mapping is commonly done by using the following relation for calculation of temperature as a function of depth:

$$T(Z) = T_o + q \sum_{i=1}^n \frac{(Z_i - Z_{i-1})}{K_i}, \text{ where} \quad (1)$$

$T(Z)$  is temperature as a function of depth,  $T_o$  is surface temperature,  $q$  is heat flow,  $Z_i$  is depth to the base of layer  $i$ ,  $K_i$  is conductivity of layer  $i$  and  $n$  is the number of layers. The necessary conditions for using Eq. 1 is that temperature is constant in time, heat flow is vertical, the radioactive heat production of the sediments can be neglected, and there is no movements of masses, e.g. water circulation. The surface temperature is easily measured,

and the heat flow is determined from the calculated temperature gradient and from the knowledge of the conductivity of the rocks. The conductivity is determined for each layer. The temperature is then computed and compared with the observed values. If measured and computed temperatures do not coincide, the heat flow and the conductivity parameters used must be adjusted.

At locations outside wells computations are done by using surface temperature and interpolated values of conductivity and heat flux.

The principle of temperature mapping outlined above has not been used in the case of the Central Graben (Jensen 1983). The reason for this is that there are no measurements of conductivity and no general study of porosity distribution in the area. Furthermore, it became clear that extensive laboratory effort would be necessary to give any significant contribution to the temperature mapping. As a typical example for a shale a variation of porosity from 16% to 70% would change the conductivity from 1.5 to 3.5 Wm<sup>-1</sup> K<sup>-1</sup> (Robertson 1979).

Eq. 1 can be rewritten using  $q = V_i K_i$ , where  $V_i$  is the mean gradient of the  $i$ 'th layer:

$$T(Z) = T_o + \sum_{i=1}^n V_i (Z_i - Z_{i-1}) \quad (2)$$

From the equation it may be seen that the heat flow and the heat conductivity are not present and only knowledge of the mean gradients,  $V_i$ , and the surface temperature,  $T_o$ , is necessary for obtaining the temperature profile. Between wells interpolated values of the formation gradient is used. It is not important for the temperature calculations whether lateral variations of the mean gradient within a formation is caused by variation of conductivity or by heat flow or both. This principle of temperature mapping is best illustrated through the temperature mapping of the Central Graben.

By taking the relations of mean gradients for a sedimentary sequence we obtain ratios of the corresponding mean conductivities:

$$\frac{V_i}{V_{i+1}} = \frac{K_{i+1}}{K_i} = \frac{V_{i+1}}{V_{i+2}} = \frac{K_{i+2}}{K_{i+1}} = \dots = \frac{V_{n-1}}{V_n} = \frac{K_n}{K_{n-1}} \quad (3)$$

In some cases this relation can be used to find unknown gradients. If one of the layers has a well-determined measured heat conductivity, the conductivity of the other formations in the sequence can in principle be found. At the same time the heat flux is also obtained.

If we want to calculate the temperature at a given point in a well at some



depth we first must see if there are at least two temperature measurements within the formation. If this is the case the temperature is calculated by linear interpolation. A mean gradient for the formation is obtained at the same time. If there is only one temperature measurement within the formation, the formation gradient cannot be calculated and has to be estimated by interpolating between values from nearby wells. The temperature can then be calculated. If there are no measurements within the formation the gradient is estimated by interpolation from nearby wells and the temperature is calculated using formation temperature of the overlying layer. For points outside wells the surface temperature is used together with interpolations of gradients to calculate the temperature downward with the help of Eq. (2). The formation boundaries are known from seismic interpretations.

Eq. (3) can be used to find the mean gradient for a given formation if it cannot be obtained by interpolation due to insufficient data. It has then to be assumed that the ratio  $V_i/V_{i+1}$  is laterally constant or that it can be obtained by interpolation.

## Conclusion

Problems associated with the mapping of the Danish Central Graben are different from mapping associated with the mapping on the Danish land area due to different type of data (log of thermal conductivity measurements from Danish North Sea Wells). The proposed method may of course also be used in cases where larger amount of conductivity measurements are available. Use of the mean gradient concept makes it possible to obtain continuous temperature profiles in cases where there are insufficient conductivity data. Measurements of rock conductivity can contribute significantly to the temperature mapping if intense sampling is performed and if a relation between thermal conductivity and the porosity of the formation is established.

## Dansk sammendrag

Temperaturkortlægning af undergrunden kan ske ved brug af målte temperaturer i borer, overfladetemperaturer samt ved interpolering mellem borer og mellem borer og overfladetemperaturer for hver formation. Forhold mellem middelgradienter for formationerne i de enkelte lagsøjler gør det muligt at beregne gradienter, som ikke kan findes ved interpolering på grund af mangelfulde data. Måling af bjergarternes varmeledningsevne kan bidrage signifikant til temperaturberegningerne, hvis der er foretaget intensiv prøvetagning. Desuden må porøsitetfordelingen i de enkelte formationer være kendt, idet varmeledningsevnen afhænger af porøsiteten.

## References

- Balling, N., Kristiansen, J. I., Breiner, N., Poulsen, K. D., Rasmussen, R. and Saxov, S. 1981: Geothermal measurements and subsurface temperature modelling in Denmark. Geoskrifter No. 16. Department of Geology, Aarhus University.
- Jensen, P. K. 1983: Formation temperatures in the Danish Central Graben. *Danm. geol. Unders., Årbog 1982*: 91–106.
- Oxburgh, E. R. and Andrews-Speed, C. P. 1981: Temperature, thermal gradients and heat flow in the south-western North Sea. *Petrol. Geol. Cont. Shelf North-West Europe*: 141– 151. Institute of Petroleum.
- Robertson, E. C. 1979: Thermal conductivities of rocks. U.S. Geological Survey, Open File Report 79–356: 1–31.

# Formation temperatures in the Danish Central Graben

Peter Klint Jensen

Jensen, P. K.: Formation temperatures in the Danish Central Graben. *Dann. geol. Unders., Årbog 1982*: 91–106. København, 1983.

The formation temperatures are mapped in the depths of 1, 2, 3, and 4 km in the Central Graben (Danish North Sea). The general trend is increasing temperatures towards the north-eastern fault boundary of the graben. Positive temperature anomalies are found around the Tyra Field in a depth of 1 km. Fluid movements in this area is possible. The observed temperature is high around the top of salt structures. The temperature is high where there is a thick cover of the low conductive, Lower Cretaceous and Jurassic shales. The top Jurassic temperature is mainly a function of the burial depth with increasing temperatures from about 80°C at the southern part of the Central Graben to about 125°C at the northern part. Locally the temperature is higher than 140°C. The temperature maps reflect the general geological trend and the temperature seems to be of conductive origin, except in the area of the Tyra Field where convection of fluids may occur. Temperature as a function of time is calculated for top and base of the J-4 Unit at some locations. Temperature through time of the J-4 Unit is increasing from the Southern Salt-dome Province towards the northern Tail End Graben. The Eocene rise of surface temperature has heated the subsurface temperature.

*Peter Klint Jensen, Slesvigsgade 14–311, DK-1762, Copenhagen V, Denmark.*

About forty off-shore wells have been investigated to evaluate the formation temperatures.

Values of approximate geothermal gradients in the Danish North Sea sector have been evaluated and published by Madsen (1975) who mentions that the values obtained are probably 10–15% too low as no corrections are applied on the collected bottom hole temperatures.

An important question is, if transfer of heat by water circulation is comparable with transfer of heat by conduction. This point is discussed in three recent papers (Oxburgh & Andrews-Speed 1981, Andrews-Speed et al. 1982, and Carstens & Finstand 1981) describing the present temperature field in the southwestern and northern North Sea.

The results of a preliminary study of the formation temperatures for the central and northern part of the Danish Central Graben (Michelsen 1982) are revised and included in the present work.



The formation temperatures are related to the structural style of the area especially to the salt structures, which are an important factor in the Danish area.

## Principles of temperature mapping

Temperature mapping is usually based on temperature measurements and heat flow determinations, but as pointed out in Jensen (1983b) temperature mapping can also be carried out simply by observing borehole temperatures and variations of temperature gradients within the formations, if sufficient temperature measurements are available.

The method of correcting the bottom hole temperature values used in this paper was used by Evans and Colemann (1974). Observed and corrected temperatures are shown in table 1. Mean gradients are calculated with reference to the measured temperature at sea floor (Evans and Colemann 1974)

Table 1. Temperatures and mean gradients.

Well	Depth b. ML (m)	Last temp. (°C)	Corr. temp. (°C)	Mean grad. (°C km <sup>-1</sup> )	Corr. grad. (°C km <sup>-1</sup> )	Type	TSC (hrs.)	Drill rate ft hr. <sup>-1</sup>
A-1	1740	52	—	26	30	Logs	?	—
A-2	982	43	—	38	44	Logs	?	50
	1967	74?	—	35	38	Logs		20
Adda-1	1139	41	45	33	39	Logs	6	0.4?
	2074	74	—	32	36	Tests	—	—
	2206	72	76	31	34	Logs	18	1
	2976	94	101	31	34	Logs	18	3
B-1	1000	40	40	33	40	Logs	5	80
	2280	79	80	32	35	Logs	15	50
	3039	106	104	32	34	Logs	13	40
	3497	116?	118	32	34	Logs	12.5	8
Bo-1	1302	42	44	28	34	Logs	6	100
	2085	75	—	32	36	Tests	—	—
	2248	70	74	30	33	Logs	17	20
	2667	93	102	36	38	Logs	25	4
D-1	996	52	55	48	55	Logs	8	90
	1730	67?	67	34	39	Logs	11	22
	3375	74	76	21	23	Logs	30	9
E-1	1000	46	47	40	47	Logs	6	90
	1997	66	—	29	33	Tests	—	—
	2028	67	—	30	33	Tests	—	—

Well	Depth b. ML (m)	Last temp. (°C)	Corr. temp. (°C)	Mean grad. (°C km <sup>-1</sup> )	Corr. grad. (°C km <sup>-1</sup> )	Type	TSC (hrs.)	Drill rate ft hr. <sup>-1</sup>
	2391	80	81	31	34	Logs	26	6
	3171	94	—	27	30	Logs	6	27
	3865	122	—	30	32	Tests	—	—
	4012	122	—	29	30	Logs	10	8.0
	4012	126	—	30	31	Logs	13	8.0
E-2	992	42	—	35	43	Logs	?	90
	2124	68	70	29	33	Logs	7	35
E-3	1013	38	—	31	38	Logs	4	120
	2217	73	75	30	34	Logs	15	40
	2594	63	—	22	24	Logs	?	30
E-4	1161	62	68	52	58	Logs	5	60
	1942	71	—	33	37	Tests	—	—
	2223	73	73	30	33	Logs	20	40
G-1	987	43	45	39	46	Logs	5	90
	2114	73	74	32	35	Logs	22	12
	3732	117	122	31	33	Logs	10	11
H-1	991	41	43	36	43	Logs	6	80
	1986	67	—	30	34	Tests	—	—
	2076	67	68	29	32	Logs	26	50
I-1	1142	43	47	35	41	Logs	6	90
	2708	108	—	37	40	Tests	—	—
	2818	92	97	32	34	Logs	24	13
	3257	105	110	32	34	Logs	18	10
	3822	129	139	35	36	Logs	10	2
L-1	1137	38	38	28	34	Logs	6	90
	2620	74	78	27	30	Logs	12	6
M-1	990	38	38	32	38	Logs	4	48
	1969	70	—	32	36	Logs	?	240
	2024	66	65	29	32	Logs	8	240
	2232	70	70	29	31	Logs	6	240
M-2	1042	26	26	17	25	Logs	8	80
	2019	71	71	31	35	Logs	14	43
M-3	1966	70	80	37	41	Logs	6	75
M-4	1890	63	—	30	33	Logs	6	40
	1996	62	62	28	32	Logs	15	40
M-5	1974	66	—	30	33	Logs	5	13
M-6	1993	66	—	30	33	Logs	3	30
M-7	2007	64	68	30	34	Logs	10	20
M-8	1207	44	—	31	37	Logs	3	100
	2728	84	90	31	33	Logs	12	8
	3325	119?	161?	46?	48?	Logs	10	15
	3580	114	—	30	32	Logs	?	?
	3581	119	124	33	35	Logs	10	16
N-1	978	34	41	34	42	Logs	4	80

Well	Depth b. ML (m)	Last temp. (°C)	Corr. temp. (°C)	Mean grad. (°C km <sup>-1</sup> )	Corr. grad. (°C km <sup>-1</sup> )	Type	TSC (hrs.)	Drill rate ft hr. <sup>-1</sup>
N-2	2483	70	70	25	28	Logs	9	33
	2220	79	83	34	37	Logs	18	100
N-3	1031	35	39	31	38	Logs	5	60
	1811	56	66	32	36	Logs	8	40
O-1	2224	76	84	34	38	Logs	12	50
	1153	44	45	33	39	Logs	6	12
	2527	77	79	29	31	Logs	9?	12
	2664	93	–	32	35	Logs	3	3
	3217	110	106	31	33	Logs	12	3
	3395	177	177	33	35	Logs	12	2
P-1	1324	33	33	20	25	Logs	6	60
	3040	83	89	27	29	Logs	15	8
Q-1	3388	102	–	28	30	Logs	?	25
	1778	44	46	22	26	Logs	7	40
	3680	106	108	28	29	Logs	21	10
	4090	127	–	29	31	Logs	6	12
Ruth-1	4434	129	–	28	29	Logs	6	10
	1152	36	–	25	31	Logs	?	50
	1638	61	66	37	41	Logs	15	10
T-1	1148	32	–	22	28	Logs	6	90
	2047	70	75	33	37	Logs	18	75
	2321	89	95	38	41	Logs	14	46
U-1	2564	107	113	42	44	Logs	21	55
	1332	39	39	24	29	Logs	6	?
	2985	98	110	35	37	Logs	25	10
	3748	149	157	40	42	Logs	13	18
	4334	144	147	33	34	Logs	16	18
V-1	4818	172	177	36	37	Logs	19	13
	1135	36	39	28	34	Logs	6	50
	3234	97	114	33	35	Logs	22	8
	3774	113	–	28	30	Logs	5	?
Vagn-1	1144	46	53	40	46	Logs	11	90
W-1	1396	36	40	23	28	Logs	9	100
	3748	107	109	27	29	Logs	24	7

and corrected gradients are computed by using 0°C (accepted mean value for the Quarternary) as sea floor temperature. Table 2 contains values of observed and assumed temperature gradients, which were used for the temperature mapping.



Table 2.

Well	Cen-1 to Cen-4 and chalk units	L. Cretaceous and Jurassic shales
A-1	—	54*
Adda-1	28	35
B-1	31	30
Bo-1	32	67
E-1	20	31
E-3	26*	—
E-4	6	—
G-1	26	30
H-1	22	44*
I-1	30	42
M-1-M-8	37*	—
N-1	33	—
O-1	25	36
P-1	28	—
Q-1	32	—
U-1	26*	72
V-1	26*	62
Vagn-1	56	—
W-1	28	—

\* = assumed

For the wells B-1 and D-1 pre Rötligendes gradient of 31° C/km was assumed. For the Well P-1 a pre Jurassic gradient of 36° C/km was assumed and for the U-1 well a gradient of 37° C/km was assumed in the Triassic.

## General comments about the temperature maps

The temperature maps for 1, 2, 3, and 4 km depth and “Top Jurassic” temperatures are shown in figs. 2–6. The locations of the wells are shown in fig. 1.

For all the maps the preliminary contouring was based on wells which are believed to be regionally representative of temperature as these wells were drilled outside salt structures. However, an occurrence of flat salt bodies could not be excluded beneath some of them, but as they are flat the temperature influence will be small. Wells which are drilled near fault zones have also been regarded as regionally representative, as the heat refracting effect usually is small around faults, and as there are no clear evidence of temperature disturbance caused by water and gases moving in these zones. An exception from this may be the upper 1–2 km around the Tyra Field (see later).

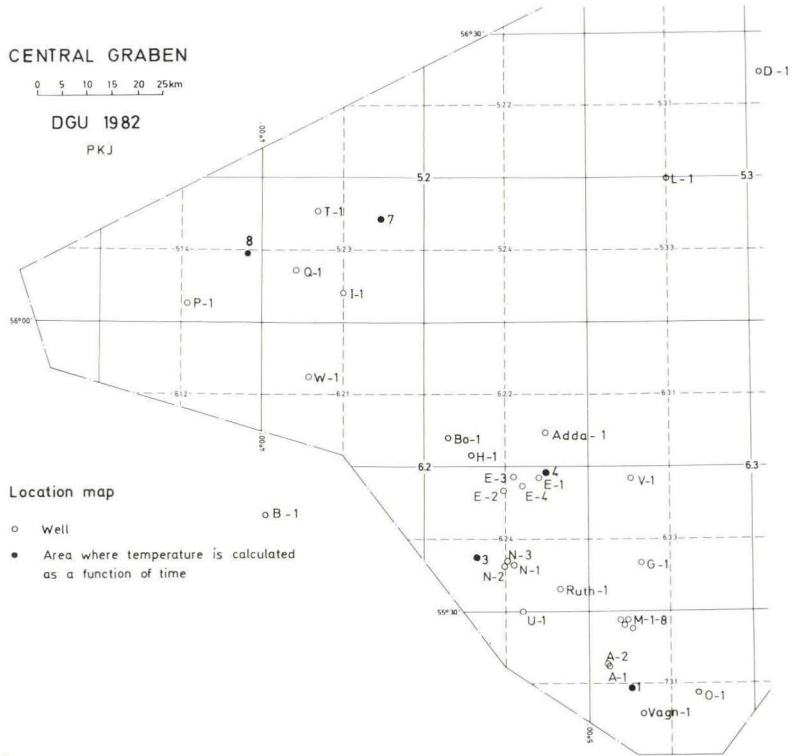


Fig. 1.

After the preliminary temperature maps were drawn, the influence of the salt structures were included by using measured temperature values and theoretical modelling (Jensen 1981). Wells which are accepted as regional thermal representative are Q-1, P-1, W-1, Bo-1, Adda-1, E-1, G-1, U-1, M-8 and, O-1, although flat salt pillows have been interpreted beneath the last three wells on basis of seismics.

### Temperature map, 1 km depth, *fig. 2*

All measurements close to 1 km depth are extrapolated or interpolated linearly to 1 km depth. The general trend of the temperature variation in the Central Graben is characterized by increasing temperatures, from 25 to 40°C, from SW- to NE-direction. Temperature anomalies are found around the Tyra Field where temperatures exceeds 50°C.

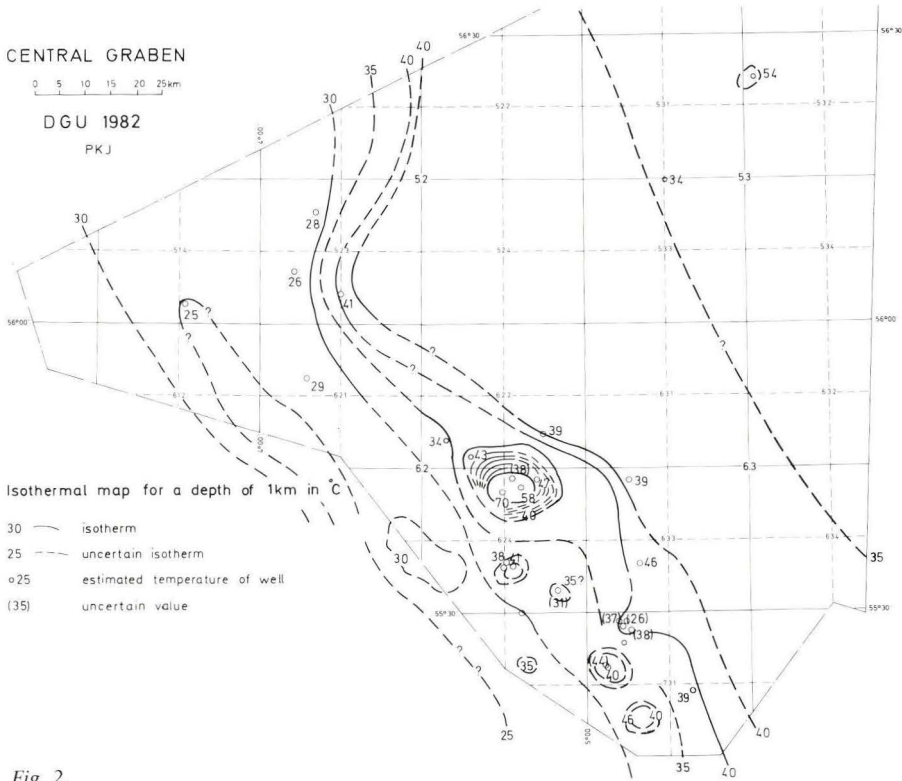


Fig. 2.

Temperature map, 2 km depth, *fig. 3*

Extrapolation or interpolation of temperatures in a well are normally based on the observed gradient in the Tertiary Cen 1–4 Units and the Chalk Group. If this gradient cannot be obtained, an assumed gradient from nearby wells is used. There is no evidence of increasing gradients towards the main faults at the NE-boundary of the Graben. A mean regional gradient for the Cen 1–4 Units and the Chalk Group of 26°C/km is accepted. Above salt structures the gradient is clearly higher. There is no evidence of change of gradient from the Cen 1–4 Units to the Chalk Group.

The higher temperature gradients which may be observed close to the NE-fault boundary are characteristic for the first kilometer only and this tendency disappears for the deeper levels.

The temperature anomaly around the Tyra Field is not seen at a depth of 2 km. The extremely high temperature anomalies which are obtained for the 1 km depth around the Tyra gas field and the normal conditions in 2 km depth could be an indication of escaping formation fluids (or gasses?) towards the



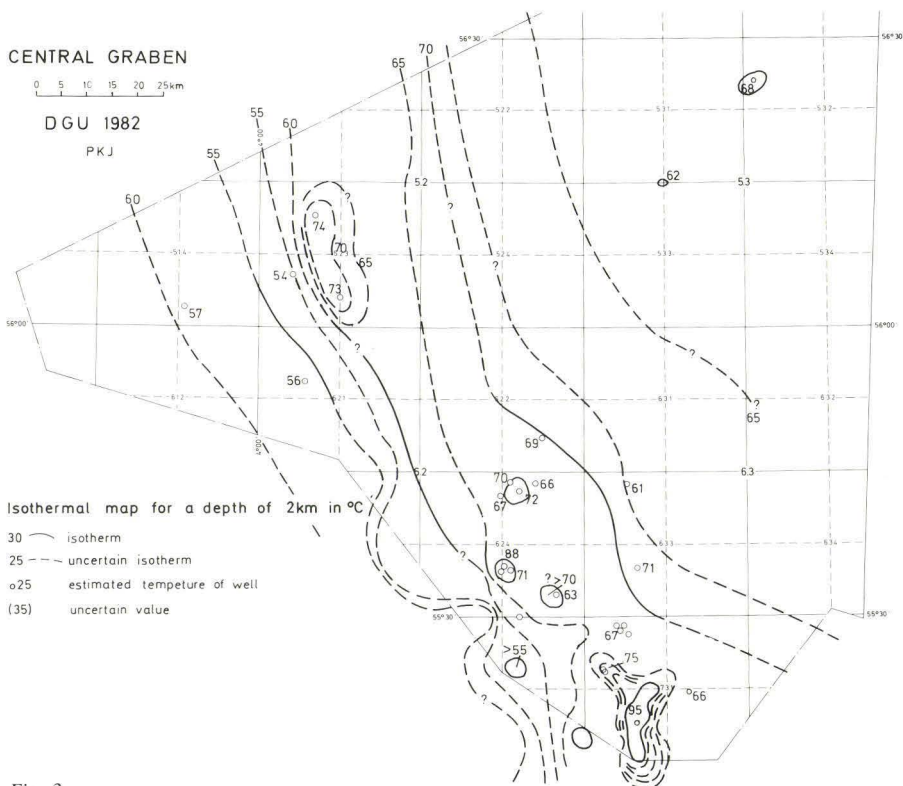


Fig. 3.

surface from a level between 1 and 2 km. In deeper levels temperature conditions seem to be normal.

Depths to Base Upper Cretaceous are found by using approximate depth conversion of two way time map of Top Lower Cretaceous and isopach map of the Chalk Group (Michelsen 1982).

Temperature map, 3 km depth, *fig. 4*

For the calculations of the temperature field for this depth it is necessary to include the value of the mean gradient corresponding to the Lower Cretaceous/Jurassic shales. A regional value of 42°C per km is estimated. This gradient is characteristic for Lower Cretaceous and Jurassic shales, as a high gradient is typical for a high porous overpressured shale. The lower conductivity of the biotumen content will also contribute to a higher gradient. The temperatures are now increasing towards areas with a thick cover of Lower Cretaceous/Jurassic shales making a good insulater (see Top Jurassic

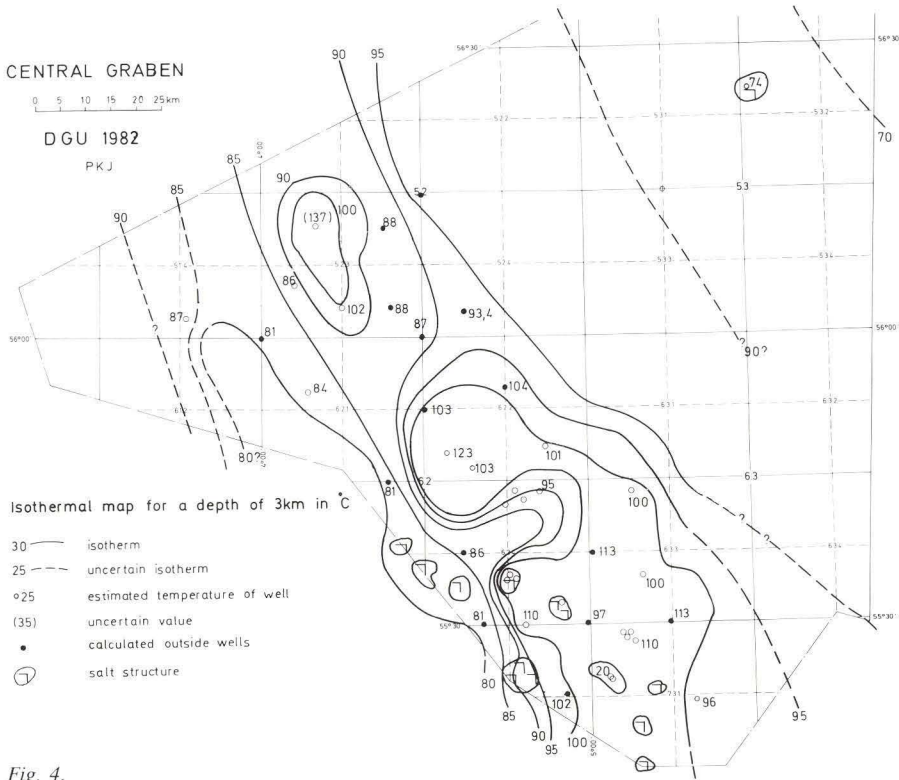


Fig. 4.

temperature map fig. 6). The temperature field around the salt structures in the Southern Saltdome Province is uncertain.

Temperature map, 4 km depth, fig. 5

Temperatures are strongly increasing towards areas with a thick Jurassic sequence, because of the low conductivity of the shales as explained above.

Temperature map, “Top Jurassic”, fig. 6

The “Top Jurassic” isothermal map reflects the major trend of the “Top Jurassic” depth map as the depth is varying considerably. The temperatures are low, about 80°C in the southern part, where the depth to the “Top Jurassic” is about 2300 m and it is increasing towards the NE with maximum about 130°C at a depth of 3600 m. In local, deep subbasins the temperature increases to more than 140°C. For this map the temperature anomalies

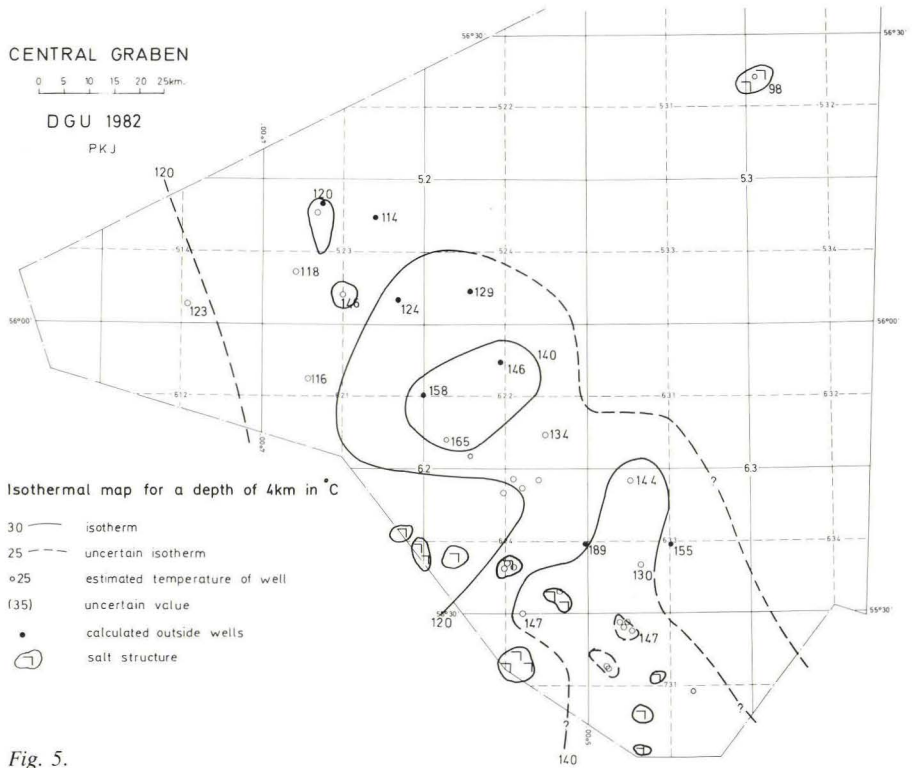


Fig. 5.

around salt structures have not been quantified due to insufficient data. The influence of salt structures is discussed later.

The temperature of about 110°C at the I-1 well is supposed to be locally influenced by the underlying salt.

## Temperature controlling mechanisms

The validity of the temperature maps depends on our knowledge of a number of temperature controlling mechanisms. According to the report: Geology of the Danish Central Graben (Michelsen 1982) chap. 4.0. the main temperature controlling mechanisms may be summarized as follows:

- 1) *Heat flow.* As there are no heat flow determinations in the Danish North Sea sector, we can only guess that the heat flow is enhanced beneath the Central Graben, which usually is the case for graben systems.

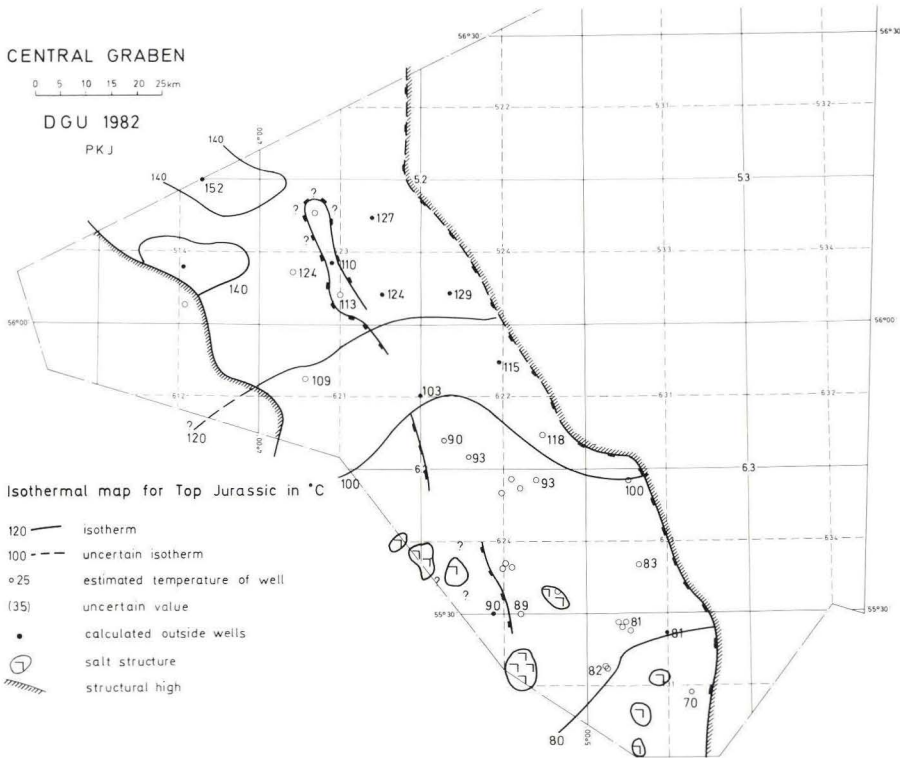


Fig. 6.

- 2) *Influence of salt structures.* Various numerical calculations have been made to determine the influence of the highly conductive salt structures on temperature, i.e. Balling (1978), and Jensen (1983a). It is clear, that there is a positive anomaly around the top of a salt structure and a negative anomaly around the root of the structure.
- 3) *Rock movements.* In the North Sea rock movements caused by faulting or folding are too slow to give any influence on subsurface temperature.
- 4) *Deep circulation of water.* The paper of Andrews-Speed et al. (1982) points out that deep circulation of water influence the temperature distribution in the British North Sea sector. Also Carstens and Finstad (1981) find identification of circulation connected to the fracture system in Norwegian North Sea. The data from the Danish North Sea do not give a definite answer whether deep water circulation influence the temperature field. It may be observed that the temperature gradient at 1 km depth increases towards the main fault boundary at the eastern margin of the Graben. Untill now it seems that the upper 1 km of the unconsolidated





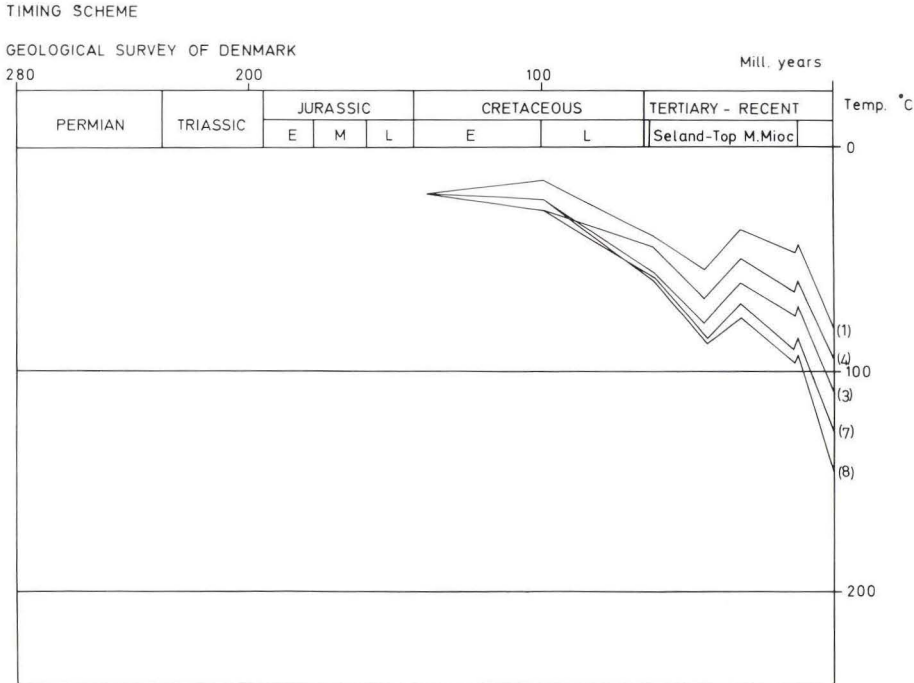


Fig. 8. Temperature of top J-4 Unit. See fig. 1 for localities.

Using depth of top and base of the J-4 Unit through time (see diagrams for the post-Triassic sequence in the Danish Central Graben, Holm 1983) and using recent temperature gradients together with surface temperature as a function of time, temperature at the top and at the base of the J-4 Unit has been estimated, figs. 7-9. The burial depth as a function of time is not corrected for hiati and compaction and the temperature gradients of the formations are assumed constant through time. A simplified surface temperature curve has been used in the present work based on Buchardt (1978) where information about surface temperature during the Tertiary and the Cretaceous is given.

The trend for the Central Graben shows clearly increase of J-4 Unit temperature from the Southern Salt-dome Province towards the northern Tail End Graben (see fig. 8). Assuming equal compounds of organic matter for the whole Central Graben area (an assumption which very well may be violated), we conclude that the maturity increases from south to north. This implies that the oil and gas developed firstly towards the north. Examining figs. 7 and 8 shows that the maturity of the top J-4 Unit at the I-1 well is probably higher than at the E-1 well but lower than the surrounding areas.

TIMING SCHEME

GEOLOGICAL SURVEY OF DENMARK

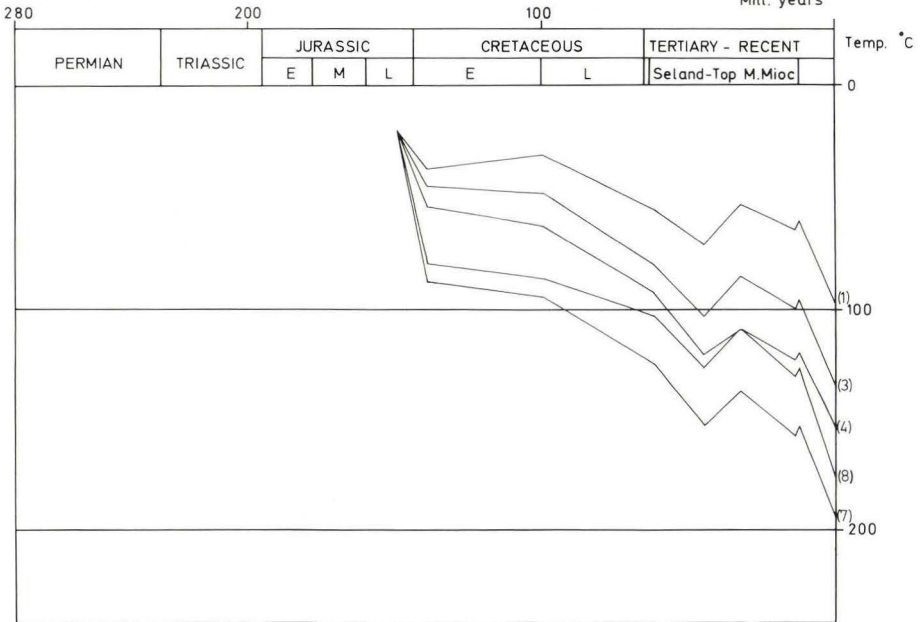


Fig. 9. Temperature of base J-4 Unit. See fig. 1 for localities.

The rise of surface temperature during the Eocene by approximately about 20°C is clearly reflected in the subsurface temperature and there is no doubt that this influence the maturation evolution.

Fig. 9 also shows a similar trend for the base J-4 Unit as for the top J-4 Unit concerning the areas (1), (4) and (7). Enhanced maturation of organic matter on top of salt structures is expected. Examples of this are given in Rashid and McAlary (1977) and Rashid (1978). It must be expected that maturation is restrained for rocks around the bases of the salt structures, due to the negative temperature anomalies there.

### Identification of salt structures

The positive temperature anomalies which may be observed above salt structures are caused by a very high heat conductivity of halite. The structural highs North- and South-Arne are influenced by salt. At North-Arne a thick layer of salt was penetrated at the bottom of the T-1 well. The temperature measured at the I-1 well indicate that also the South-Arne structure is influenced by thick accumulations of salt. If we use high temperature anomalies as

identifications of salt structures, the following structures or fields in the Southern Salt-dome Province are probably situated above salt structures: Gorm, Anne and Vagn.

## Validity of the temperature maps

It is difficult to quantify the uncertainties of the temperature calculations. The difficulties of obtaining reliable temperatures have been discussed by Carstens and Finstad (1981). Uncertainties of the depth to Top Jurassic could be of the order of 600 m, which means an error of up to 25°C in areas, where there are no well control.

The validity of the curves fig. 7–9 is restricted by the lack of a study of hiati, compaction, age of more horizons, past heat flow conditions and past heat conductivities.

## Conclusions

Subsurface mapping has been carried out in the Danish Central Graben based on all the temperature data available. The temperature maps reflect the general geological trend. An increase of temperature gradient from 25°C to 40°C is observed towards the fault boundary of the Graben in the NE-direction for a depth of 1 km. For deeper levels a similar trend cannot be detected. Around the Tyra gas field a positive temperature anomaly is found. A high gradient of 42°C km<sup>-1</sup> is believed to be representative for the Lower Cretaceous and Jurassic shales. Positive temperature anomalies are identified above salt structures. Temperatures for the top J-4 Unit are increasing from about 80°C at the Southern Salt-dome province at depth of 2300 m to about 130°C at the Tail End Graben at a depth of 3600 m. The temperature controlling mechanism seems to be heat conduction, although influence from deep circulation of water cannot be excluded. Temperature through time of the Top J-4 Unit is increasing from the South to the North.

*Acknowledgements.* A special thank is given to O. Michelsen, L. Holm and E. Gosk for constructive advises.

## Dansk sammendrag

Formationstemperaturer er kortlagt i den danske del af Centralgraven (Nordsøen). Temperaturkort gives for dybderne 1, 2, 3 og 4 km. Herudover præsenteres et "Top Jura" temperaturkort. Middelgradienten til en dybde af 1 km viser stigning fra ca. 25°C/km i den østlige del til ca.



40°C/km i den vestlige del. En tilsvarende tendens kan ikke spores i dybere niveauer. En positiv temperaturanomali er konstateret omkring Tyra feltet. En høj middelgradient (42°C/km) i de nedre kretasiske og jurassiske skifre præger temperaturbilledet i disse skifre samt i underliggende formationer. Positive temperaturanomali er konstateret over saltstrukturer. Top J-4 Unit temperaturen stiger fra ca. 80°C i den sydlige del af Centralgraven i en dybde af 2300 m til ca. 130°C i den nordlige del i en dybde af 3600 m. Temperaturbilledet kan forklares ved varmeledning, men dyberegående cirkulation af formationsvand kan ikke udelukkes. Temperaturer for Top J-4 Unit som funktion af tid er stigende fra syd mod nord.

## References

- Andrews-Speed, C. P., Oxburgh, E. R., and Cooper, B. A. 1982: Temperatures and depth dependent heat flow in the western North Sea. (In preparation).
- Balling, N. 1978: Geofysiske metoder til lokalisering af geotermiske energiresourcer. Dansk geol. Foren., Årsskrift for 1977: 13–27.
- Buchardt, B. 1978: Oxygen isotope palaeotemperatures from the Tertiary North Sea area. *Nature*, 275: 121–123.
- Carstens, H. and Finstad, K. G. 1981: Geothermal gradients of the northern North Sea Basin, 59–62 degrees North. *Petroleum geology of the continental shelf of North-West Europe*: 152–161.
- Evans, T. R. and Colemann, N. C. 1974: North Sea geothermal gradients. *Nature*, 247: 29–30.
- Holm, L. 1983: Subsidence history of the Jurassic sequence in the Danish Central Graben. *Danm. geol. Unders., Årbog 1982*: 39–51.
- Jensen, P. K. 1981: Geotermiske modelberegninger ved endelige elementers metode og analytiske metoder specielt med henblik på saltstrukturer. Upubliceret specialearbejde, Inst. for Geofysik, Københavns Universitet.
- Jensen, P. K. 1983a: Calculations on the thermal conditions around a salt diapir. *Geophysical Prospecting*, 31, 3: 481–489.
- Jensen, P. K. 1983b: Principles of temperature mapping. *Danm. geol. Unders., Årbog 1982*: 87–90.
- Madsen, L. 1975: Approximate geothermal gradients in Denmark and the Danish North Sea sector. *Danm. geol. Unders., Årbog 1974*: 5–16.
- Michelsen, O. (edit.) 1982: *Geology of the Danish Central Graben*. *Danm. geol. Unders., Ser. B, No. 8*: 1–133.
- Oxburgh, E. R. and Andrews-Speed, C. P. 1981: Temperature, thermal gradients and heat flow in the southwestern North Sea. *Petrol Geol. Cont. Shelf North-West Europe*: 141–151. Institute of Petroleum.
- Rashid, M. A. 1978: The influence of a salt dome on the diagenesis of organic matter in the Jeanne d'Arc Subbasin of the northeast Grand Banks of Newfoundland. *Organic Geochemistry*, 1: 67–77.
- Rashid, M. A. and McAlary, J. D. 1977: Early maturation of organic matter and genesis of hydrocarbons as a result of heat from a shallow piercement salt dome. *Journ. Geochem. Explorat.*, 8: 549–569.

# *Bathichnus* and its significance in the trace fossil association of Upper Cretaceous chalk, Mors, Denmark

Erik Nygaard

Nygaard, E.: *Bathichnus* and its significance in the trace fossil association of Upper Cretaceous chalk, Mors, Denmark. *Dann. geol. Unders., Årbog 1982*: 107–137. 3 pls., København, 1983.

The ichnogenus *Bathichnus* is given a supplementary description. Many cross-sections of side branches, leading away from the main vertical shaft, are described, which should aid in the recognition of the trace fossil in limited exposures such as drilled cores. *Bathichnus* is interpreted to reflect the behavior of an animal, which responded to rapid sediment accumulation by extending its burrow to the new sediment surface.

Trace fossils in redeposited beds may either precede the redeposition, reflect an escape from burial under the redeposited sediment, mirror an adaptation of the animal to rapid episodic deposition, or they may represent the time interval between major depositional episodes.

The diagenetic coronas around the vertical shafts of *Bathichnus* including the paramoudra flints, were developed on chemical gradients away from the shafts. The gradients were established contemporaneously with sedimentation, in part because reducing pore water from below was forced, owing to compaction, to move upwards through the vertical shafts.

*Erik Nygaard, Geological Survey of Denmark, Thoravej 31, DK-2400, Copenhagen NV, Denmark.*

The trace fossil assemblage in chalk includes as one of its more exceptional species *Bathichnus paramoudrae*, which was established by Bromley, Peake & Schulz (1975). The extraordinary dimensions of this long and slender vertical trace fossil would reduce its recognizeability in field exposures and drilled cores were it not for the characteristically associated diagenetic features. The paramoudra flints which may surround the vertical part of the trace are particularly prominent and draw attention to the trace, but also a pyrite enriched corona is often present.

Previous work on the trace fossil and giant flints was reviewed by Bromley et al. (1975), and this stimulated further observations on these structures (Jordan 1981, Clayton 1982, Nygaard 1982, Schmid 1982). Bromley et al. (1975) with hesitation suggested that *Bathichnus paramoudrae* might have been produced by a long nemertean worm or pogonophore, which worked



Fig. 1. The localisation of the study area on top of the Mors salt dome is given in relation to the generalized Upper Cretaceous isopachs (in metres). The studied wells were drilled in a village named Erslev.

its way down into the sediment, and which had a length comparable to that of the trace. Apart from *Bathichnus paramoudrae*, chalk often contains a wide variety of trace fossils (cf. Kennedy 1970), but their sedimentological significance is poorly understood except where they are associated with hardgrounds (Bromley 1975). In the depocenters of the Late Cretaceous sea the trace fossil assemblage is dominated by a few ichnogenera and as an indication of relatively deep water, *Thalassinoides* is sparse (Kennedy 1980). Some depositional implications of the trace fossils in such a setting, suggested by Nygaard (1982), are documented here. In a more general way it has been suggested that the presence in a chalk sequence of only *Chondrites* could mirror relatively fast sedimentation, while *Zoophycos* may be taken to indicate relatively slow deposition (Nygaard, Lieberkind & Frykman 1983).

Upper Cretaceous chalk with contorted internal structures is well known in onshore areas. Brotzen (1945) found thick redeposited units in the Höllviken well, and Steinich (1967, 1972 a,b) described a number of these beds with large lateral extent from Rügen as "subaquatische gleitmaterial". In the German Turonian, Voigt (1962) demonstrated examples of early diagenetic deformation that were as spectacular as those in the Cenomanian of Northern France (Kennedy & Juignet 1974). Despite the early evidence about physical sedimentary processes in chalk, their more general application was not ac-



cepted however, until the investigations in connection with the exploration for hydrocarbons in the North Sea chalk proved redeposited chalk to be common. Gigantic units were interpreted to be redeposited in the Ekofisk field by Perch-Nielsen et al. (1979), but since then, a multitude of types of allochthonous beds have been found (cf. Watts et al. 1980, Kennedy 1980, Hardman 1982, and Ofstad 1983).

An investigation of the Santonian to Maastrichtian chalk, which overlies a salt piercement dome on the island Mors, Denmark (fig. 1), showed *Bathichnus* and other long vertical trace fossils, to be present throughout the sequence in six out of thirty, one meter long drilled cores. The Mors salt dome is situated in the north-western axial part of the Danish Basin. The Late Cretaceous chalk, which covers the salt dome, is relatively thin (600 m) compared to the regional thickness (1000–1500 m). The salt movement was in part contemporaneous with the sedimentation and caused extensive reworking and allochthonous redeposition of the chalk (Nygaard & Frykman 1981). The geologic setting as well as the mode of deposition is therefore comparable to the North Sea.

## Methods

Most of the cores have been studied on the round but carefully smoothed outer surface, where the structures have first been recognized. This must be kept in mind as for instance a photographic figure may show two sections of a linear element, which crosses the core. Some cores have been slabbed to improve the examination of physical sedimentary structures. A three-dimensional impression of a trace fossil has been achieved by carefully digging away the sediment around it. This work was greatly facilitated by weathering of the mineralized trace fill, which expanded and thereby loosened the chalk. For the purpose of better preservation of the structures in the chalk, various techniques have been tested. The oil staining technique (Bromley 1980), which improves the visibility of structures so dramatically on dry outcrop samples, turned the moist cores into an ideal substrate for mildew. Therefore, the photographic technique, which was developed by Bromley (1980), has been the only useful means of visual improvement and has been applied in the cores which contain physical sedimentary structures.

## Description

Most of the long vertical trace fossils, in the cores from Mors, can either



directly be identified as *Bathichnus paramoudrae* or they bear a gross similarity to it and are therefore termed *Bathichnus* sp. The similarities are the vertical dimensions, the sizes of branches, the colouration and the presence of pyrite enriched coronas. These traces are found in five cores, of which mainly two are considered here as they are exceptionally well documented in the material.

*Bathichnus paramoudrae* (plate 1 a) has an almost vertical shaft, filled with light grey structureless chalk. The diameter is 0.5–0.7 cm and the length, over which it can be followed in the core, is 70 cm. Side branches diverge downwards and become horizontal away from the vertical shaft (plate 2).

*Bathichnus* sp. (plate 1 b) has a vertical shaft of a considerably greater diameter than *Bathichnus paramoudrae*. It seems to terminate downwards in

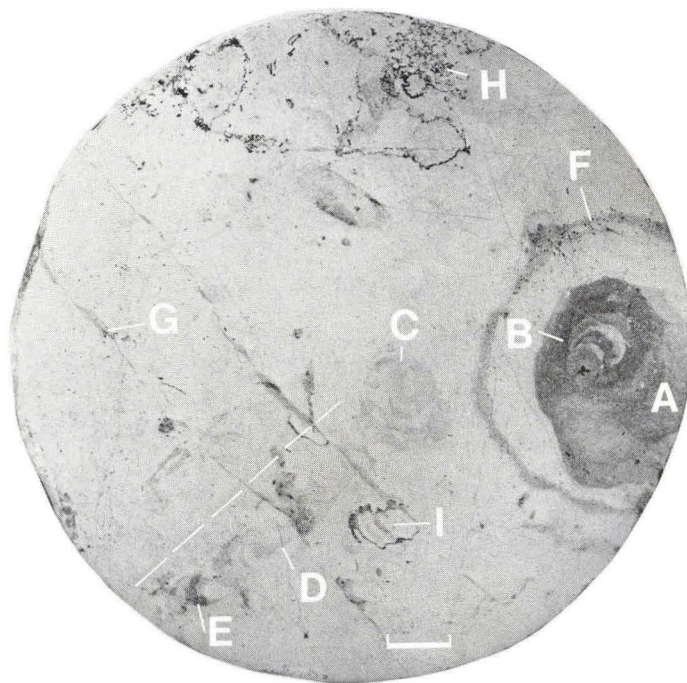


Fig. 2. Horizontal cross section through the *Bathichnus* sp. shaft, A, showing the eccentric and slightly spiralling arrangement of grey and white fill, B. The high colour contrast in the youngest fill (in the centre) fades backwards through successive older generations. Note also the accessory shaft, with similar coarse irregular internal structures, C, which is connected to a side branch, D (stippled). The side branch has backfill structures which indicate movement towards the shaft, E. Pyritic corona, F, fractures, G, stylolite plane, H, and shell fragment, I. Scale bar = 1 cm.

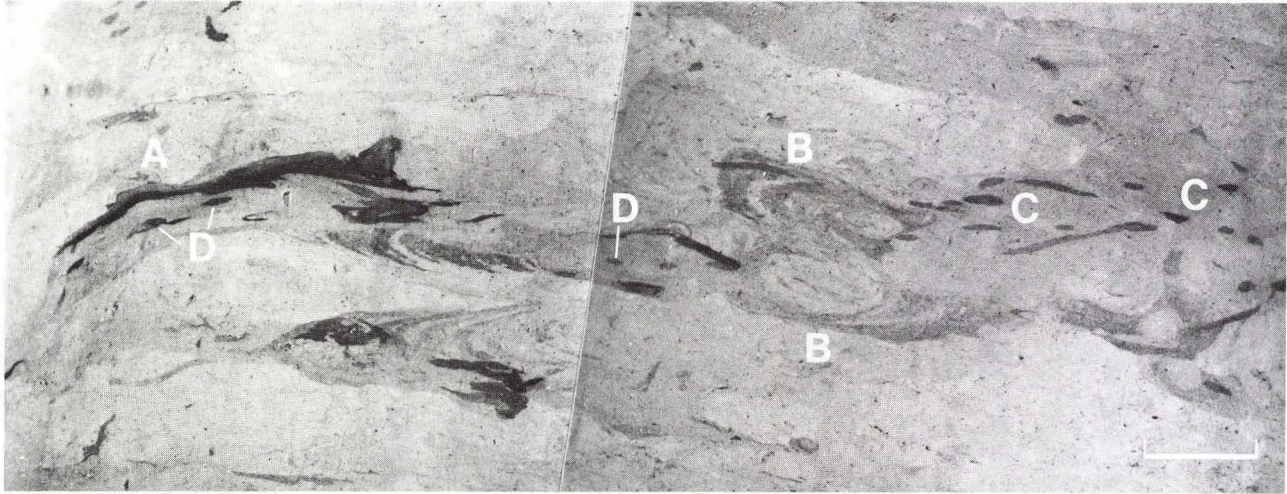


Fig. 3. Side branches of *Bathichnus paramoudrae* which are almost exposed in longitudinal section at A. The internal structures show great irregularity but a concentric system seems to dominate, B. *Chondrites* is present outside the side branches, C, and as reexcavations, D. The figure is composed of two photos of the round core surface. Scale bar = 1 cm.



an expanded chamber from where side branches protrude. The upper part of the *Bathichnus* sp. shaft is 2–3 cm in diameter and the core surface intersects three subhorizontal sections (plates 1 b and 3). In this part of the core the trace fill is homogeneously grey. Midway down the shaft the diameter increases to 4 cm and a pronounced eccentric wall coating system of chalk in grey and white colours is present (fig. 2). The grey/white colour contrast is greatest in the youngest part of the trace fill and fades into homogeneous grey in the oldest part.

The lower bulbous termination of the vertical shaft is 7 cm in diameter and demonstrates a complex relationship between generations of homogeneous grey fill. The youngest fill consists of grey/white wall drapes like the main shaft and more of the successive wall drapes may have glauconite linings. Some of the youngest fill does extend into side branches which protrude from the shaft (plates 1b and 3).

At one side of the main shaft a smaller vertical shaft is present. This accessory shaft has a coarse, irregular, concentric structure and is seen to be connected to a side branch at a cut surface (fig. 2). Downwards the accessory shaft crosses into the main shaft and disappears (plate 3).

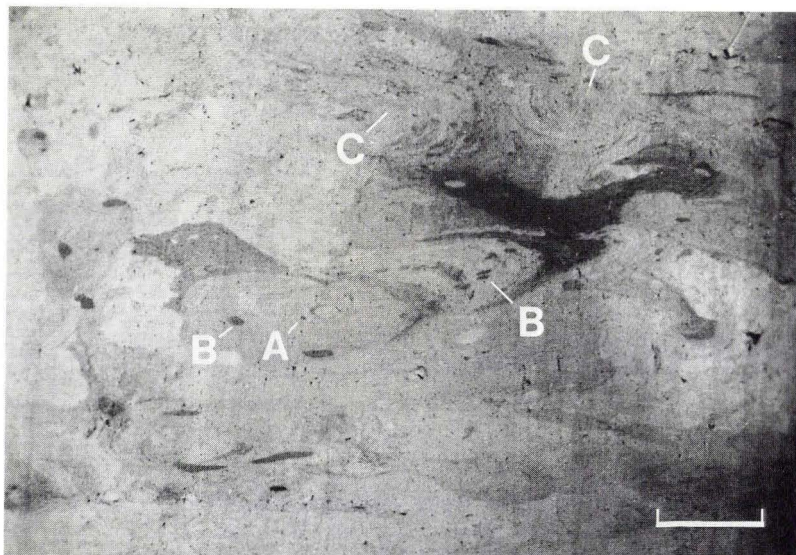


Fig. 4. Oblique section through side branches of *Bathichnus paramoudrae*. Note the concentric internal structures in the final tube, A, and the re-excavation by *Chondrites*, B. Also some other traces which possibly may be side branches have concentric internal structures, C. Scale bar = 1 cm.

*Side branches:* The vertical *Bathichnus* shafts are directly connected to a few side branches at the exposed surfaces. A large number of other sections through side branches surround the shafts and are, with few exceptions, identical for the *Bathichnus* specimens under consideration. The core surfaces intersect most of the cylindrical side branches, which generally appear as ovals, at a high angle and the long axis is mostly subhorizontal. Fully longitudinal sections are not found on the round core surfaces (figs. 3 and 4). The sections through side branches are described in groups with gross similarity:

Sections with homogeneous grey fill (figs. 5 a, d and 6). Often two generations of fill can be seen. The oldest fill constitutes a thin drape on the wall of the trace and totally encircles the next generation (figs. 5 b, c and 7 d). More side branches of this type may overlap (figs. 6 and 7 b), and sometimes the section through the older trace has lenticular shape while the younger is oval (fig. 9 b).

Sections which have a young cylindrical generation of internal fill situated centrally (figs. 7 c and 8). In a third of the cores presented here, in which *Bathichnus* is present, sections through side branches of this type have a young central fill which consists of intraclast containing chalk (fig. 10).

Sections with multiple more or less concentric generations of fill (figs. 3 and 7 d).

Sections with an irregular backfill structure, with a tendency to alternate from side to side. Usually these indicate downward movement in the cross section and have no visible terminal passage (figs. 9 a, c and d). These cross sections are only found in association with *Bathichnus* sp.

Sections with a highly irregular concave periphery filled with two generations of fill. The older is homogeneous grey chalk and the younger is a cylindrical fill with high colour contrast and in a central position (figs. 5 c and 7 a).

Whereas the outer dimensions of the above side branches all correspond to those of the vertical shafts, others have a more dubious relationship. Such a peculiar side branch is found at the top of the *Bathichnus paramoudrae* shaft. This trace system is partly glauconitized and pyritized, and the oxidation upon exposure of these minerals has caused the core to break. In this way the trace has been exposed in three dimensions (fig. 11 a). The trace system consists of flat mineralized sections, up to 1 cm wide and 0.3 cm thick. At the one discovered branching point the mineralisation is thicker. The glauconitized sections have "digging traces" on the surface, some of which are spiralling (fig. 11 b). These sections have abrupt terminations and are intercon-



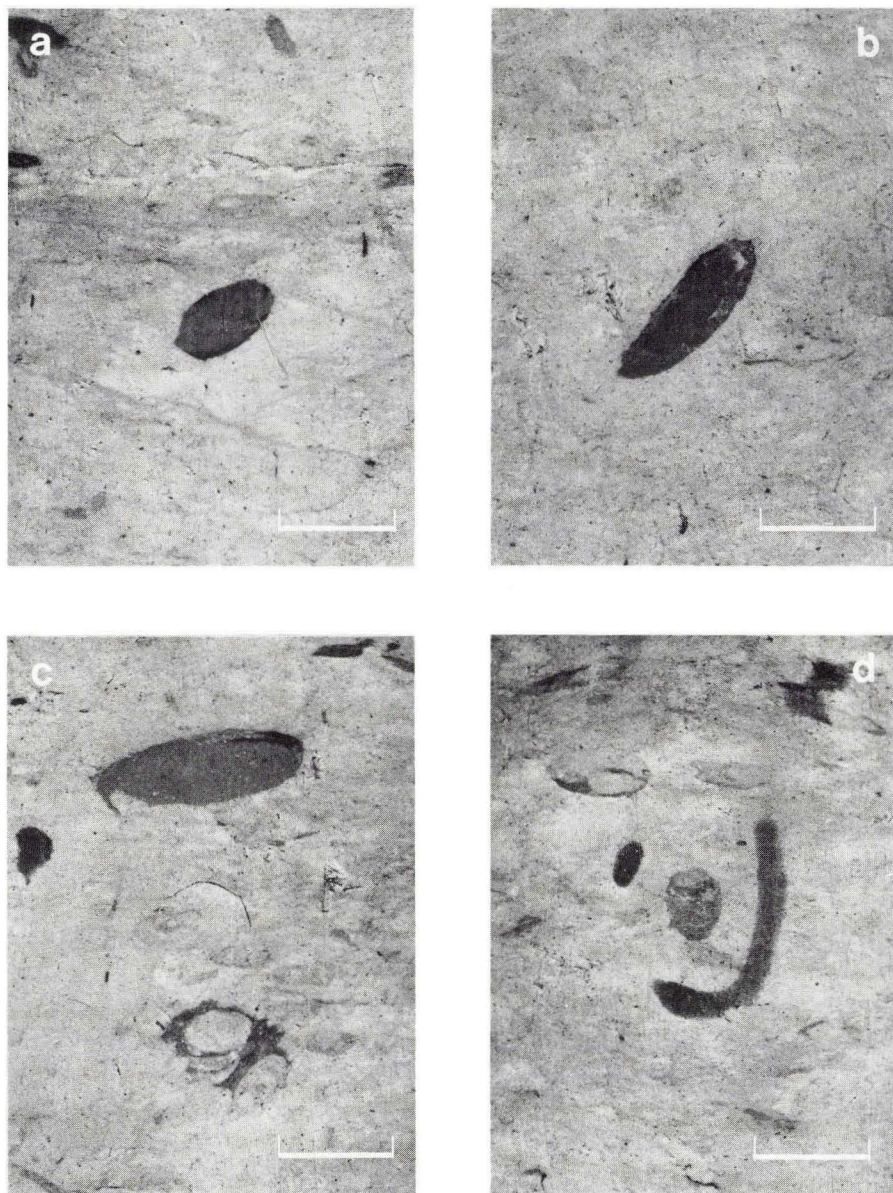


Fig. 5. Cross sections through side branches of *Bathichnus paramoudrae*. There are no linings around the cross sections, but apart from d/ all of them have two generations of fill. The youngest fill which is homogeneous and grey has a large diameter so that only a thin rim of the first generation is preserved. Note the concave periphery and light coloured final fill in the centre of the lower side branch in c/, which resembles *Spongiomorpha*. The side branch in d/ is surrounded by a discontinuous pyritic corona. Scale bar = 1 cm.

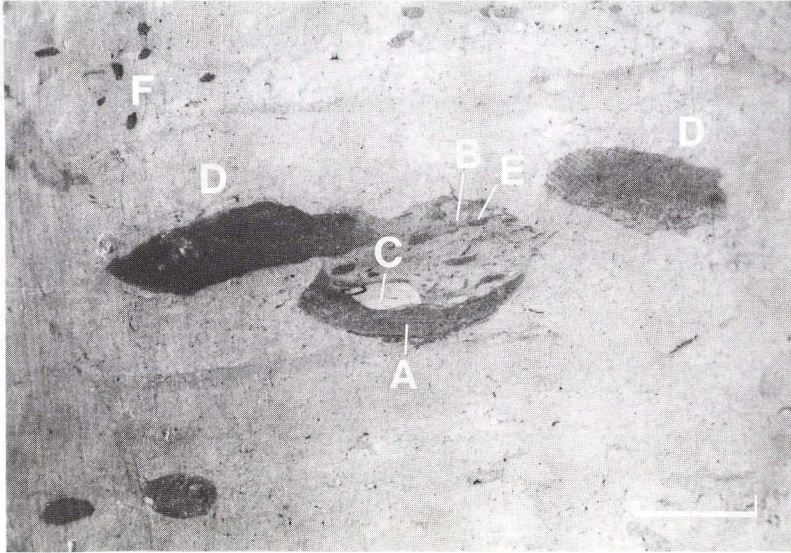


Fig. 6. Cross sections through side branches of *Bathichnus paramoudrae*. Note the relation between the first generation of side branches with homogeneous fill, A, and the first generation of re-excitation which is offset slightly, B. The white, youngest trace fill is fully internal, C. The youngest generation of side branches partly re-excite the former and are filled with homogeneous fill, D. *Chondrites* is found inside one of the generations of side branches, E, as well as outside them, F. Scale bar = 1 cm.

nected through sections of the trace with much smaller diameter (0.1–0.3 cm). This trace system is connected to the vertical *Bathichnus* shaft through straight horizontal, 1–2 mm wide and 2 cm long sections with circular cross sections and light grey fill.

*Other trace fossils: Chondrites*, von Sternberg 1933. *Chondrites* is a common trace fossil in many of the cores from Mors. In the upper third of the core, which contains *Bathichnus paramoudrae*, *Chondrites* is present in characteristic clusters and as reexcavations (figs. 6 and 12). In the middle section of the core, *Chondrites* is sparser (plate 2) and in the lower part of the core, intersections of what may have been single branches in a *Chondrites* cluster are individually scattered and have suffered mechanical deformation (fig. 13). In the core which contains the *Bathichnus* sp., *Chondrites* is very sparse (plate 3).

*Zoophycos*, Massalongo 1855. *Zoophycos* is also common in the chalk on Mors. Within the material considered here, only two windings of *Zoophycos* are present in the topmost part of the core which contains *Bathichnus*



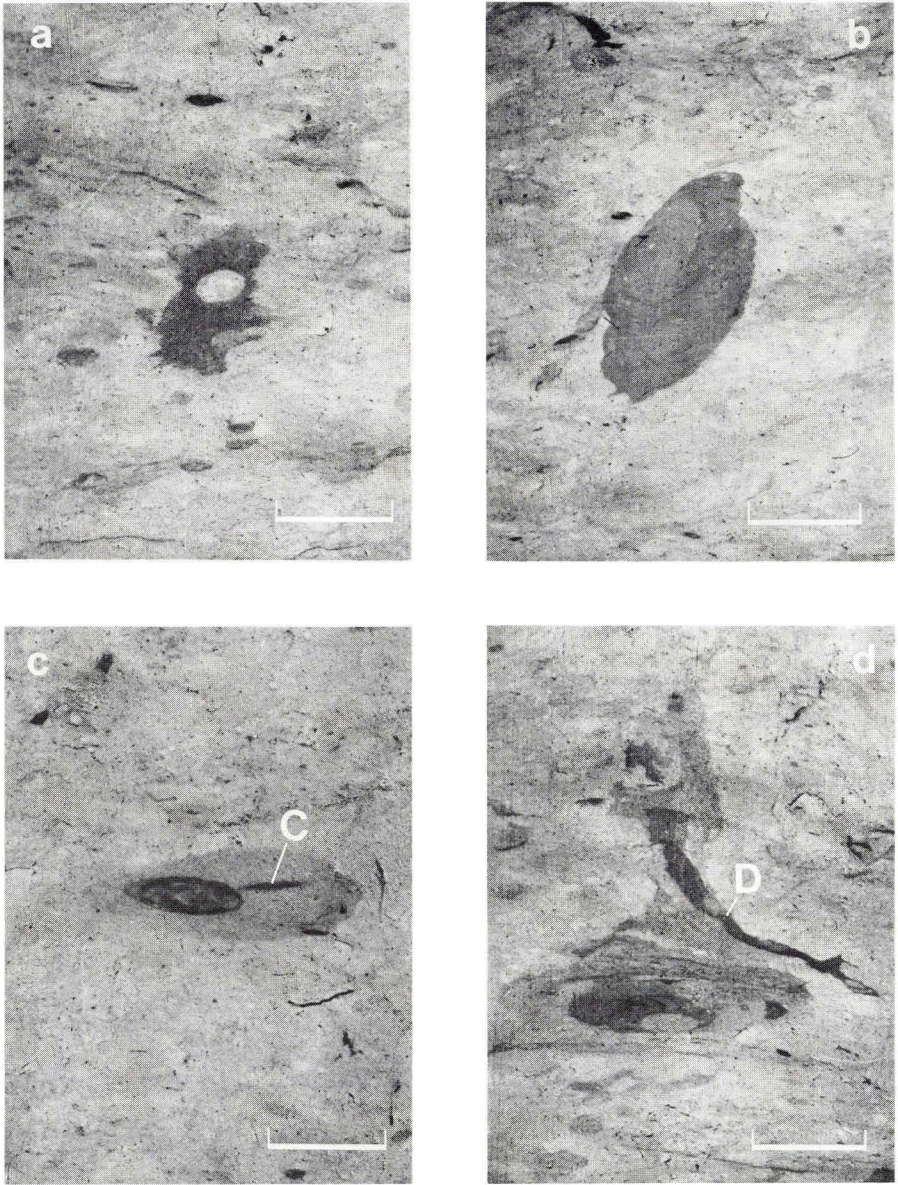


Fig. 7. Cross sections through side branches of *Bathichnus paramoudrae*. a/ a *Spongiomorpha* like side branch with concave periphery and light coloured central fill. b/ overlapping branches which show that the first lower side branch has been first filled and then re-excavated by the upper. The internal structures indicate that the side branches were gradually filled. c/ faint side branch with dark fill in the centre. Also *Chondrites* may be present, C. d/ cross section with multiple "concentric" wall drapes which totally encircle each other. The significance of the long slender trace, D, is uncertain. Scale bar = 1 cm.

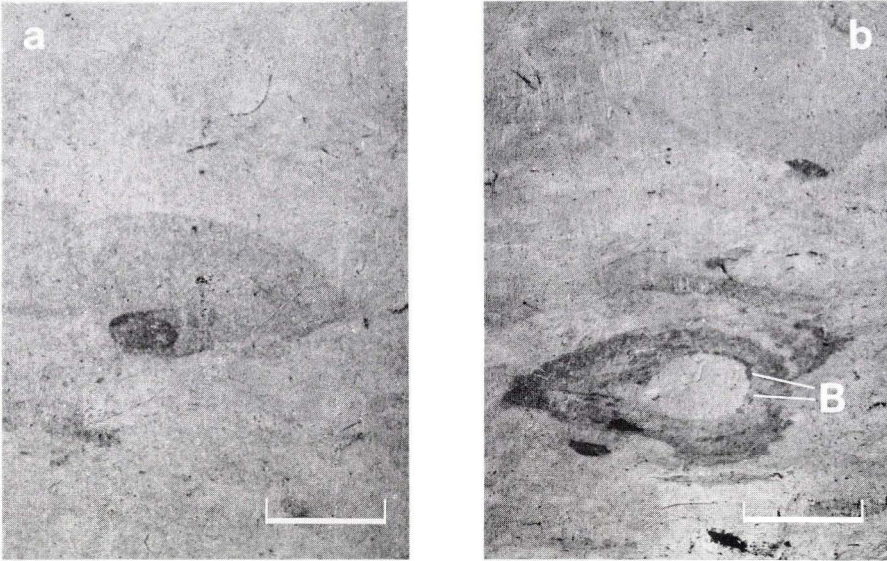


Fig. 8. Cross sections through side branches of *Bathichnus paramoudrae* with young cylindrical fill. a/ faint section with dark terminal fill at the lower edge. b/ section with light coloured central fill and small *Chondrites*, B. Scale bar = 1 cm.

*paramoudrae* (plate 2 and fig. 11a). As mentioned for *Chondrites*, some of the trace fossils in the lower end of the core which contains *Bathichnus paramoudrae* have suffered physical deformation. This is evident in fig. 13, which, apart from deformed *Chondrites*, shows a large trace that has been sectioned by a number of parallel subhorizontal planes of slight movement. The mechanical distortion of the biogenic structures in the chalk is even more prominent in other cores in which the rock largely consists of intraclasts. Here, trace fossils have in a few examples survived as intraclasts, although they are strongly deformed due to the packstone texture of the rock (fig. 14). Some of the intraclast containing sedimentary units in the Mors chalk are rather thick (> 70 cm, Nygaard & Frykman 1981) and in one of these, a special trace fossil is present. This trace is a straight, vertical hairline, with circular cross section. Its diameter is a fraction of a mm, and often it is filled with micro crystalline pyrite. The trace is referred to *Trichichnus*, Frey 1970 although it is considerably longer than the type. The chalk in the immediate vicinity of *Trichichnus* is enriched in micro crystalline pyrite and it transects an entire allochthonous unit unaffected by its internal structures (figs. 15 and 16).



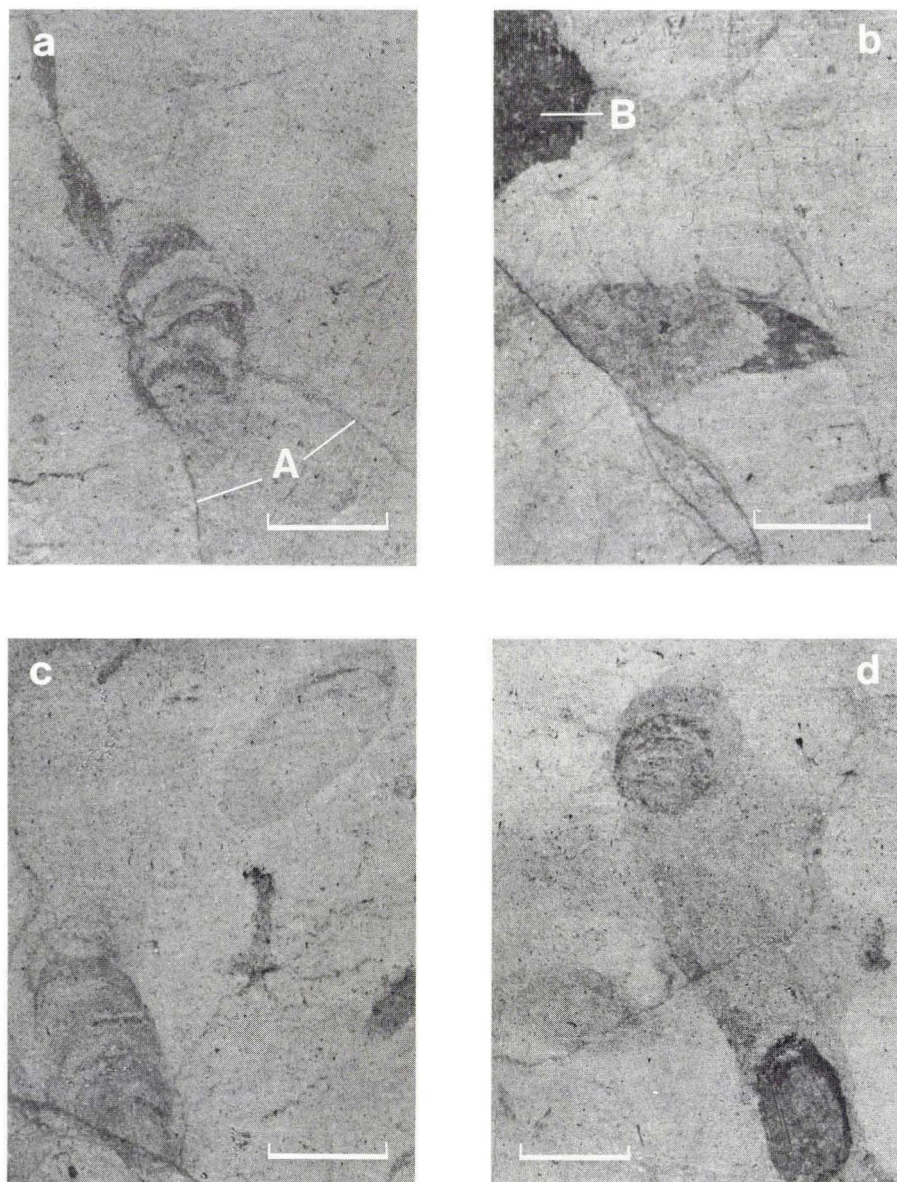


Fig. 9. Cross sections through side branches of *Bathichnus* sp. a/ section with irregular backfill which indicates downward movement. There is no terminal passage. Fractures, A. b/ a side branch with lenslike periphery re-excavated in a slightly offset position by a side branch with oval shape. This suggests the chalk to have been compacted in between the two excavations. B is the basal part of the vertical shaft. c/ faint sections, – one with subtle concentric internal structures and the other with backfill indicating downward movement like in a/. d/ faint section through steeply inclined side branch which is re-excavated by other side branches. One of these has backfill. Scale bar = 1 cm.

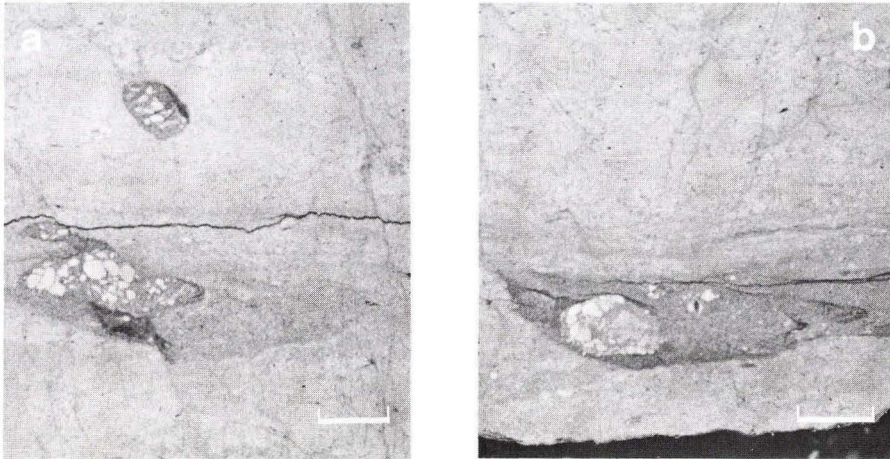


Fig. 10. Side branches of *Bathichnus* from a third core. Note that the central fill consists of a packstone of chalk intraclasts in a darker chalk matrix. This demonstrates that the central cavities in the side branches were open until they became suddenly filled with allochthonous material. Erslev 3S, core 4. Scale bar = 1 cm.

*Burial and diagenesis:* The vertical main shafts of *Bathichnus*, and one of the side branches are surrounded by a corona of chalk, which is enriched in micro crystalline pyrite, fig. 5 d. This corona is most prominent along the basal part of the shafts and has a distance of up to one cm from it. In other instances the corona is situated in the outskirts of the shaft itself (plate 3).

A broader and less easily recognized zone of relatively light coloured and hard chalk also surrounds the vertical *Bathichnus* shafts. Flint is only present within the cores under consideration as a small irregular body, which directly surrounds the *Bathichnus paramoudrae* in its upper end (plate 2). Small fractures and faults are present throughout the cores and they are especially frequent in the core with the *Bathichnus* sp., where also stylolites are abundant. The stylolites have up to two mm thick clay drapes, which split up into horsetail structures where they intersect the vertical shaft of the *Bathichnus* sp. (plate 1 b).

## Results and discussion

*Characterisation of Bathichnus:* The three trace systems, the *Bathichnus paramoudrae*, *Bathichnus* sp., and the shaft associated with *Bathichnus* sp. possess important similarities but also noteworthy differences. The points of similarity are the dominating outer dimensions of side branches and reexca-



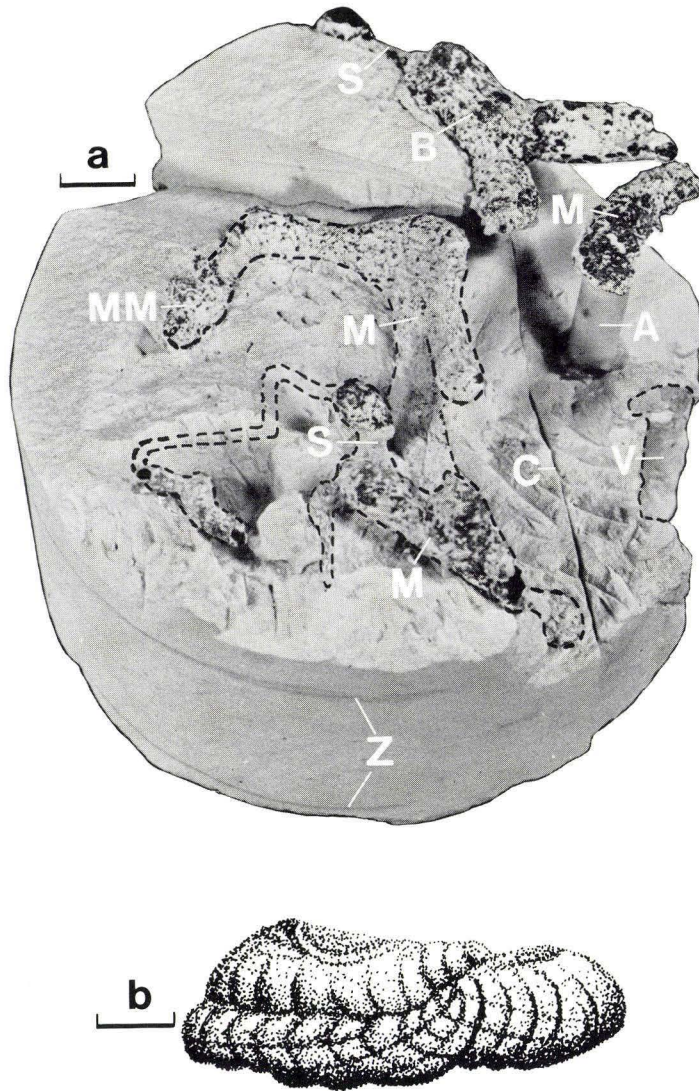


Fig. 11. The upper part of the *Bathichnus paramoudrae* exposed in three dimensions. a/ note the presence of *Zoophycos*, Z, the vertical shaft, V, the glauconite and pyrite mineralized sections of side branches, M, one of which does branch, B, and the small diameters of the trace between the mineralisations, S. Artificial support, A, Saw cut, C. Scale bar = 1 cm. b/ a mineralized section of a side branch in side view, showing slightly spiralling "digging marks". This mineralisation is indicated by MM on fig. 11a. Scale bar = 2 mm.



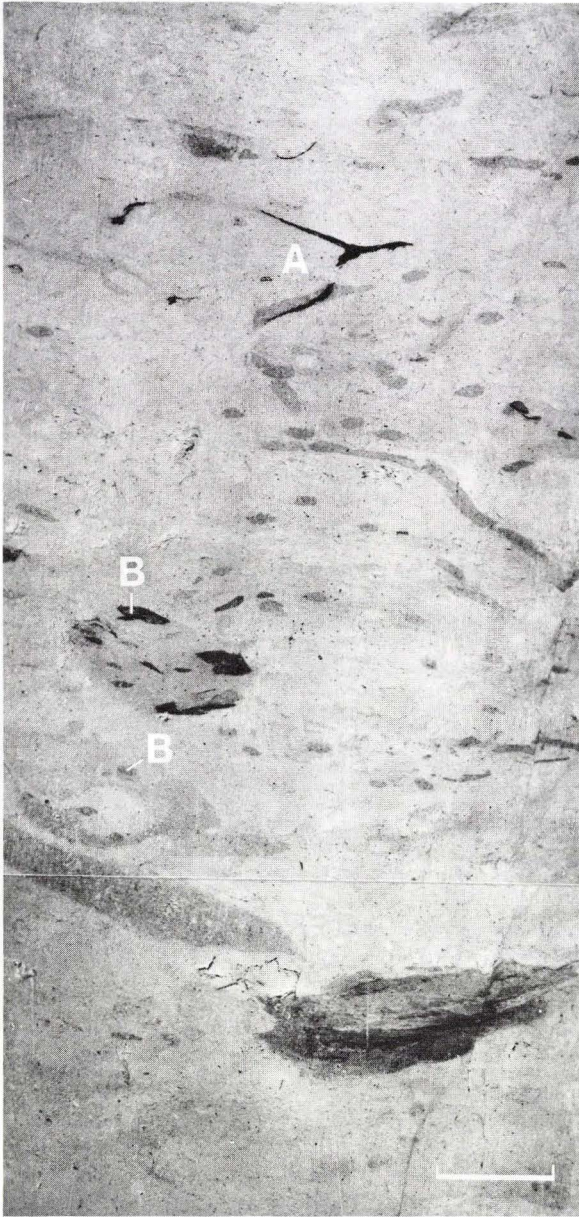


Fig. 12. Chondrites in characteristic clusters in the matrix, A, and inside side branches, B. From the upper part of the core which contains *Bathichnus paramoudrae*. Scale bar = 1 cm.

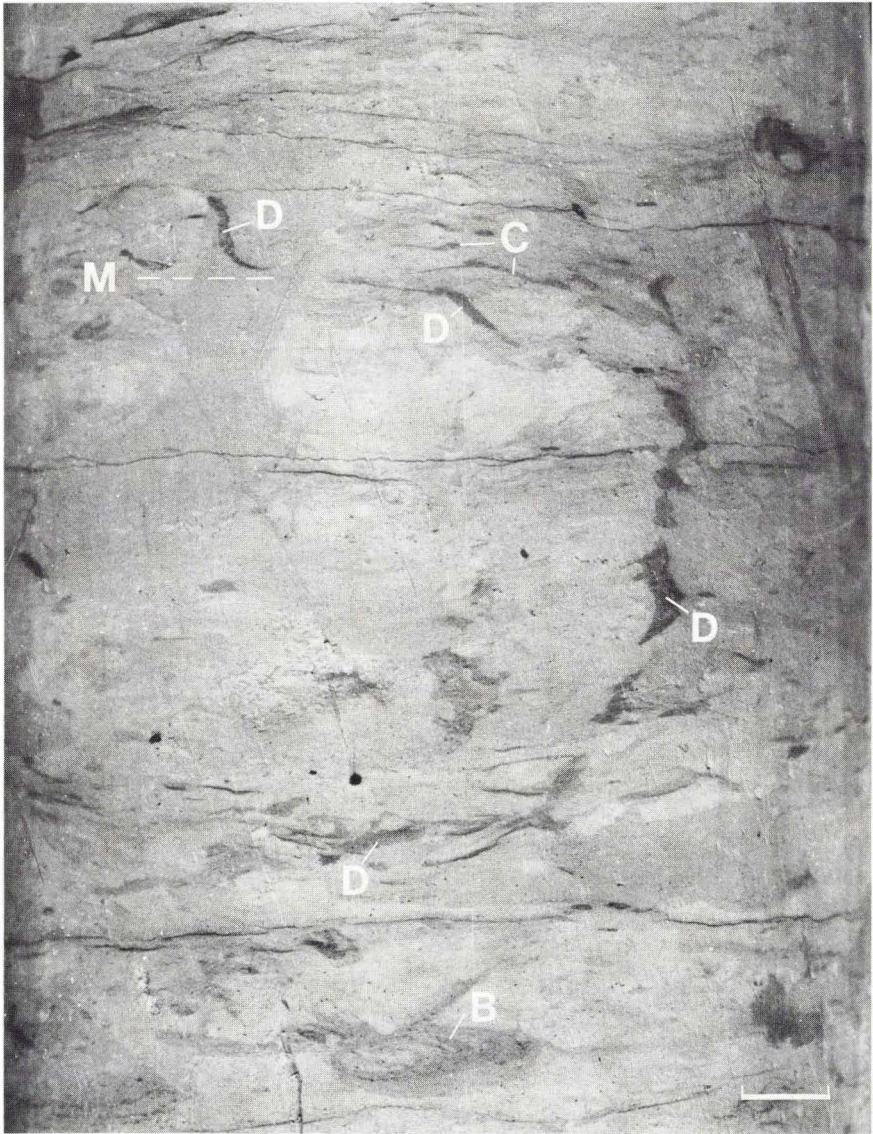
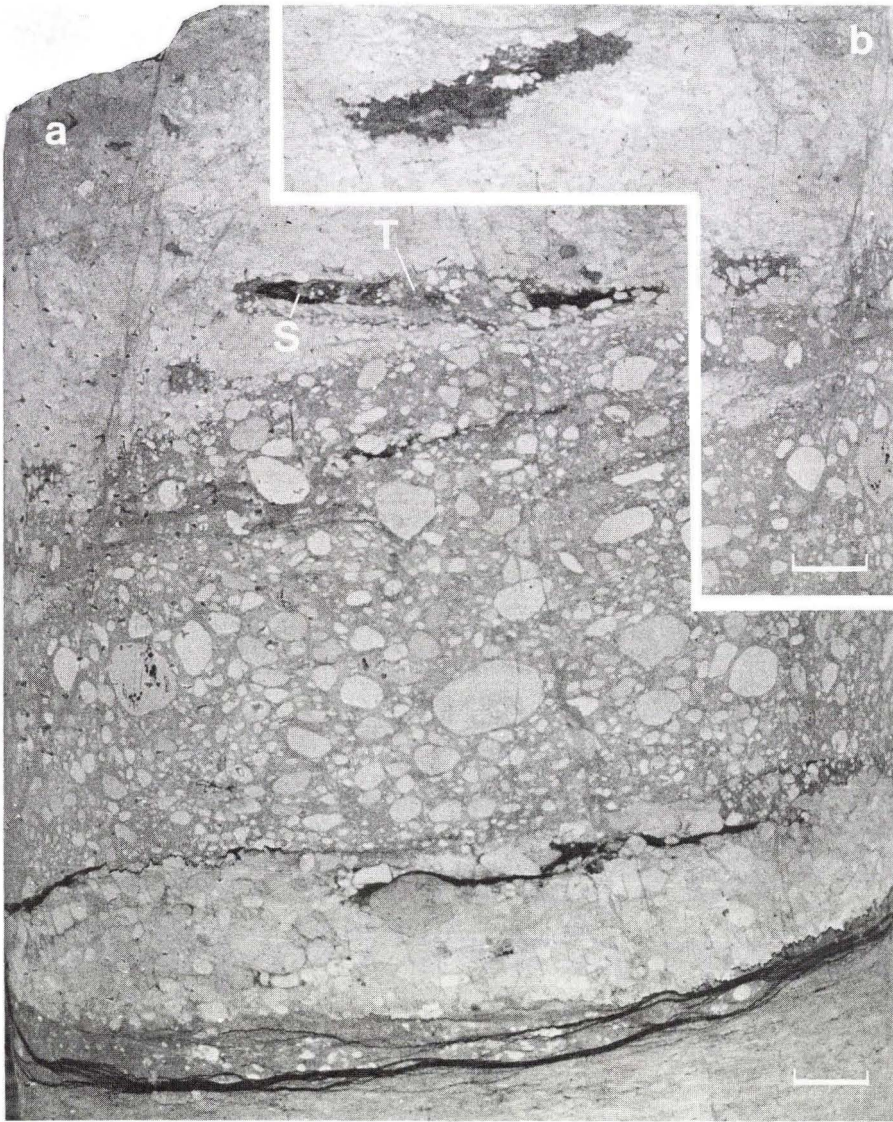


Fig. 13. Deformed trace fossils in the lower slightly marly end of the core which contains *Bathichnus paramoudrae*. Individual sections of smeared out *Chondrites*, C. Discontinuous deformed trace, D, which is sectioned by horizontal planes of movement, M. Side branches of *Bathichnus* are undeformed, B. Scale bar = 1 cm.





*Fig. 14.* Trace fossils that predate an episode of redeposition and which have behaved as relatively buoyant intraclasts. a/ a trace fossil with internal backfill or spreite (S), which is isolated in a rock which consists of fine intraclasts. A tongue of the intraclast containing host rock is injected into the trace (T). b/ an other example where the surrounding intraclasts have severely deformed the periphery of the trace. Erslev 3S, core 4. Scale bar = 1 cm.





Fig. 15. The lower end of a very long, straight, and vertical *Trichichnus*. The lower end of the trace coincides with the basal part of a debris flow (see Nygaard & Frykman 1981). Note the black microcrystalline pyrite inside the trace and the pyrite enriched zone around the trace. See the continuation of the trace on fig. 16. Erslev 3S, core 2. Scale bar = 1 cm.

vations, the presence of a long vertical shaft from which side branches diverge, and the presence of identical internal structures in the majority of side branches associated with the *Bathichnus paramoudrae* and *Bathichnus* sp. trace systems. The differences comprise variations in outer diameters of the shaft, colourations, presence of absence of eccentric internal structures, and the presence of reexcavations in the wide lower end of the *Bathichnus* sp. shaft.

Here the similarities are considered to be most important as already indicated through the naming of *Bathichnus* sp. The close relationship is further



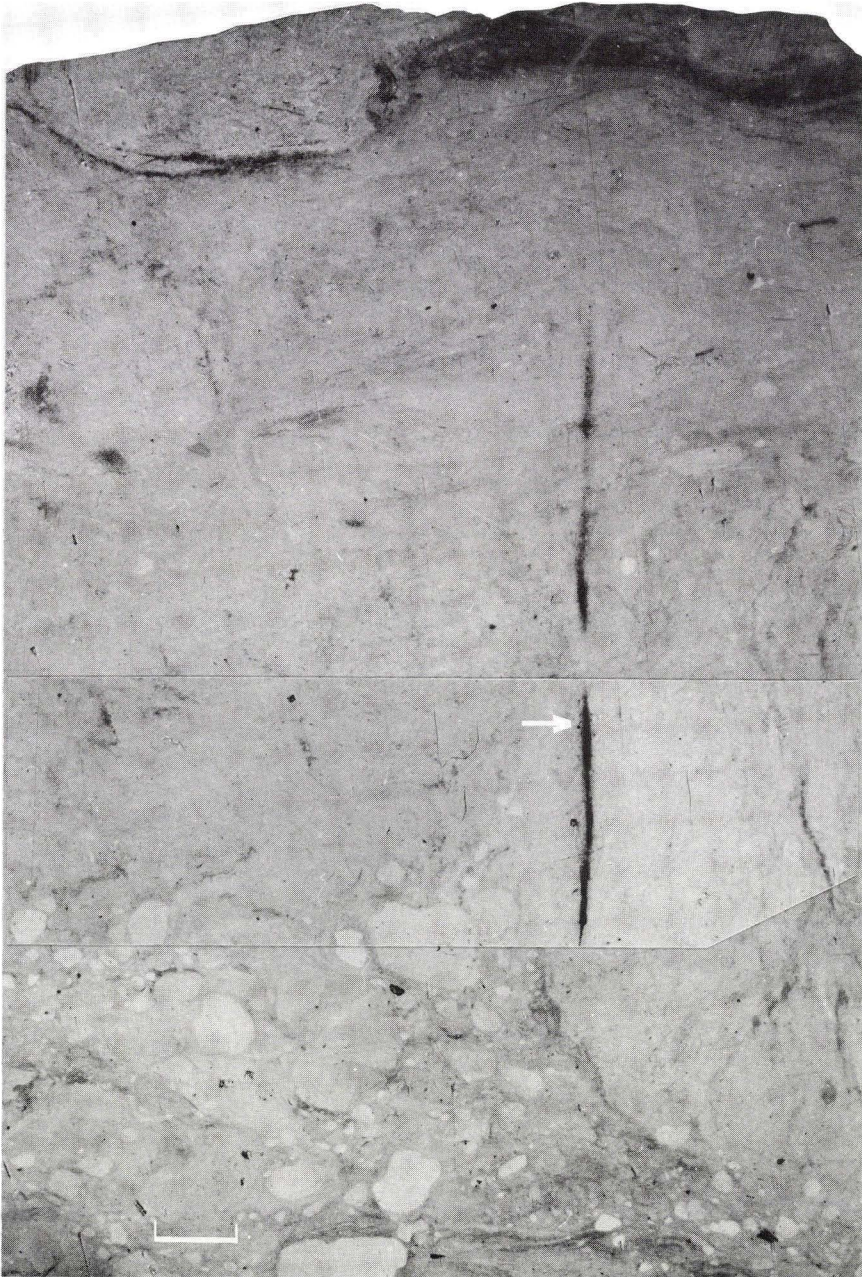


Fig. 16. The central part of the long vertical *Trichichnus* which transects an entire re-deposited unit (> 70 cm thick). Note that the trace transects the matrix unaffected by its internal structures. See also fig. 15. Erslev 3S, core 2. Scale bar = 1 cm.

stressed by the direct entry of the accessory shaft into that of *Bathichnus* sp. in its lower end (plate 3). According to the original description by Bromley et al. (1975), only the trace fossil in plate 1a can be assigned to the ichnospecies *Bathichnus paramoudrae*. The present examples suggest a need for extending the diagnosis of the genus to: Burrows that comprise vertical shafts 0.2–7 cm, typically 0.5 cm in diameter and up to 9 m long, from all parts of which side branches with diameters from 0.2–1.5 cm diverge irregularly.

Of greater importance, however, than this suggested revision of diagnosis is the supplementary description of the side branches. Knowledge of the variability, in the side branches especially, will facilitate the future recognition of *Bathichnus* in drilled cores, in which there is normally little chance of encountering the vertical shafts.

Individual cross sections of the vertical shafts and side branches of *Bathichnus* could easily and correctly have been assigned to a variety of the trace fossil genera that are well known from onshore areas, see Kennedy (1970) and Bromley (1975). Most noteworthy is the resemblance between some of the side branches and *Planolites*, Nicholson 1873 (figs. 5 and 6) *Thalassinoides*, Ehrenberg 1944 (plate 1b), and *Spongeliomorpha*, de Saporta 1887 (figs. 5c and 7a). It is therefore essential to note, that the present material invites the suggestion that *Bathichnus* is characterized by a great variety in types of side branches and shafts.

Most side branches have more generations of fill, which lines the walls in what seems to be a cylindrical manner, rather than as backfill. Good longitudinal sections which could clarify the question are not present, however (figs. 3 and 4).

A special interpretational problem is posed by the mineralized side branch (fig. 11). Although it is connected to the *Bathichnus paramoudrae* shaft it has not been possible to verify with certainty that this is anything but a random intersection of the shaft by a later independent trace. The dimensions of this trace, however, and the behaviour it seems to reflect, does suggest that it may be a part of the *Bathichnus* trace system.

The side branch, which is connected to the accessory shaft, has irregular backfill structures which indicate that it was filled from the distal end towards the shaft (fig. 2). Other sections through side branches also have irregular backfill (fig. 9a, c, d). This means that the animal, in some cases, relocated the worked chalk within the trace system. Some steeply inclined side branches have retrusive backfill structures (fig. 9 a,c). It is possible that these side branches are connected in their lower ends to other side branches or to a shaft since the animal is unlikely to have disappeared downwards.

Bromley et al. (1975, plate 5E) found a slender internal structure in the *Bathichnus paramoudrae*, which spiralled slightly down the vertical shaft.



Spiralling is also reflected here (fig. 2), and is therefore apparently a fundamental, behavioristic pattern in the vertical shafts. A spiralling behaviour is reflected too, in the peculiar glauconite mineralized side branch system (fig. 11 b) and finally the side branches are often reexcavated in a slightly offset position (figs. 6, 7b and 9b). The spiralling arrangement of fill in the shafts may be the result of climbing. A slender worm in a wide, open hole can only climb it from the bottom by applying a, *in casu* spiralling, contact to its walls (fig. 2), unless it swims. Further, in most sections through the trace system, the youngest trace fill occupies a narrow cylindrical space in the center of older generations. A genetic model for the trace system must account for these observations.

*The animal:* Bromley et al. (1975) tentatively suggested “a predatory or filter feeding nemertinean worm or pogonophore” to have produced *Bathichnus paramoudrae*. If only one genus is responsible for the trace, the Mors material would suggest it to have been a deposit feeding worm: The side branch system with strongly varying diameter (fig. 11a) has “digging traces” on the surface of its glauconite mineralized parts. The causal animal must thus have been slender enough to enter through the narrow (0.2 cm) passages and might have widened the intervening sections by eating its way along the chalk wall of the trace in a spiralling manner (fig. 11b).

The apparent contradiction, between the smaller diameter of the youngest trace fill in most cross sections of the *Bathichnus* system and the larger outer diameter of the entire trace, may be explained by the behaviour of the speculative animal. The pattern seems to reflect a widening of the trace to a diameter which is larger than the diameter of the animal (figs. 2, 7a, c, d and 8). A slender, deposit feeding worm, could have produced a relatively wide burrow in the sediment, by eating it up to what seems to have been its customary diameter of action (0.5–0.6 cm). This is the diameter of the *Bathichnus paramoudrae* and most of the side branches. Referring all the traces and structures in the *Bathichnus* trace system to one causal animal or animal species is not necessarily correct, although the possibility has been argued above. *Bathichnus* may well be a polygenetic trace fossil, reflecting that a group of animals utilized a vertical shaft over, may be, even more generations.

Bromley et al. (1975) suggested with hesitation, that the trace producing animal had a length comparable to the maximum length of the vertical shaft, which is up to 9 m. In the light of the behavioral and sedimentological considerations given above, it is not necessary to consider a burrowing animal with such exceptional dimensions, although it is still considered to have been very slender.

*The trace-sediment relation:* The lower end of the thick *Bathichnus* sp. shaft has more generations of homogeneous fill, which have been repeatedly reexcavated by shafts and side branches. As the reexcavations are, in turn, filled by several generations of wall draping sediment, the open trace must now and then have become narrower until it was finally totally filled.

The sediment that fell into the vertical shaft and the side branches, must have been loosely packed and it partly or fully filled the trace. Despite this infilling, the animal seems to have preferred to stay on *locus* and it just pushed the fill aside, and maybe removed a small amount by reexcavation. Sometimes the traces were so massively filled with sediment, however, that the animal chose a new route (figs. 7b and 9b) and the old one was abandoned (fig. 10). This could happen at a variety of stages of infilling.

If this interpretation is correct, sediment from the sediment surface was filled into the *Bathichnus* in episodes. The animal stored the sediment on the walls of the burrow whereby its diameter was reduced. The reason why a smaller diameter of the burrow was so often acceptable to the animal, would be that it served for access and not for nutrition when sediment fell into it. The animal thus seems to have gone to great effort to re-open filled parts of the trace before it finally had to abandon it. In this way the animal, which produced *Bathichnus*, was forced to move upwards through the sediment, as a response to deposition of sediment on the sea bottom.

The vertical *Bathichnus* shafts are probably not reflections of a general preference for that orientation, since the side branches are dominantly horizontal, but rather a necessity. Many sections through *Bathichnus* show that sediment was passively emplaced in the open trace system in episodes rather than by active action of an animal. The indications are that after a wall drape was applied, the remaining cavity in the trace occasionally stayed open long enough for glauconite linings to develop, and this may be seen on more of the concentric fills. Another argument is that along a filled part of a side branch a new excavation has often taken place. Finally, intraclasts are sometimes found as fill in the traces. This may be taken to indicate that the animal did not abandon the trace by free will.

The internal structures in *Bathichnus*, and the occasional intraclast containing fill, are thus indirect indications of episodic sedimentation on the sea bottom.

To argue for the latter interpretations, it is necessary to consider also, the physical sedimentary structures of the chalk matrix as well as other trace fossils. The *Bathichnus paramoudrae* is found in a core which is rich in signs of gentle physical deformation in the lower part (fig. 13). The loss of physical sedimentary structures upwards through the core, combined with the simultaneous gain of *in situ* trace fossils other than *Bathichnus*, suggest the entire

core to represent a single depositional event. The deformed traces at the base indicate that the sediment had been burrowed before the final deposition. The cored interval can therefore be taken to consist of allochthonous chalk. The *in situ* *Chondrites* and *Zoophycos* in the top of the core must have been produced by animals, which populated the upper surface of the settled allochthonous unit. The presence of a *Bathichnus* shaft in this unit, suggests that the vertical orientation of the shaft was applied as a response to rapid sedimentation.

The *Bathichnus* sp. is found in chalk where, except for very few *Chondrites*, neither other trace fossils nor bioturbation is present. Also, physical sedimentary structures are absent, and in line with Nygaard et al. (1983) the cored interval may therefore consist of chalk, which was deposited so fast that the infauna, except the one which was responsible for the *Bathichnus* sp., had difficulty in surviving.

The *Bathichnus* sp. shaft continues in subhorizontal sections in its upper part. This is a well known feature, since many sections of vertical shafts in field exposures are inter-connected in this way (Bromley et al. 1975). In the context of the present interpretation, the subhorizontal sections reflect intermediate stages of slow or non-deposition.

The reason why the deeper part of the *Bathichnus* trace system was constantly reexcavated could likewise be the fast episodic deposition, which would leave comparatively many nutrients in the deeper levels (Seilacher 1978). These levels may have been abandoned when they were out of reasonable reach rather than because their content of nutrients was exhausted.

The use of trace fossils to designate the topmost part of depositional beds, is well-known from siliciclastic as well as carbonate turbidites (e.g. Seilacher 1962, 1978, Scholle 1971, Robertson 1976, Ekdale 1980), and Nygaard (1982) suggested a similar significance for the chalk on Mors.

If on the other hand the deposited sediment units are thin, the bioturbation will erase the bed boundaries. The preserved traces, from the "historic layer" (Berger et al. 1979), will therefore in this case constitute one continuous sequence in which the trace fossil genera, rather than their relation to bed boundaries, characterize the rate of sedimentation (Nygaard et al. 1983).

It is possible that the present interpretation of *Bathichnus* has a wider application since there is a close resemblance between some of the side branches presented here and the trace fossils referred to *Asterosoma* von Otto 1854, by Chamberlain (1978, figs. 81–83). This would support Frey & Howard's (1970) documentation, that identical behavioral patterns are sometimes reflected in the chalk and siliciclastic sand environments.



*Physical deformation:* The inferences about the genesis of *Bathichnus* and mode of sedimentation are supported by physical signs of rapid and allochthonous accumulation, which are known to be common in the Mors area (Nygaard & Frykman 1981). The deformed trace fossils at the base of the core which contains *Bathichnus paramoudrae* must obviously have had almost the same buoyancy as the sediment around them, when the deformation took place. But other examples show that trace fossils can also have responded in a buoyant way while the sediment around them suffered brittle deformation (fig. 14). In these cases the pre-redepositional origin of the traces can be verified because intraclasts have deformed their periphery (fig. 14a).

The chalky sediment seems often to traverse the sea bottom by internal sliding along parallel planes during redeposition (fig. 13). This implies a preferential preservation of mechanically isolated horizontal elements. Hereby the preservation of *Zoophycos* is favoured, because it has a pronounced horizontal element, as is possibly the case in Steinich (1972b, fig. 3) and Bromley and Ekdale (1983).

*Trichichnus:* An active response to a major depositional event is reflected in *Trichichnus* which, although it is less than a millimetre in diameter, crosses vertically from base to top through an allochthonous unit (figs. 15 and 16). Similar traces which are up to 6 m long are described by Scholle (1971) from the Monte Antola carbonate flysch. Due to the setting of the trace in the Mors core it is suggested to reflect the escape of a shallow infaunal or surface dwelling animal on the pre-redeposition seafloor, which survived the sudden burial and escaped to the new sediment surface.

*Compaction:* A very early phase of compaction of the chalk on Mors seems to be reflected in some of the *Bathichnus* side branches, which have been reexcavated after an intermediate stage of compaction (fig. 9b). A possible explanation for this early compaction, which is in line with the general interpretation of the *Bathichnus*, is that a major depositional episode caused the side branches in the underlying chalk to be filled. Due to the new load, the chalk sediment was gradually compressed before a new side branch was produced. The main part of the compaction in the chalk on Mors is much later, however, as indicated by stylolites (plate 1b).

*Diagenesis:* The vanishing colour contrast from the youngest back through the older generations of fill in the *Bathichnus* sp. shaft (fig. 2), indicates that the structures in the trace vanished with age until the moment when the shaft was totally filled. From the onwards, the colour contrast of these structures

has remained largely unchanged despite the vast time that has been available. Therefore, homogeneous dark trace fill seems sometimes to be the product of chemical alterations due to ventilation in the central part of the shaft, while it was still used by a burrower.

One of the most characteristic features related to *Bathichnus* is the prominent diagenetic alteration coronas, which are produced on steep chemical gradients away from the vertical shafts (plates 1–3 and fig. 2). These features may consist of an inner corona of micro crystalline pyrite set in a relatively hard chalk, and an outer corona consisting of chert (Bromley et al. 1975). A small flint nodule surrounds the *Bathichnus paramoudrae* shaft (plate 2), but no other flint seems to be present, as neither the drilling rate of penetration was changed, nor the cuttings enriched in flint in the cored interval. Also *Trichichnus* (figs. 15 and 16) is surrounded by a pyritic corona.

The many signs of a biogenic origin of *Bathichnus* which are given here, preclude Jordan's (1982) genetic interpretation of the trace as fluid or gas escape tracks, but his basic concept that the chemical gradients forming the coronas are caused by invasion from below is well in line with these data.

The coronas are related to the vertical trace fossils. As the vertical trace fossils in turn seem to be related to fast and episodic sedimentation, this may also have caused the coronas to develop: During fast episodic accumulation, relatively large amounts of organic matter are trapped (Seilacher 1978) and the sediment is compacted.

As a consequence of compaction, the vertical trace fossils are turned into drains, which function in the same way as Middleton & Hampton's (1976) fluid escape funnels.

Such a selective permeability through recent vertical traces of *Trichichnus* type was observed by Weaver & Schultheiss (1983) in siliciclastic turbidites. On Mors *Trichichnus* is only found to transect one depositional unit, whereas *Bathichnus* may cross more of them. Escaping pore water may therefore be allowed into the overlying strata over a comparatively long period through *Bathichnus*.

The accessory vertical shaft has no pyritic corona, and as it directly crosses into the *Bathichnus* sp. shaft (plate 3), this may reflect that no pore water passed through this shaft while it was an effective conduit to the sediment surface.

The chemical conditions in the pore fluid become more reducing downwards towards a redox barrier (cf. Eder 1982, Weaver & Schultheiss 1983), which is established due to decay of entrapped organic matter. Water escaping through the vertical trace fossils would therefore bring relatively reducing water up into beds, where less reducing or even oxidizing conditions prevailed.

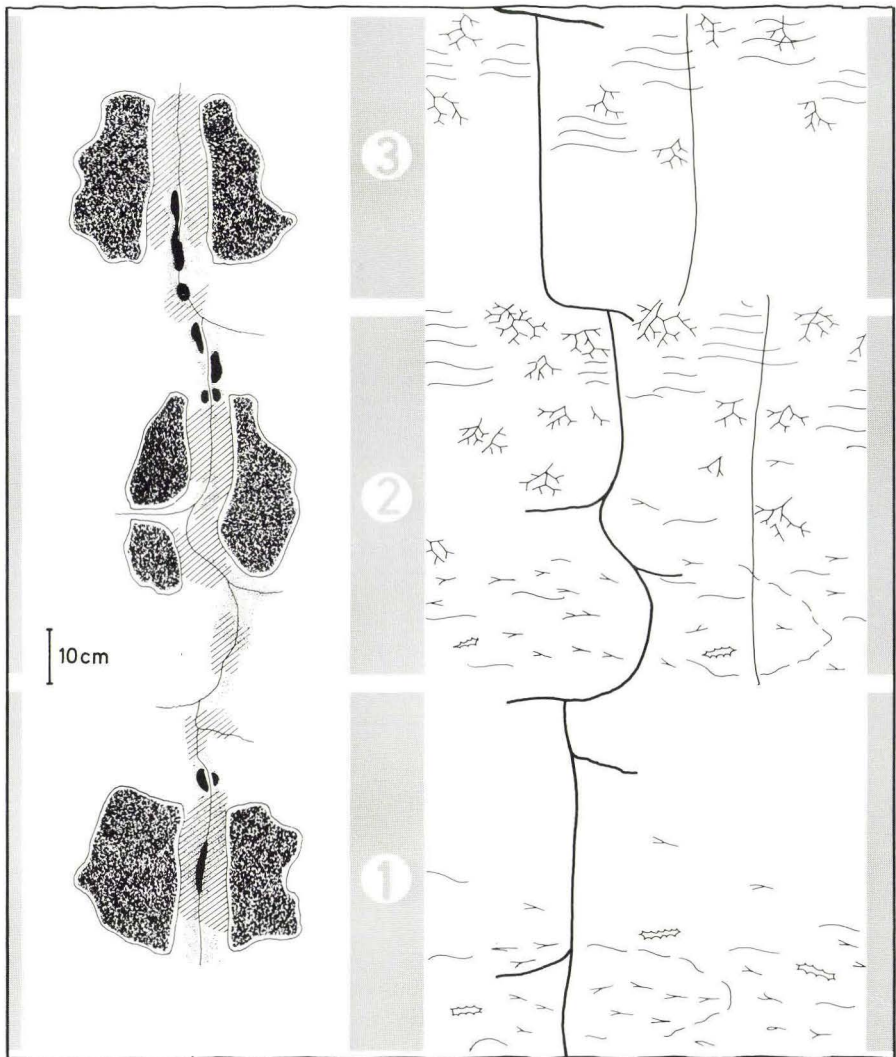


Fig. 17. Suggested relationship between trace fossils, diagenesis and episodic sedimentation. On the left hand side the *Bathichnus paramoudrae* and the associated diagenetic coronas from Bromley et al. (1975, fig. 5) are reproduced in a suggested succession of three depositional episodes. On the right all the trace fossils, which are considered in the text, are presented and related to the same episodes.

In the first depositional episode (1) only deformed traces which predate the final deposition are drawn, except *Bathichnus* which transects all the depositional units.

In the second depositional episode (2) all traces are drawn. They include *Bathichnus*, deformed traces which predate the depositional episode, the slender escape trace *Trichichnus*, and the in situ trace fossils, *Chondrites* and *Zoophycos* that have been produced in the top of the unit during its exposure to the sea water.

In the third episode only the trace fossils, which post date the deposition, are drawn.



Bromley et al. (1975) and Clayton (1982) explained the chemical gradients away from the vertical shafts by the establishment of a reducing environment inside and in the close vicinity of the shaft, through reduction of organic matter in the trace. The geologic evidence from Mors suggests that the chemical gradient on which the coronas, including the paramoudra flints, were developed, is caused by combined biologic and water escape effects.

## Summary

Based on some examples from the Upper Cretaceous chalk, which overlies the Mors salt dome, an extension of the genus *Bathichnus*, Bromley et al. (1975) is suggested: Burrows that comprise vertical shafts 0.2–7 cm, typically 0.5 cm in diameter and up to 9 m long, from all parts of which side branches with diameters from 0.2–1.5 cm diverge irregularly.

The vertical shafts are surrounded by numerous side branches with a variety of internal structures which would refer them to other ichnogenera was it not for their common inheritance.

Two fundamental principles seem to apply to the way *Bathichnus* is filled by sediment: drapes on walls and spiralling.

Glauconite linings and intraclasts in trace fill suggest wall linings in *Bathichnus* to have been applied as a consequence of depositional episodes on the sea bottom, which caused sediment to drop passively into the open trace. *Bathichnus* thus seems to reflect the adaptation by an animal or group of animals of a suitable behaviour for a stressful environment, where more major depositional episodes could occur within a lifetime. *Bathichnus*, taken as a type of escape trace, is therefore suggestive of episodic sedimentation and allochthony as sedimentary processes.

The evidence in the Mors material would suggest, that a deposit feeding worm was possibly the original trace producing animal. This would have produced the entire *Bathichnus* system by secondary widening of the burrow up to its customary diameter of action (c. 0.5 cm). A possible polygenetic origin cannot be rejected, however.

A re-evaluation of the genesis of *Bathichnus* in view of the behavioral and sedimentological considerations given above, as well as the gross morphology of *Bathichnus paramoudrae* (Bromley et al. 1975, fig. 5, and here on fig. 17), allows a considerably shorter animal than the originally suggested 9 m to have produced the trace fossil: Each section of the vertical shaft is connected to the next vertical shaft by a subhorizontal section, and represents a deposi-

tional episode, which forced the animal to dig its way up to the new sediment surface. The animal therefore was probably not longer than the individual vertical sections.

Other trace fossils in the Mors core material are deformed and predate events of re-deposition. *Trichichnus* seems to reflect an escape from sudden overburden, and *Chondrites* and *Zoophycos* reflect relatively stable sediment surface conditions.

The evidence from the Mors cores about trace fossils in relation to rapid and episodic sedimentation in a setting close to the depo-centre of the Upper Cretaceous sea has been summarized in fig. 17.

Paramoudra flints either protrude downward from a bed surface (R. G. Bromley pers. comm. 1982), or they constitute an irregular columnar stack (Felder 1971, Bromley et al. 1975). This way of occurrence of the paramoudras may readily be explained in the present depositional context: By each major depositional event, the sediment surface rose a distance comparable to the height of the single sections of the paramoudra column. The depositional episodes caused excess porewater to be squeezed out from below and this created the chemical gradient on which a new upper section of the paramoudra was developed (fig. 17).

The geologic evidence from Mors therefore shows that the chemical gradients on which the coronas, including the paramoudra flints, were developed, may be caused not by organic decay alone, but also by reducing pore water escaping in the very early compaction history of the chalk, while the vertical shafts were still effective conduits to the sediment surface.

The suggested potential of trace fossils, in the chalk on Mors, as indicators of mode and rate of deposition may be more generally applicable. The trace fossil analysis may therefore be a valuable additional tool for the depositional interpretation of chalk in those parts of the Late Cretaceous sea where the sediment accumulated episodically.

*Acknowledgements:* During the preparation of this paper I have received help from P. Frykman and T. F. Jensen of the Geological Survey of Denmark. R. G. Bromley carefully reviewed an early draught of the paper and gave valuable criticism. The drawings were prepared by K. Andersen, the photos by J. and C. Torres, and H. Nylander typed the script. For this they are all gratefully acknowledged.

## Dansk sammendrag

I fire borerer, der gennemsætter det meste af Øvre Kridttids lagserien over saltstrukturen på Mors, er der udtaget 30 kerner. I seks af disse findes usædvanlig lange lodrette sporfossiler. De

fleste af disse spor svarer enten direkte til *Bathichnus paramoudrae* (Bromley et al. 1975) eller har stor lighed med dette (planche 1 og 2). Baseret på en beskrivelse af et stort antal tværsnit gennem sidegrene og lodrette centralspor foreslås en udvidelse af slægts karakteristikken af *Bathichnus* til også at omfatte de bredere vertikale sporsystemer (planche 1 og 3).

Det foreslås at tværsnit af sidegrene af *Bathichnus* kan have stærkt varierende omrids og indre struktur, hvilket tolkes som et resultat af passiv sediment indfyldning i gravegangssystemet mens dette endnu var i brug. De enkelte side grene blev således forladt af den gravende organisme på forskellige stadier af brug, hvilket afspejles i de indre strukturer. Dersom sediment indfyldningen ikke var voldsommere end at den tillod genbrug af gangen, blev fyldet blot skubbet ud til siderne som en vægdrapering, mens en mere massiv fyldning forhindrede genanvendelse og derfor efterlod den centrale del af sporet med et ensartet fyld. Baseret på at *Bathichnus paramoudrae* er fundet i en borekerne hvor dets nedre del findes sammen med deformerede sporfossiler, mens det selv er upåvirket, og at toppen af kernen viser *Bathichnus* omgivet af udeformerede *Chondrites* og *Zoophycos* foreslås en samlet model.

Modellen går ud på at den lodrette orientering af *Bathichnus* afspejler hurtig aflejring. Sporet viser at det gravende dyr ønskede at bibeholde kontakten med sedimentoverfladen, og at det derfor blot forlængede sporet efterhånden som der aflejredes sediment.

På grundlag af tilstedeværelsen af deformerede spor og flugtspor (*Trichichnus*) i omlejrede enheder i Mors borerne opstilles en samlet model for relationen mellem spor og episodisk aflejrede kalkenheder. Ifølge modellen vil en sekvens af spor kunne karakterisere sådanne enheder (fig. 17):

- a deformerede spor som er dannet før den endelige aflejring
- b flugtspor dannet som reaktion på aflejringen
- c spor af tilpassede organismer (*Bathichnus*)
- d udeformerede spor som er gravet ned fra sediment overfladen efter aflejringen.

De diagenetiske reaktionsrande omkring de lodrette spor synes at passe godt i denne fortolkning. De må have fungeret som vandundvigelseskanaler i forbindelse med den hurtige kompaktion, som den hurtige aflejring afstedkom. Herved er forskellige formationsvæsker blevet bragt i indbyrdes kontakt, hvilket har været medvirkende til dannelsen af randene af mikrokrySTALLIN pyrit, hærdenet kalk og flint.

Den foreslåede mulighed for at benytte sporfossilerne i kalkstenen på Mors til at angive bjergartens aflejningsmåde og -hastighed er muligvis mere generelt anvendelig. En sådan sporfossil analyse kan derfor være et værdifuldt supplement til andre undersøgelser ved fortolkningen af aflejningsbetingelserne i de dele af kridttidshavet, hvor aflejringen foregik hurtigt og episodisk.

## References

- Berger, W. H., Ekdale, A. A. and Bryant, P. P. 1979: Selective preservation of burrows in deep-sea carbonates. *Marine Geology* 32: 205–230.
- Bromley, R. G. 1975: Trace Fossils at omission surfaces. In: Frey, R. W. (ed.): *The study of Trace Fossils*, Springer-Verlag New York Inc.: 399–428.
- Bromley, R. G. 1981: Enhancement of visibility of structures in marly chalk: modification of the Bushinsky oil technique. *Bull. geol. Soc. Denmark* 29: 111–118.



- Bromley, R. G., Schulz M.-G. and Peake N. B. 1975: Paramoudras: giant flints, long burrows and the early diagenesis of chalks. Det Kongelige Danske Videnskabers Selskab, Biologiske Skrifter 20, 10: 31 p.
- Bromley, R. G. and Ekdale, A. A. 1983: Flint and fabric in the European chalk. In press.
- Brotzen, F. 1945: De geologiska resultaten från borrhningarna vid Höllviken (in swedish with english summary). Sveriges Geologiska Undersökning, Ser. C 465: 1–64.
- Chamberlain, C. K. 1978: Recognition of trace fossils in cores. SEPM Short Course 5: 125–183.
- Clayton, C. J. 1982: Geochemistry and origin of paramoudras. IAS 3rd Eur. MTG., Copenhagen, Abstr.: 108–110.
- Eder, W. 1982: Diagenetic redistribution of carbonate, a process in forming limestone – marl alternations (Devonian and Carboniferous Rheinisches Schiefergebirge, W. Germany). In: Einsele, G. & Seilacher, A. (eds.): Cyclic and Event Stratification, Springer-Verlag: 98–112.
- Ekdale, A. A. 1980: Trace fossils in deep sea drilling project Leg 58 cores. DSDP Init. Rep. Vol. LVIII: 601–605.
- Felder, W. M. 1971: Een bijzondere vuursteenknol. Grondboor – Hamer, 2: 30–38.
- Frey, R. W. and Howard, J. D. 1970: Comparison of Upper Cretaceous ichnofaunas from siliceous sandstone and chalk, Western Interior Region, U.S.A. In: Crimes, T. P. & Harper, J. C. (eds.): Trace Fossils, Geol. J. Spec. Issue 3: 141–166.
- Hardman, R. F. P. 1982: Chalk reservoirs of the North Sea. Bull. geol. Soc. Denmark 30: 119–137.
- Jordan, R. 1981: Sind submarine Gas- und Schlammvulkane in der Schreiekreide-Fazies Nordwesteuropas Anlass für die Genese der Paramoudras?. N. Jb. Geol. Paläont. Mh. 7: 419–426.
- Kennedy, W. J. 1970: Trace fossils in the chalk environment. In: Crimes, T. P. and Harper, J. C. (eds.): Trace Fossils, Seel House Press, Liverpool: 263–282.
- Kennedy, W. J. 1980: Aspects of chalk sedimentation in the southern Norwegian offshore. Proceedings of symposium: “The sedimentation of North Sea reservoir rocks”, Norwegian Petroleum Society, Geilo: 29 p.
- Kennedy, W. J. and Juignet, P. 1974: Carbonate banks and slump beds in the Upper Cretaceous (Upper Turonian-Santonian) of Haute Normandie, France. Sedimentology 21: 1–42.
- Middleton, G. V. and Hampton, M. A. 1976: Subaqueous sediment transport and deposition by gravity flows. In: Stanley, D. J. and Swift, D. J. P. (eds.): Marine sediment transport and environmental management. John Wiley and Sons Inc.: 197–218.
- Nygaard, E. 1982: Trace fossils in redeposited chalk, Mors, Denmark. IAS 3rd Eur. MTG., Copenhagen, Abstr.: 55–56.
- Nygaard, E. and Frykman, P. 1981: Alloktone aflejringer i Maastrichtien kalken på Mors (in danish with english abstract). – Dansk geol. Foren., Årsskrift for 1980: 57–60.
- Nygaard, E., Lieberkind, K. and Frykman, P. 1983: Sedimentology and reservoir parameters of the Chalk Group in the Danish Central Graben. Geol. Mijnb. 62: 177–190.
- Ofstad, K. 1983: Geology of the southernmost part of the norwegian section of the Central Trough. Oljedirektoratet, NPD Paper 32: 41 p.
- Perch-Nielsen, K., Ullberg, K. and Evensen, J. A. 1979: Comments on “The terminal Cretaceous event: a geologic problem with an oceanographic solution”. Proceedings of the Cretaceous-Tertiary boundary symposium. University of Copenhagen: 106–111.
- Robertson, A. H. F. 1976: Pelagic chalk and calciturbidites from the Lower Tertiary of the Troodos Massif, Cyprus. Jour. Sed. Petrology 46: 1007–1016.
- Schmid, F. 1982: Das erweiterte Unter-/Ober-Maastricht-Grenzprofil von Hemmoor, Niederelbe (NW-Deutschland). Geol. Jb. A 61: 7–12.

- Scholle, P. A. 1971: Sedimentology of fine-grained deep-water carbonate turbidites, Monte Antola Flysch (Upper Cretaceous), Northern Apennines, Italy. *Geol. Soc. Amer. Bull.* 82: 629–658.
- Seilacher, A. 1962: Paleontological studies on Turbidite sedimentation and erosion. *Jour. Geology* 70: 227–234.
- Seilacher, A. 1978: Use of trace fossil assemblages for recognizing depositional environments. *SEPM, Short Course* 5: 185–201.
- Steinich, G. 1967: Sedimentstrukturen der Rügener Schreibkreide. *Geologie, Jahrg.* 16, heft 5: 570–583.
- Steinich, G. 1972a: Endogene tektonik in der Unter-Maastricht-vorkommen auf Jasmund (Rügen). *Geologie, Beiheft zur Zeitschrift* 20: 1–205.
- Steinich, G. 1972b: Pseudo-Hardgrounds in der Unter-Maastricht-Schreibkreide der Insel Rügen. *Wiss. Z. Univ. Greifswald* 21, Mathematisch-Naturwissenschaftliche Reihe 2: 213–223.
- Voigt, E. 1962: Frühdiagenetische Deformationen der turoner Plänerkalk bei Halle/Westf. als folge einer Grossgleitung unter besondere Berücksichtigung des Phacoides-Problem. *Mitt. Geol. St. Inst. Hamburg* 31: 146–275.
- Watts, N. L., Lapre, J. F., van Schyndel-Goester, F. S. and Ford, A. 1980: Upper Cretaceous and Lower Tertiary chalks of the Albuskjell area, North Sea: Deposition in a slope and base-of-slope environment. *Geology* 8: 217–221.
- Weaver, P. P. E. and Schultheiss, P. J. 1983: Vertical open burrows in deep-sea sediments 2 m in length. *Nature* 301: 329–331.

# Publications issued 1982

## *Årbog – Yearbook*

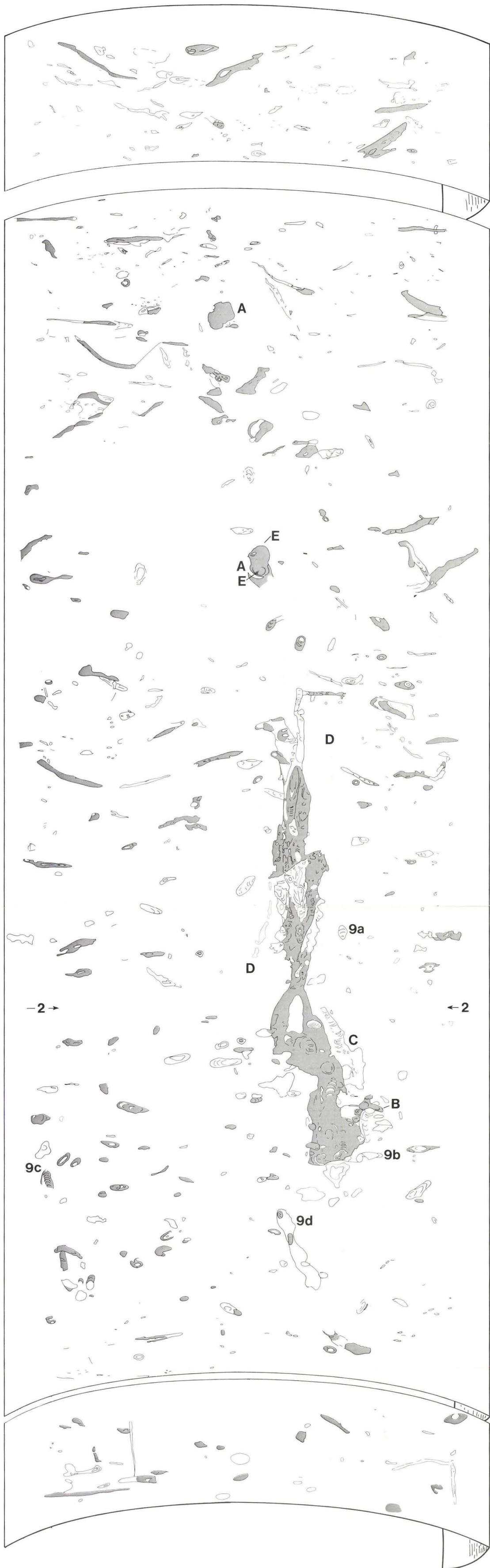
1981 Editor: *Bent Aaby*, 1982, 137 pp.

Contents: *Bent Vad Odgaard*: A Middle Weichselian moss assemblage from Hirtshals, Denmark, and some remarks on the environment 47.000 BP: 5–46. *Niels Balslev Jørgensen*: Turbidites and associated resedimented deposits from a tilted glacio – deltaic sequence, Denmark: 47–72. *Peter Gravesen*: Lower Cretaceous sedimentation and basin extension on Bornholm, Denmark: 73–100. *P. Hedeboel Nielsen, Regin Waagstein, Jóannes Rasmussen and Birger Larsen*: Marine seismic investigation of the shelf around the Faroe Islands: 101–110. *Jóhannes Jóhansen*: Vegetational development in the Faroes from 10.000 BP to the present: 111–136. Publications issued 1981: 137.

## *Serie B – Series B*

6. *Roger J. Davey*: Dinocyst stratigraphy of the latest Jurassic to Early Cretaceous of the Haldager No. 1 borehole, Denmark: 1–57.
7. *Peter Gravesen, Flemming Rolle and Finn Surlyk*: Lithostratigraphy and sedimentary evolution of the Triassic, Jurassic and Lower Cretaceous of Bornholm, Denmark: 1–51.
8. *Olaf Michelsen* (ed.): Geology of the Danish Central Graben: 1–135.





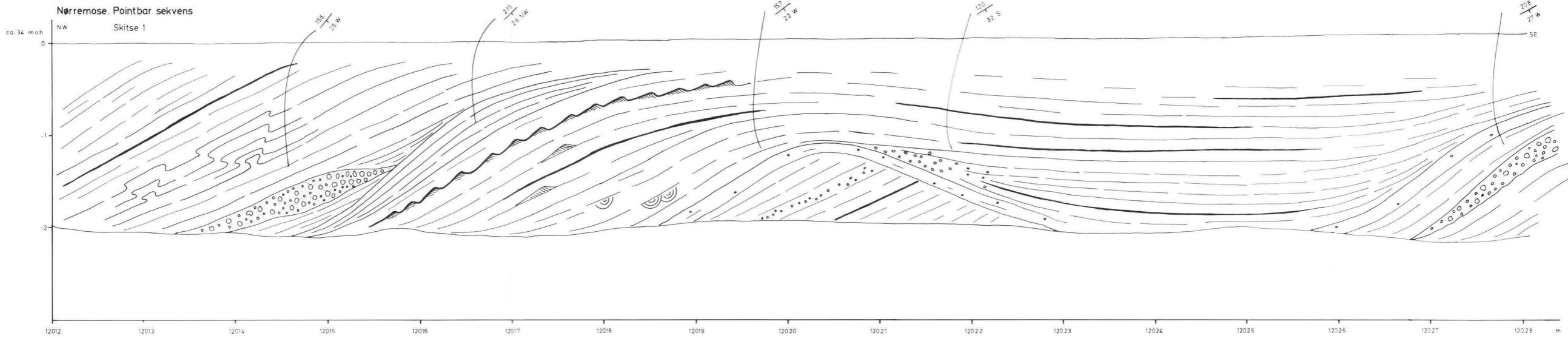
Dispersed microcrystalline pyrite

Relative dark trace fossils

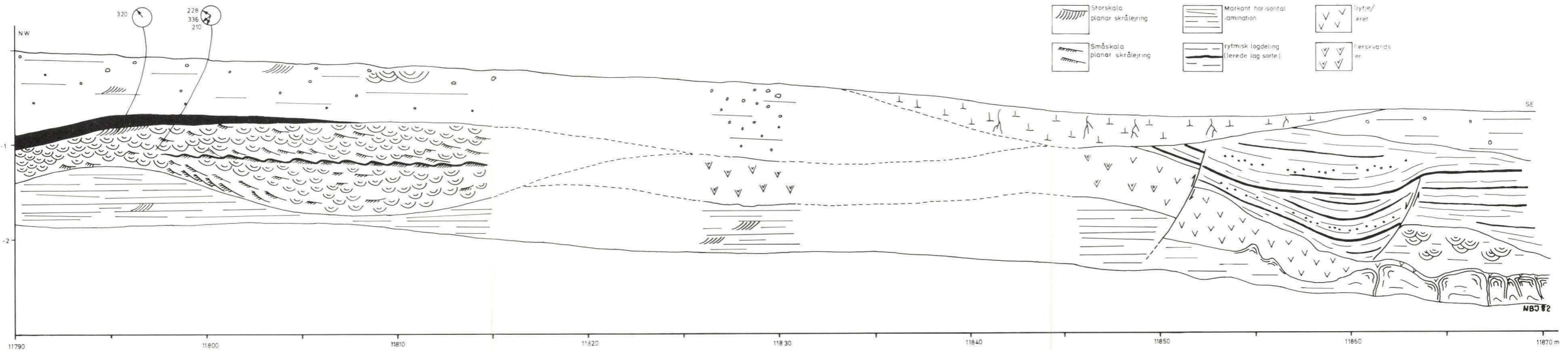
Relative light trace fossils

Plate 3. *Bathichnus* sp. from plate 1b, drawn together with all other recognized biogenic structures all the way round the core surface.

The numbers refer to figures which illustrate some of the details. Note the subhorizontal sections through the *Bathichnus* shaft A, young generations of trace fill which protrude from the shaft into a side branch B, the entry of the accessory shaft into the main shaft C, the sparse presence of *Chondrites*, and the localisation of the pyritized corona outside the shaft D, or in its outskirts E. Erslev 4S, core-4.



	Storskala skrælejrning		Klatrende ribber		Diamiktite
	Småskala skrælejrning		Svag horisontal lamination		Taru
	Storskala planar skrælejrning		Markant horisontal lamination		Silt/sand
	Småskala planar skrælejrning		rytmisk lagdeling (lerede lag sorte)		Finskandede ler

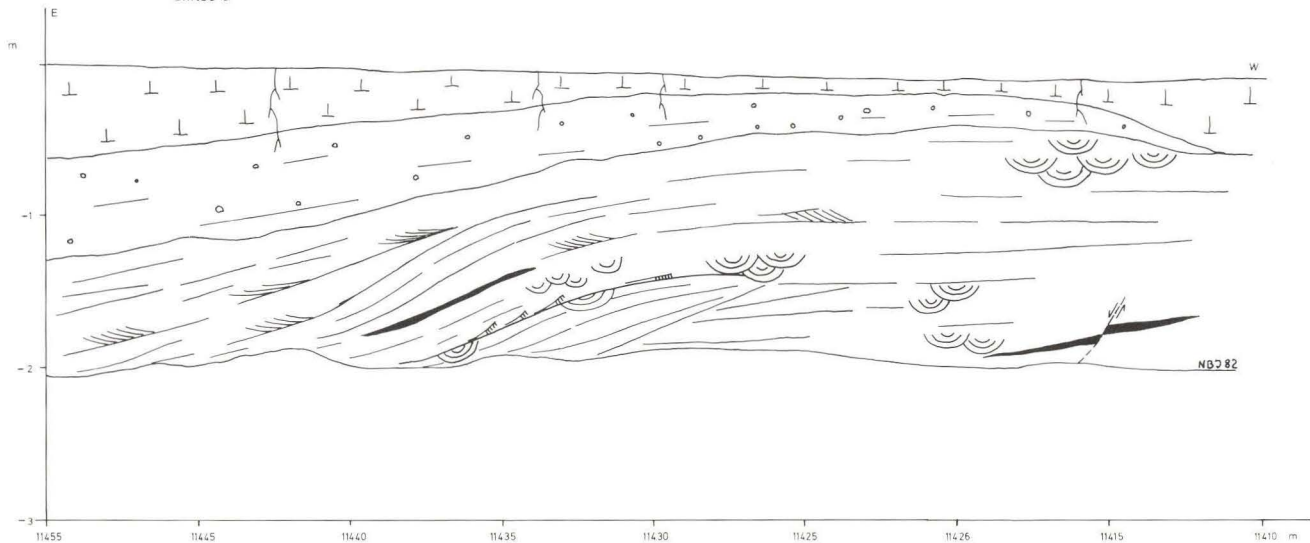


Skitse 1: Se tekst.





Vester Nebel Ådal. Pointbar sekvens  
Skitse 3



Skitse 3: Pointbar sekvens umiddelbart øst for V. Nebel Å, se i øvrigt teksten.

NATURGAS 1982

NIELS BALSLEV JØRGENSEN



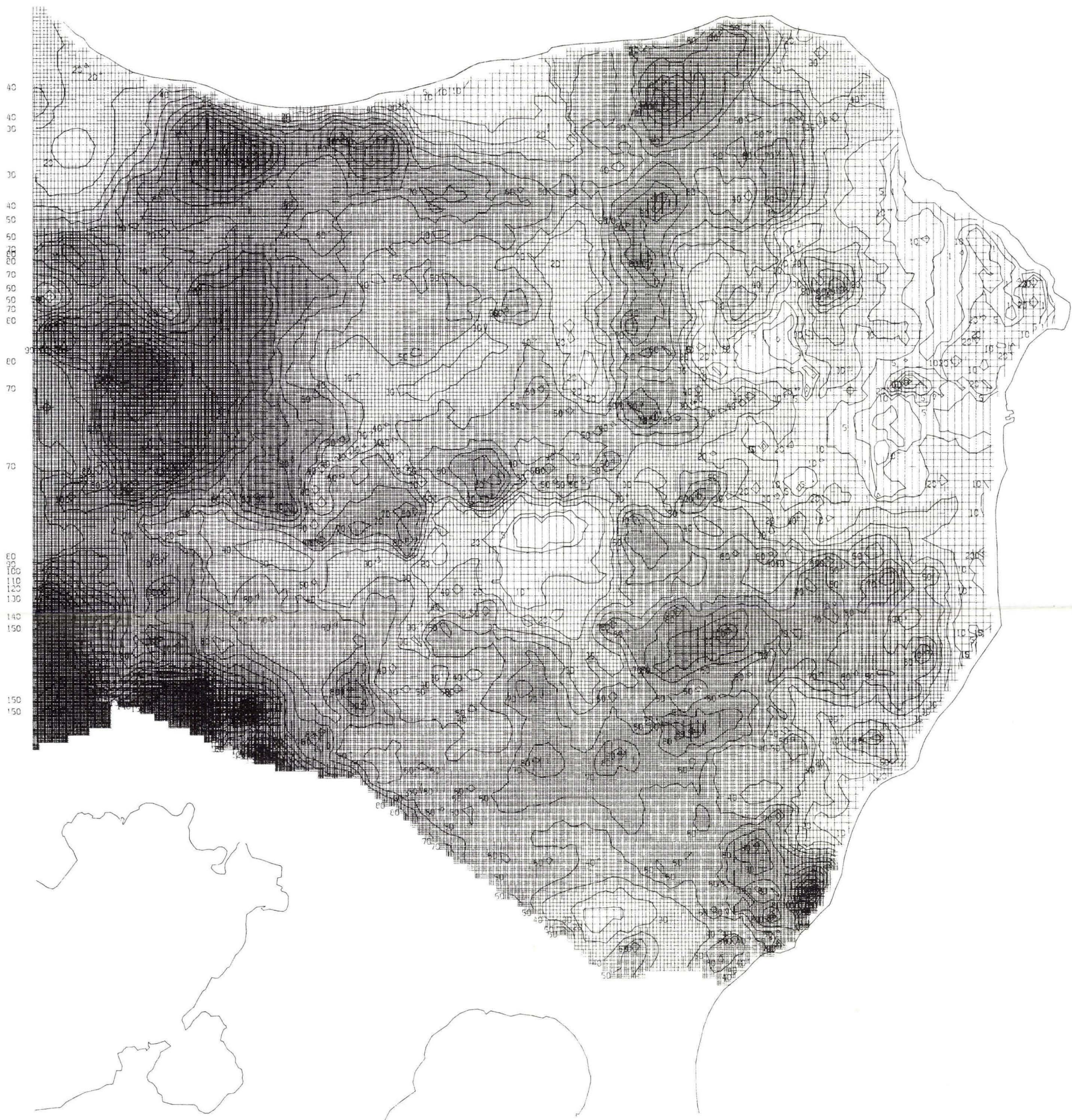


Plate 1. Hydraulic percolation time to the Danian aquifer, given in approximate years.



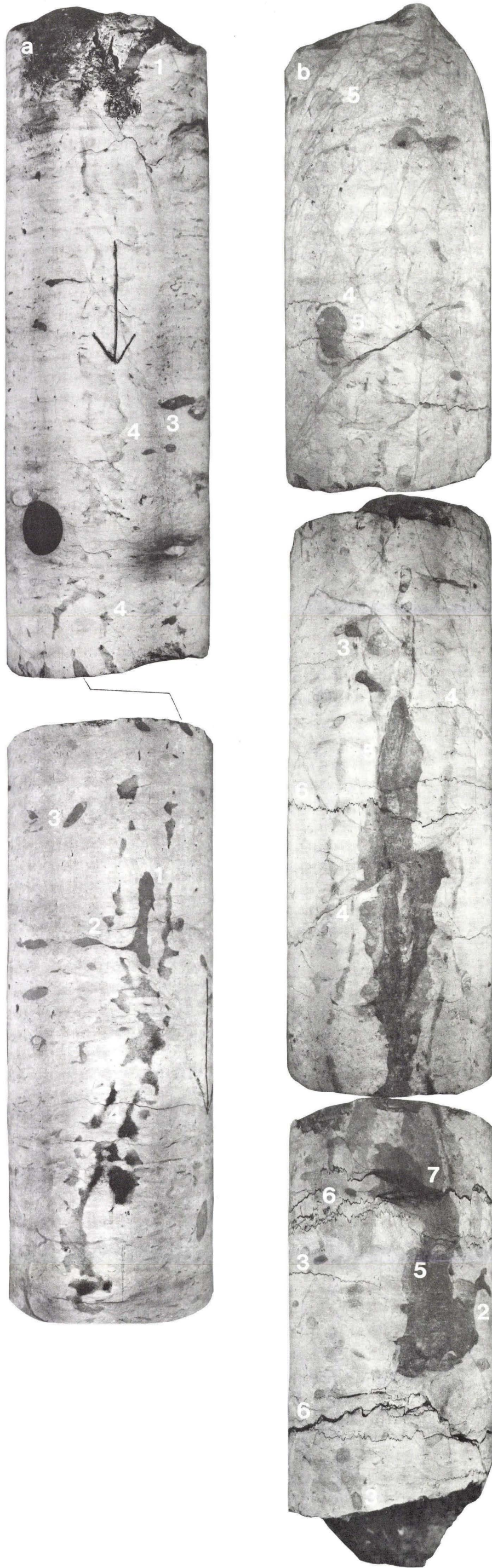


Plate 1. a/ *Bathichnus paramoudrae*,  
 b/ *Bathichnus* sp.

The two cores demonstrate the general morphology of the *Bathichnus* shafts and side branches. Also the pyrite enriched coronas round the shafts are seen. The arrow, which indicates the direction of drilling, is located on a tangential section through the corona. Note that the core pieces in a/ are rotated relative to each other. *Bathichnus* sp. in b/ increases considerably in diameter downwards towards its lower termination. 1 *Bathichnus paramoudrae* shaft with grey homogeneous fill and with branching point into subhorizontal side-branch 2, and sections through side branches 3. The discontinuous pyrite enriched intervals 5. Note the stylonites 6, with up to 2 mm clay mineral drape, shaft and laterally into horsetail flasers 7, where they cross the shaft. The uppermost section of the core in plate 1a is shown in fig. 11a. a/ Erslev 3S, core-3, b/ Erslev 4S, core-4.



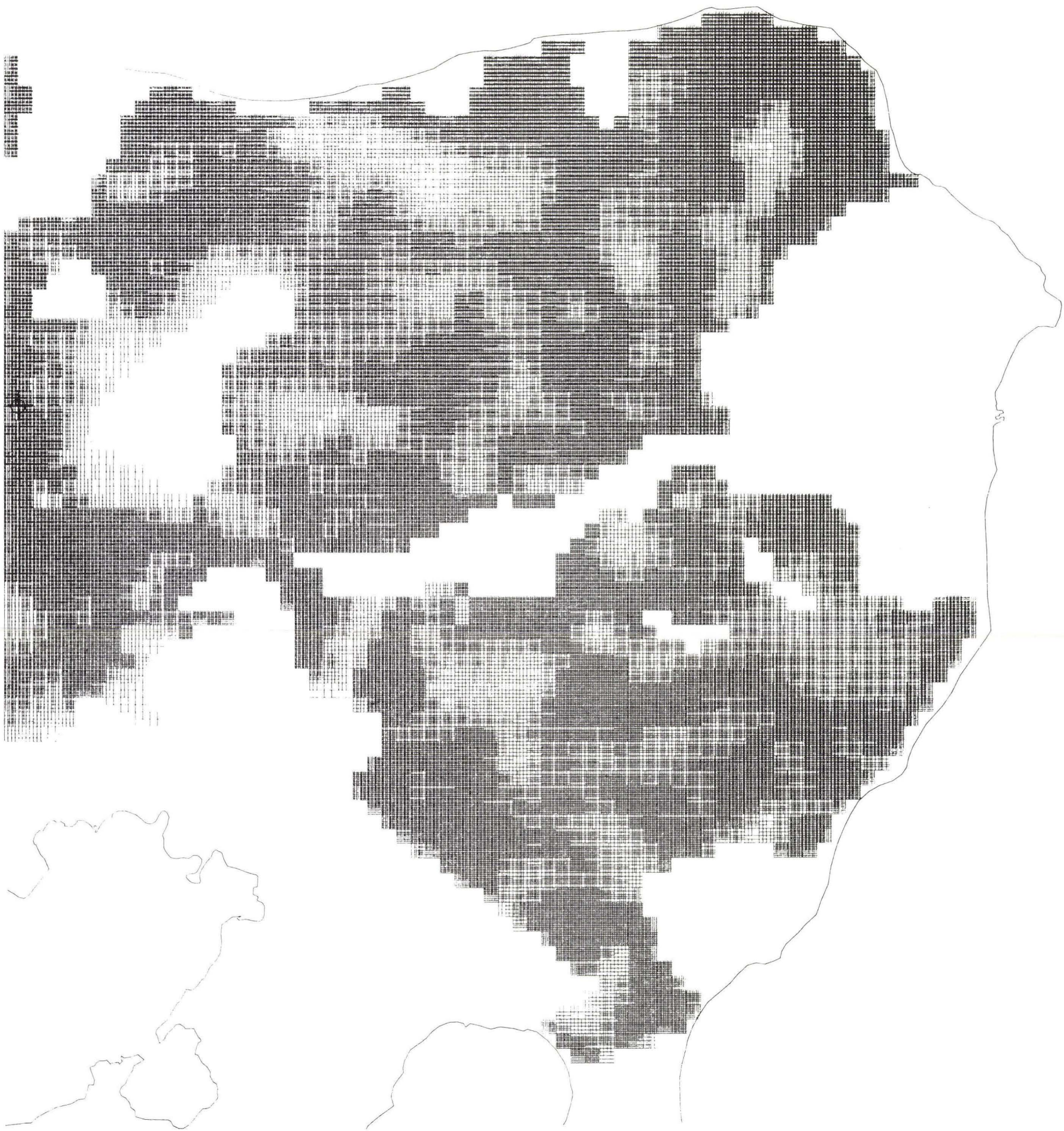





Plate 2. Vulnerability of upper glacial aquifers in the test area. Increasing shading corresponds to increased vulnerability. White areas are undefined.





 Chert

 Relative dark trace fossils

 Dispersed microcrystalline pyrite


 Relative light trace fossils

Plate 2. *Bathichnus paramoudrae* from plate 1a, drawn together with all other recognized biogenic structures all the way round the core surface. The numbers correspond to figures which illustrate some of the details.

Note the sparse presence of *Chondrites* in the middle part of the core, the deformed and individually located sections through *Chondrites* at the base A, and the undeformed *Chondrites* in the upper part B. Note also *Zoophycos* in the topmost part of the core Z. Erslev 3S, core-3.